

Geology and geochemistry of Precambrian rocks, central and south-central New Mexico

by KENT C. CONDIE and A. J. BUDDING





New Mexico Bureau of Mines & Mineral Resources

A DIVISION OF
NEW MEXICO INSTITUTE OF MINING & TECHNOLOGY

**Geology and geochemistry of Precambrian rocks,
central and south-central New Mexico**

by Kent C. Condie and A. J. Budding

NEW MEXICO INSTITUTE OF MINING & TECHNOLOGY

KENNETH W. FORD, *President*

NEW MEXICO BUREAU OF MINES & MINERAL RESOURCES

FRANK E. KOTTELOWSKI, *Director*GEORGE S. AUSTIN, *Deputy Director*

BOARD OF REGENTS

Ex Officio

Bruce King, *Governor of New Mexico*
Leonard DeLayo, *Superintendent of Public Instruction*

Appointed

William G. Abbott, 1961-1985, *Hobbs*
Judy Floyd, Secretary-Treasurer, 1977-1981, *Las Cruces*
Owen Lopez, President, 1977-1983, *Santa Fe*
Dave Rice, 1972-1983, *Carlsbad*
Steve Torres, 1967-1985, *Socorro*

BUREAU STAFF

Full Time

ORIN J. ANDERSON, <i>Geologist</i>	NORMA J. MEEKS, <i>Department Secretary</i>
WILLIAM E. ARNOLD, <i>Scientific Illustrator</i>	ARLEEN MONTOYA, <i>Librarian/Typist</i>
VIRGINIA BACA, <i>Staff Secretary</i>	ROBERT M. NORTH, <i>Mineralogist</i>
ROBERT A. BIEBERMAN, <i>Senior Petrol. Geologist</i>	CONNIE OLIVER, <i>Receptionist</i>
CHARLES T. BOLT, <i>Petroleum Geologist</i>	GLENN R. OSBURN, <i>Volcanologist</i>
LYNN A. BRANDVOLD, <i>Chemist</i>	LINDA PADILLA, <i>Staff Secretary</i>
CORALE BRIERLEY, <i>Chemical Microbiologist</i>	NEILA M. PEARSON, <i>Associate Editor</i>
BRENDA R. BROADWELL, <i>Assist. Lab. Geoscientist</i>	JOAN C. PENDLETON, <i>Associate Editor</i>
FRANK CAMPBELL, <i>Coal Geologist</i>	JUDY PERALTA, <i>Executive Secretary</i>
RICHARD CHAMBERLIN, <i>Economic Geologist</i>	BARBARA R. POPP, <i>Lab. Biotechnologist</i>
CHARLES E. CHAPIN, <i>Senior Geologist</i>	ROBERT QUICK, <i>Driller's Helper</i>
JEANETTE CHAVEZ, <i>Admin. Secretary I</i>	BRUCE REID, <i>Geologist</i>
RICHARD R. CHAVEZ, <i>Assistant Head, Petroleum</i>	MARSHALL A. REITER, <i>Senior Geophysicist</i>
RUBEN A. CRESPIN, <i>Laboratory Technician II</i>	JACQUES R. RENAULT, <i>Geologist</i>
LOIS M. DEVLIN, <i>Director, Bus.-Pub. Office</i>	JAMES M. ROBERTSON, <i>Mining Geologist</i>
KATHY C. EDEN, <i>Editorial Clerk</i>	W. TERRY SIEMERS, <i>Indust. Minerals Geologist</i>
ROBERT W. EVELETH, <i>Mining Engineer</i>	JACKIE H. SMITH, <i>Laboratory Technician IV</i>
ROUSSEAU H. FLOWER, <i>Sr. Emeritus Paleontologist</i>	BARBARA J. SPENCE, <i>Geologist</i>
STEPHEN J. FROST, <i>Coal Geologist</i>	WILLIAM J. STONE, <i>Hydrogeologist</i>
JOHN W. HAWLEY, <i>Environmental Geologist</i>	DAVID E. TABET, <i>Geologist</i>
CANDACE L. HOLTS, <i>Associate Editor</i>	SAMUEL THOMPSON III, <i>Petroleum Geologist</i>
STEPHEN C. HOOK, <i>Paleontologist</i>	ROBERT H. WEBER, <i>Senior Geologist</i>
BRADLEY B. HOUSE, <i>Scientific Illustrator</i>	WILLIAM T. WILLIS, <i>Driller</i>
MEL JENNINGS, <i>Metallurgist</i>	DONALD WOLBERG, <i>Field Geol./Vert. Paleontologist</i>
ROBERT W. KELLEY, <i>Editor & Geologist</i>	MICHAEL W. WOOLRIDGE, <i>Scientific Illustrator</i>
R. E. KELLEY, <i>Field Geologist</i>	JOHN R. WRIGHT, <i>Paleont. Preparator/Curator</i>
STEPHANIE LANDREGAN, <i>Scientific Illustrator</i>	

Part Time

CHRISTINA L. BALK, <i>Geologist</i>	BEVERLY OHLINE, <i>Newswriter, Information Services</i>
NANCY H. MIZELL, <i>Geologist</i>	ALLAN R. SANFORD, <i>Geophysicist</i>
HOWARD B. NICKELSON, <i>Coal Geologist</i>	THOMAS E. ZIMMERMAN, <i>Chief Security Officer</i>

Graduate Students

SCOTT K. ANDERHOLM	STEVEN D. CRAIGG	SUSAN C. KENT
PAM BLACK	MARTIN A. DONZE	T. MATTHEW LAROCHE
JEFFREY BRUNEAU	K. BABETTE FARIS	VIRGINIA McLEMORE
GERRY W. CLARKSON	THOMAS GIBSON	SUSAN ROTH
GARY COFFIN	RICHARD HARRISON	CHARLES R. SHEARER

Plus about 25 undergraduate assistants

First Printing, 1979

Preface

This investigation of Precambrian rocks in central and south-central New Mexico serves several purposes. We bring together and summarize existing field, stratigraphic, petrographic, and geochronologic data from Precambrian terranes in central and south-central New Mexico. Additional data from our own studies are included. For the first time, we provide complete geologic maps and descriptions of Precambrian terranes in the White Sands Missile Range. We tabulate and evaluate major- and trace-element data for the principal Precambrian rock types in central and south-central New Mexico in terms of alteration, models for magma origin, and sediment provenance. Many of these tabulations are on microfiche in the envelope inside the back cover. Finally, one of our major goals is discussion of the origin and tectonic setting of the Precambrian terrane using all available geologic and geochemical evidence.

ACKNOWLEDGMENTS—The authors are grateful to R. H. Duncan, chief scientist at the White Sands Missile Range, for permission to undertake geologic studies of the Precambrian rocks on the missile range. In particular, we acknowledge Felix Sedillo for his assistance in planning our field work in the missile range and Ismael Rel for acting as our escort and guide. We could not have completed the studies in the limited time available if it had not been for Rel's knowledge of the roads. Dennis Umshler, Walter Yuras, and Larry Trom are acknowledged for their assistance in sample preparation, analytical work, and reduction of data. Theresa Cookro, Charles Beers, Paul Farquhar, David Mathewson, and William Bolton provided some of the field and analytical results as part of their theses at New Mexico Institute of Mining and Technology. Clay T. Smith and David L. White helped the authors with field investigations in the area east of Socorro and in the San Andres Mountains, respectively. We also thank the staff at the Sandia Laboratories nuclear reactor in Albuquerque for their cooperation in irradiating samples for neutron-activation studies. This study would not have been possible without the cooperation of the many ranchers and farmers who allowed the authors access to their properties. Some of the field expenses were furnished by the New Mexico Bureau of Mines and Mineral Resources. James M. Robertson, David L. White, and Christopher Rautman are acknowledged for critical reviews of the manuscript.

Kent C. Condie
Professor of Geochemistry

A. J. Budding
Professor of Geology

New Mexico Institute of
Mining and Technology

Socorro
October 19, 1978

Contents

ABSTRACT 7	STRUCTURAL GEOLOGY 31
INTRODUCTION 7	SMP BLOCK 31
METAMORPHIC ROCKS 11	SAN ANDRES MOUNTAINS 32
MICA-QUARTZ SCHIST AND PHYLLITE 11	PEDERNAL HILLS 32
QUARTZITE AND RELATED ROCKS 13	LADRON MOUNTAINS 33
MAFIC META-IGNEOUS ROCKS 16	OTHER AREAS 33
SILICEOUS META-IGNEOUS ROCKS 18	CONCLUSIONS 33
GNEISS 20	METAMORPHISM 34
STRATIGRAPHY 21	GEOCHRONOLOGY 37
GRANITIC ROCKS 24	GEOCHEMISTRY 38
NORTH AND SOUTH SANDIA PLUTONS 25	MAFIC META-IGNEOUS ROCKS 38
MANZANITA PLUTON 26	SILICEOUS META-IGNEOUS ROCKS AND GRANITIC ROCKS 40
OJITA AND MONTE LARGO PLUTONS 26	High-Ca group 40
PRIEST PLUTON 27	High-K group 42
LOS PINOS PLUTON 27	High-Si group 43
SEPULTURA PLUTON 27	Effects of alteration 44
PEDERNAL PLUTON 27	FELDSPATHIC QUARTZITES AND ARKOSITES 45
LADRON PLUTON 28	MAGMA ORIGIN 47
CAPIROTE PLUTON 28	TECTONIC SETTING AND
LA JOYITA PLUTON 28	GEOLOGIC EVOLUTION 48
POLVADERA PLUTON 28	MINERAL DEPOSITS 50
MAGDALENA PLUTON 28	REFERENCES 51
OSCURA AND CAPITOL PEAK PLUTONS 28	APPENDICES 54
MOCKINGBIRD GAP PLUTON 29	1—Composite stratigraphic sections 54
STRAWBERRY PEAK AND MAYBERRY PLUTONS 30	2—Major-element chemical analyses (microfiche
SAN ANDRES PLUTON 30	in pocket)
MINERAL HILL PLUTON 30	3—Trace-element contents (microfiche in pocket)
GRANITIC ROCKS OF THE CABALLO MOUNTAINS AND	4—Sample locations (microfiche in pocket)
RED HILLS 30	INDEX 57
MISCELLANEOUS PLUTONS 30	

Tables

1—Relative percentages of metamorphic rocks in Precambrian sections 11	9—Geochemical classification of Precambrian siliceous meta-igneous rocks and granitic plutons 40
2—Modal estimates in principal Precambrian metamorphic rocks 13	10—Comparison of average compositions, Precambrian granitic rocks, high-Ca group 41
3—Detrital-grain modal parameters of medium to coarse clastic metasedimentary rocks 24	11—Comparison of average composition of Precambrian granitic rocks, high-K and high-Si groups, from several areas 42
4—Major Precambrian granitic plutons 24	12—Average compositions, Precambrian siliceous meta-igneous rocks, central and south-central New Mexico, and Taupo rhyolite, New Zealand 44
5—Average modes of Precambrian granitic plutons 26	13—Comparison of average composition, Precambrian feldspathic quartzite-arkosite, central New Mexico, other sandstone averages 45
6—Progressive changes in metamorphic mineral assemblages 34	
7—Summary of major Precambrian events 37	
8—Average compositions of Precambrian mafic meta-igneous rocks 39	

Figures

- 1—Precambrian crustal provinces, southwestern United States **vi**
- 2—Index map, Precambrian rocks in central and south-central New Mexico **vi**
- 3—Precambrian terranes, basement of New Mexico **8**
- 4—Precambrian rocks, Pedernal Hills **Pocket 5**—**Precambrian** rocks, Ladron Mountains **Pocket 6**—**Precambrian** rocks, Magdalena Mountains **Pocket 7**—**Precambrian** rocks, Lemitar Mountains **Pocket 8**—**Precambrian** rocks, La Joyita Hills **Pocket 9**—**Precambrian** rocks, Coyote Hills **Pocket 10**—**Precambrian** rocks, east of Socorro **Pocket 11**—**Precambrian** rocks, Caballo Mountains and Red Hills **Pocket**
- 12—Precambrian rocks, Fra Cristobal Range **Pocket 13**—**Precambrian** rocks, San Diego Mountain area **Pocket 14**—View of normal fault along east side of San Andres Mountains **9**
- 15—View of San Andres Peak **9**
- 16—Views of Precambrian rocks, San Andres and Organ Mountains **10**
- 17—Precambrian rocks, northeastern Organ Mountains **Pocket**
- 18—Precambrian rocks, Pajarito Mountain **Pocket**
- 19—Photomicrographs, schists and gneisses **12**
- 20—View of ridge, north side Hembrillo Canyon **14**
- 21—Photomicrographs, quartzite, arkosite, and related quartz-rich rocks **15**
- 22—Photomicrographs, mafic meta-igneous rocks **17 23**—Photomicrographs, siliceous meta-igneous rocks **19 24**—Composite stratigraphic sections, Precambrian rocks in SMP block **22**
- 25—Miscellaneous composite stratigraphic sections, Precambrian rocks **23**
- 26—Geographic distribution of Precambrian granitic plutons **25**
- 27—Quartz-K-feldspar-plagioclase classification triangle **25**
- 28—Photomicrographs, granitic rocks **29**
- 29—ACF and AKF diagrams showing distribution of meta-igneous rocks **35**
- 30—P-T diagram of phase relations and probable course of progressive metamorphism **35**
- 31—Histograms, U-Pb zircon and whole-rock Rb-Sr isochron ages **36**
- 32—Initial $\text{Sr}^{87}/\text{Sr}^{86}$ ratios, whole-rock isochrons **36**
- 33— $\text{K}_2\text{O}-\text{SiO}_2$ variation diagram **39**
- 34—Ti-Zr-V variation diagram **39**
- 35—Average chondrite-normalized REE diagram **40**
- 36— $\text{Na}_2\text{O}-\text{K}_2\text{O}-\text{CaO}$ diagram **41**
- 37—Rb-Sr diagram for Precambrian igneous rocks from central and south-central New Mexico **41**
- 38—Chondrite-normalized average REE distributions for members of the high-Ca group **41**
- 39—Normative diagram **43**
- 40—Chondrite-normalized envelope of variation of average REE distributions for members of the low-REE subgroup **43**
- 41—Chondrite-normalized envelope of variation of average REE distributions for members of the high-REE subgroup **43**
- 42—Chondrite-normalized envelope of variation of average REE distributions for members of the high-Si group **44**
- 43—Chondrite-normalized average REE distributions for altered siliceous meta-igneous rocks from the Ladron Mountains **45**
- 44—Chondrite-normalized REE distributions in Precambrian feldspathic quartzites and arkosites **46**
- 45— $\text{K}_2\text{O}-\text{Na}_2\text{O}-\text{SiO}_2$ variation diagram, Precambrian feldspathic quartzites and arkosites (+), Los Pinos and Manzano Mountains **46**
- 46—Rock-type distribution, Precambrian of central and south-central New Mexico compared to rock-type distributions in Phanerozoic assemblages **48**
- 47—Possible tectonic settings between 1.7 and 1.9 b.y. in the southwestern United States **49**
- 48—Distribution of proposed multiple-rift system between 1.4 and 1.7 b.y., southwestern United States **50**

Sheets (geologic maps in pocket)

- 1—Precambrian rocks in SMP block and in Monte Largo Hills
- 2—Precambrian rocks from various locations in central and south-central New Mexico (includes figs. 4-13, 17, and 18)
- 3—Precambrian rocks in San Andres and Oscura Mountains

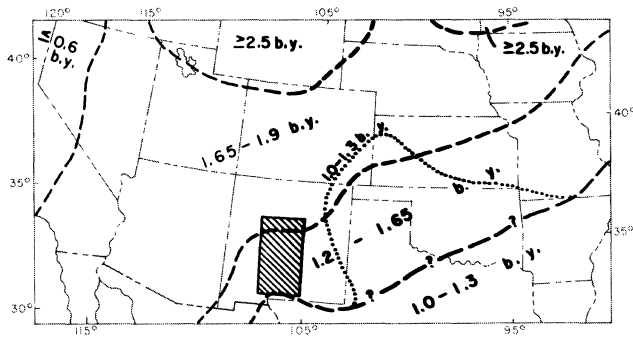


FIGURE 1-PRECAMBRIAN CRUSTAL PROVINCES IN THE SOUTHWESTERN UNITED STATES; ages in billions of years. Shaded area is subject of this report. Dotted line represents a region where igneous rocks, 1.0-1.3 b.y. old, overlie or are intruded into older crust.

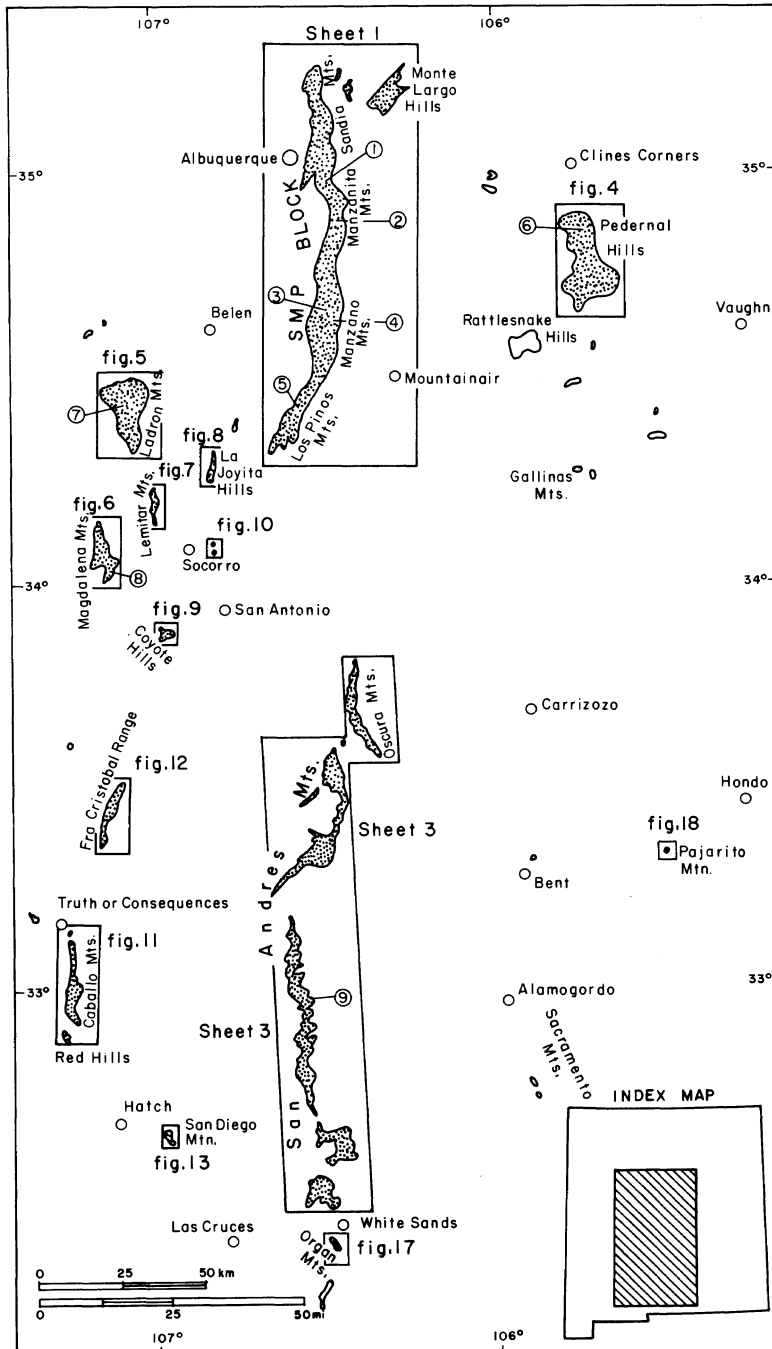


FIGURE 2-DISTRIBUTION OF PRECAMBRIAN ROCKS IN CENTRAL AND SOUTH-CENTRAL NE MEXICO (after Stipp, 1955; Foster and Stipp, 1961; and Robertson, 1976). Circled numbers correspond to stratigraphic sections in figs. 24 and 25. Fig. numbers refer to detailed geologic maps on sheet 2.

Abstract

The Precambrian terrane in central and south-central New Mexico is composed of granitic plutons (70 percent) intruded into metamorphic rocks (30 percent). The principal metamorphic rock types are phyllite and quartz-mica schist (40 percent), quartzite and arkosite (30 percent), mafic meta-igneous rocks (15 percent), siliceous meta-igneous rocks (10 percent), and gneisses (5 percent). The basement rocks upon which the section was deposited have not been found. The thickest preserved sections (10-13 km) occur in the northern Manzano and central San Andres Mountains. Granitic rocks range from granodiorite to syenite in composition, with quartz monzonite predominant. Individual plutons are syntectonic to post-tectonic and have been emplaced at depths less than 10 km. Foliation strikes north-northwest to north-northeast, and the only large fold exposed in the region is a syncline in the southern Manzano Mountains. In many areas evidence exists for at least two major periods of Precambrian deformation. Metamorphic rocks range in grade from the lower greenschist to the amphibolite facies. Geochemical model studies suggest that the Precambrian tholeiites were produced by partial melting of lherzolite in the upper mantle and that the granitic rocks were produced by partial melting of siliceous granulites in the lower crust. Magmatism and sedimentation began by 1.7 b.y. ago; major plutonism, deformation, and regional metamorphism occurred between 1.0 and 1.5 b.y. ago. The Precambrian rock association in central and south-central New Mexico bears a resemblance to associations found in young continental rift systems. A model of an evolving multiple-rift system that developed in response to an ascending mantle plume or plumes is proposed for this region between 1.0 and 1.9 b.y. ago. Basaltic magmas are derived directly from the plume; extensive heating of the lower crust produces granitic magmas. Quartzite-arkosite-shale successions are deposited in subsiding rift basins by the erosion of nearby uplifted blocks.

Introduction

Precambrian rocks exposed in the cores of the principal mountain ranges in New Mexico and west Texas are among the few surface exposures of three Precambrian crustal provinces extending across the central United States (fig. 1). Rb-Sr-whole-rock-isochron and U-Pb-zircon dates in the range of 1.65-1.9 b.y. define a province extending from southern California and Sonora to Wisconsin. Dates between 1.2 and 1.65 b.y. suggest the existence of another province extending from central New Mexico to Illinois south of and partially overlapping the 1.65-1.9-b.y. province. Existing data also indicate the presence of a third province extending from west Texas possibly as far east as Ohio, characterized by 1.0-1.3-b.y. dates. This report synthesizes and interprets available geologic and geochemical data from exposed Precambrian rocks in central and south-central New Mexico (fig. 2). The rocks studied represent the principal exposures of the 1.2-1.65-b.y. province.

From oil tests penetrating the Precambrian basement in west Texas and eastern New Mexico and from surface exposures of Precambrian rock, basement terranes can be characterized by specific rock types or rock associations. Existing data from surface exposures and from some well data in the remainder of New Mexico suggest that most of the state is underlain by a terrane composed of granitic (70 percent) and low- to medium-grade metamorphic rocks (30 percent). Basement terranes in New Mexico are shown in fig. 3. Most of the area covered by this report is underlain by the granitic-metamorphic terrane. The southeastern area is underlain by clastic sediments of the De Baca terrane, which is locally intruded by the Pajarito syenite complex north

east of Alamogordo. The Franklin Mountains igneous terrane may underlie a small area along the southeastern border; its relationship to the De Baca terrane is unknown.

The largest exposure of Precambrian rocks in central and south-central New Mexico occurs in the core and along the western escarpment of the Sandia, Manzanita, Manzano, and Los Pinos Mountains south of Albuquerque (sheet 1). This exposure, bounded by young high-angle normal faults on the west (adjacent to the Rio Grande rift) and by high-angle Laramide thrusts and/or the Phanerozoic unconformity on the east, will be referred to here as the SMP block. The block is characterized by a northeast-striking section of phyllite-schist, quartzite, and siliceous and mafic meta-igneous rocks metamorphosed to the upper greenschist or lower amphibolite facies. The Phanerozoic unconformity is best exposed along the crest of the Sandia Mountains and in the vicinity of Bosque Peak in the Manzano Mountains. At these locations, the Sandia Formation (Pennsylvanian) overlies the Precambrian rocks. The Precambrian section is intruded by one pretectonic or syntectonic granitic pluton (the Manzanita pluton southwest of Albuquerque) and seven late-tectonic to post-tectonic plutons. Precambrian rocks also form the core of the Monte Largo Hills east of the Sandia Mountains. At this location, the Precambrian rocks, principally quartzofeldspathic gneisses and amphibolite, are bordered by Cenozoic faults on the northwest and southeast and are overlain unconformably by the Sandia Formation on the northeast and southwest.

Precambrian rocks are poorly exposed in the Peder-

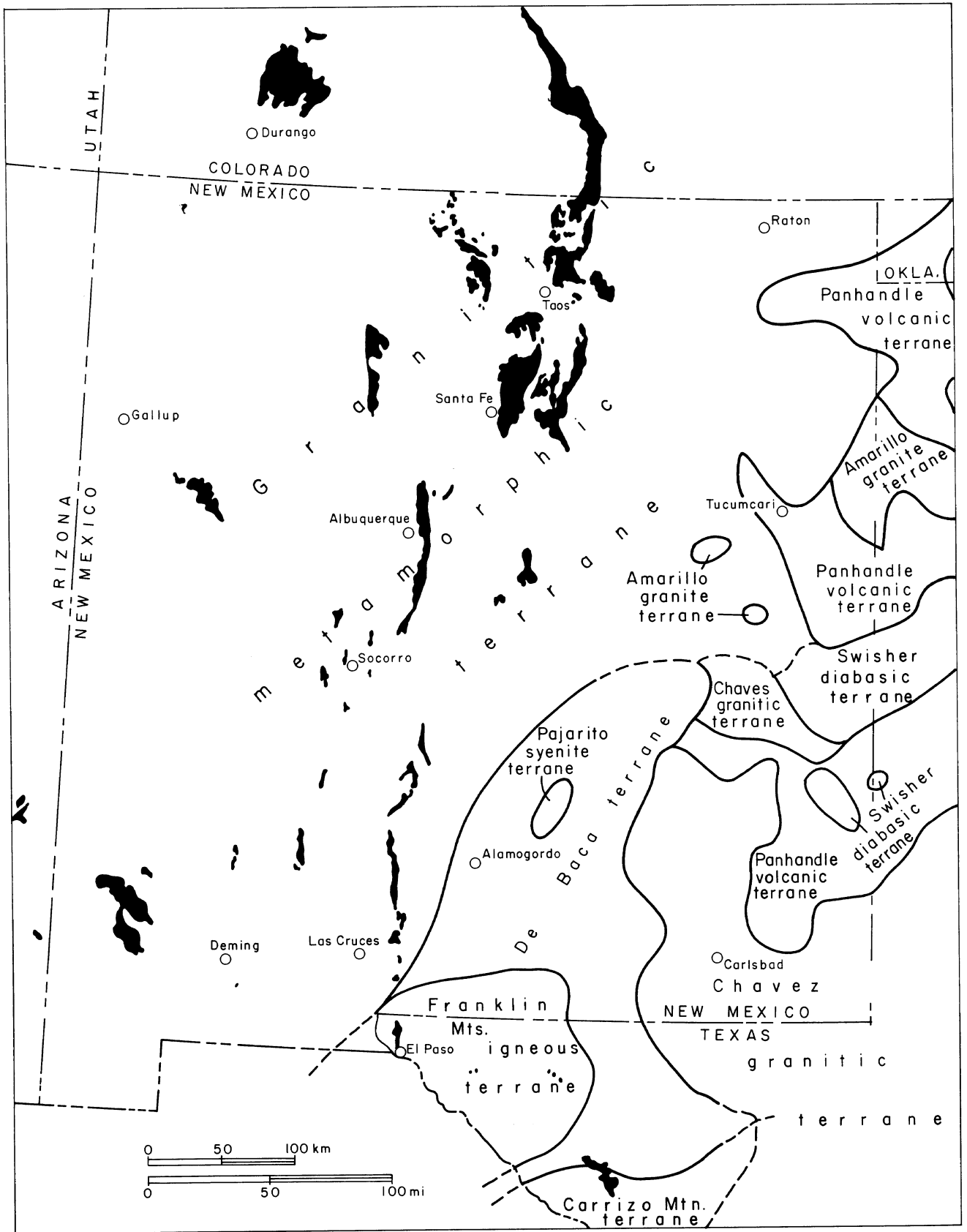


FIGURE 3—PRECAMBRIAN TERRANES IN THE BASEMENT OF NEW MEXICO. (Terranes in eastern New Mexico and west Texas from Flawn, 1956; Muehberger and others, 1967; Denison and Hetherington, 1969; and Foster and others, 1972.)

nal Hills south of Clines Corners (fig. 4 on sheet 2). The Yeso Formation of Permian age here unconformably overlies the Precambrian terrane, characterized by schists, quartzites, and minor amphibolites—all intruded by the Pedernal granitic pluton. Isolated exposures of mica and chlorite schist occur northwest of the Pedernal Hills at Cerrito del Lobo, and small outcrops of granitic rocks are found in the Rattlesnake Hills and in and near the Gallinas Mountains (Perhac, 1964; Kelley, 1972).

Most of the Ladron Mountains southwest of Belen are composed of a structurally complex exposure of quartzites, phyllites, amphibolites, and siliceous metaigneous rocks intruded by two granitic plutons (fig. 5 on sheet 2). Cenozoic faults almost completely surround this range. The unconformity with the overlying Sandia Formation is well exposed at only one location on the extreme northwestern tip of the range. Precambrian rocks also compose the northeastern slope of the Magdalena Mountains west of Socorro (fig. 6 on sheet 2). Here again the Sandia Formation unconformably overlies the Precambrian rocks. Isolated exposures of granitic rocks occur in the vicinity of Socorro along the eastern slope of the Lemitar Mountains (fig. 7 on sheet 2), in the La Joyita and Coyote Hills (figs. 8 and 9 on sheet 2), and in the vicinity of Socorro (Smith, 1963, and fig. 10 on sheet 2).

In the southwestern part of the study area, Precambrian rocks occur along the western escarpment of the Caballo Mountains and in the Red Hills south of Truth or Consequences (fig. 11 on sheet 2). This exposure is bounded by a Cenozoic fault system on the west and by the unconformity with the Bliss Sandstone on the east. The Precambrian terrane in this area is composed dominantly of granitic rocks. In the south-central part of the Caballos, granitic rocks also occur along the northwestern slope of the Fra Cristobal Range north of Truth or Consequences (fig. 12 on sheet 2). They are bounded by a high-angle Cenozoic normal fault on the west and by either steep thrusts or an unconformity with the Magdalena Group (Pennsylvanian) on the east. Isolated exposures occur at San Diego Mountain near Hatch (fig. 13 on sheet 2), northwest of Truth or Consequences, and northwest of the Fra Cristobal exposure in the Sierra Cuchillo (Jahns, 1955).

The second largest exposure of Precambrian rock in the study area is the thin strip along the eastern face of the San Andres Mountains northeast of Las Cruces. Brief descriptions of the Precambrian rocks in this area are given by Kottlowski (1955, 1959) and Kottlowski and others (1956). The exposure is bounded on the east by Cenozoic normal faults (fig. 14) and on the west, most commonly, by the Phanerozoic unconformity (fig. 15). At this unconformity, well exposed at arroyo level in Hembrillo Canyon (fig. 16), the dark-brown Bliss Sandstone of probable Ordovician age overlies the Precambrian section (Kottlowski and others, 1956). Most of the Precambrian rocks in the San Andres Mountains are granitic rocks intrusive into schists, quartzites, and amphibolites.

Similar Precambrian granitic rocks occur along the western escarpment of the Oscura Mountains west of Carrizozo. In this range, the Precambrian rocks are bounded on the west by a Cenozoic normal fault and are

unconformably overlain on the east by Paleozoic formations. With the cooperation of the White Sands Missile Range, the authors have mapped the Precambrian rocks in the San Andres and Oscura Mountains (sheet 3). Two exposures of Precambrian rock (one shown by fig. 17 on sheet 2) occur in the Organ Mountains south of White Sands. In the southeast part of the study area, small isolated Precambrian outcrops are found at Pajarito Mountain near Hondo (fig. 18 on sheet 2), at Bent Dome north of Bent, New Mexico (Denison and Hetherington, 1969), and at the base of the western escarpment of the Sacramento Mountains near Alamogordo (Pray, 1961).

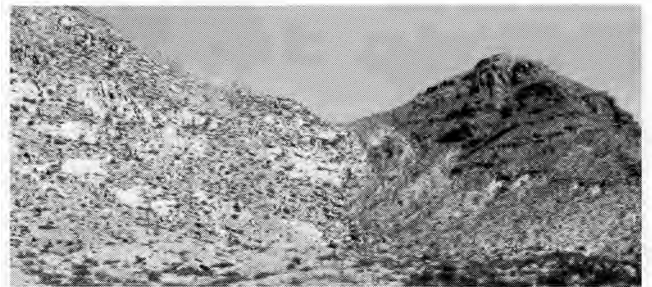


FIGURE 14—NORMAL FAULT ALONG THE EAST SIDE OF THE SAN ANDRES MOUNTAINS NEAR THE ENTRANCE OF JOHNSON PARK CANYON. Fault trace passes through saddle. Light outcrops are granitic rocks of the Capitol Peak pluton; dark layered rocks on the right are Paleozoic.

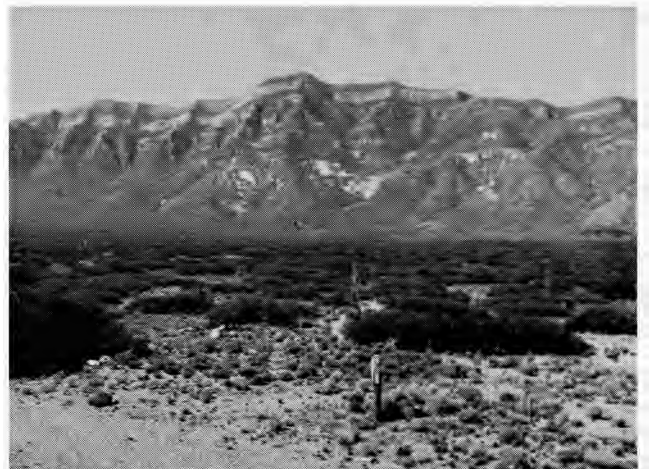


FIGURE 15—SAN ANDRES PEAK IN THE SOUTHERN SAN ANDRES MOUNTAINS VIEWED FROM THE EAST. Paleozoic rocks unconformably overlie the San Andres pluton; unconformity about halfway up the mountain face.



FIGURE 16—PRECAMBRIAN ROCKS IN THE SAN ANDRES AND ORGAN MOUNTAINS. A) Angular unconformity in Hembrillo Canyon; vertical, light-colored Precambrian quartzite overlain by Bliss Sandstone dipping gently to the west. B) Crossbedding in quartzite, Hembrillo Canyon. C) Amphibolite inclusion in Capitol Peak pluton. D) Two ages of aplite dikes cutting granitic rocks of the White Sands pluton.

Metamorphic rocks

Mica-quartz schist and phyllite

Mica-quartz schists and phyllites compose about 40 percent of the metamorphic rocks in the exposed Precambrian of central and south-central New Mexico (table 1). True thicknesses of schist-phyllite sections are difficult to estimate because drag folding has caused thickening. Maximum cumulative thicknesses of about 4 km occur on the western limb of the syncline between Comanche and Monte Largo Canyons in the central Manzano Mountains and in the North Canyon area in the Manzanita Mountains (sheet 1). An exposed thickness of about 3 km occurs in the central Pedernal Hills (fig. 4 on sheet 2) and in the central San Andres Mountains between Sulphur and Howinahell Canyons (sheet 3). A maximum of 1.5 km is exposed in the Blue Springs Muscovite Schist in the Los Pinos Mountains. A section, 3.5 km thick, of mixed schist-phyllite, feldspathic quartzite, and quartzite occurs beneath the angular unconformity at Comanche Canyon in the Manzano Mountains. Smaller amounts of schist and/or phyllite are interlayered with quartzite and amphibolite in the

Ladron Mountains, in the central San Andres Mountains between Hembrillo and Mayberry Canyons, in the Coyote Canyon area and in the Tijeras Greenstone in the northern Manzanita Mountains, in the Coyote Hills west of San Antonio, and in the Magdalena Mountains in and north of Water Canyon. A small exposure (150 m by 2.5 km) of shale-siltstone with minor interbedded quartz sandstone occurs south of Alamogordo along the escarpment of the Sacramento Mountains. The total exposed thickness is only about 25 m (Pray, 1961).

The schist-phyllite sections generally form valleys and embayments or rubbly slopes and are often poorly exposed, such as they are in the Pedernal Hills. The best exposures are in the canyons along the western escarpment of the southern Manzano Mountains. The schists and phyllites are generally fine grained and exhibit well-developed foliation, parallel to or at angles of 15 degrees or less with bedding. They are most commonly gray, light green, or lavender, although locally they are buff or reddish orange. Minor folds are common. Schist and phyllite commonly contain interbedded quartzite or feldspathic quartzite layers, which range from 3 cm to

TABLE 1—RELATIVE PERCENTAGES OF METAMORPHIC ROCKS IN PRECAMBRIAN SECTIONS OF CENTRAL AND SOUTH-CENTRAL NEW MEXICO: tr = trace, — = absent, * = includes corresponding siltites.

Section location	Total thickness Exposed (m)	Quartzite feldspathic quartzite*	Arkosite*	Conglomeratic quartzite and arkosite	Mafic meta-igneous rock	Siliceous meta-igneous rock	Mica-quartz schist and phyllite	Gneiss
Northern Manzanita Mountains	4,100	28	5	0	45	1	6	15
Northern Manzano Mountains	12,000	4	14	tr	23	tr	59	0
Central Manzano Mountains (west)	5,830	20	6	tr	5	19	50	0
Central Manzano Mountains (east)	3,200	43	15	tr	12	16	8	0
Northern Los Pinos Mountains	3,610	26	5	tr	6	23	40	0
Northern Pedernal Hills	6,500	37	tr	tr	20	0	43	tr(?)
Ladron Mountains	4,660	13	21	10	12	34	10	0
Magdalena Mountains	1,650	45	50	2	3	tr	tr	0
Central San Andres Mountains	9,500	8	38	tr	11	tr	43	0
Weighted average of sections 1 and 2		10	12	tr	30	tr	43	4
Weighted average of sections 3 to 9		23	18	1	11	11	36	0

100 m thick and taper laterally. Chloritoid porphyroblasts are common in schist samples from the Ladron Mountains and from the mixed section beneath the Precambrian unconformity at Comanche Canyon in the Manzanos. Almandite porphyroblasts are uncommon. Relict graded bedding in phyllitic siltstones occurs in the Blue Springs Muscovite Schist in the southern Los Pinos Mountains (Beers, 1976) and in the mixed metaclastic section beneath the central Manzano unconformity. In Hembrillo Canyon in the San Andres Mountains, a thin talc bed (1-5 m thick) is conformably interbedded with the major phyllite unit crossing the canyon (sheet 3). The talc layer has sharp contacts with the surrounding phyllites. Although the origin of this bed is unknown, existing data favor an origin by decarbonation of a siliceous dolomite bed or recrystallization of a montmorillonite-rich volcanic unit during low-grade metamorphism.

Locally schists and phyllites are highly sheared and mylonitized—for instance, in parts of the Pedernal section and in the Sulphur Canyon area in the central San Andres Mountains. Varying stages in the production of boudins from thin quartzite beds within a dominantly mica-schist section can be observed near Sulphur Canyon. The boudins are rounded and randomly dispersed through the schist matrix about 2 km southwest of Strawberry Peak. The resultant rock superficially resembles a metamorphosed pebbly mudstone. In the mixed metaclastic section beneath the angular unconformity in the central Manzanos, mica-quartz-chloritoid schists and phyllites (40 percent) are intimately associated with medium- to coarse-grained arkosite, feldspathic quartzite, and quartzite (60 percent), Channel-fill deposits and crude graded bedding occur in some of the units. Locally, quartz veins crosscut schist-phyllite succession.

In the southern Manzano and Los Pinos Mountains, the mica-schist-phyllite unit—the thickest and most continuous exposure in New Mexico—has been named the Blue Springs Muscovite Schist (Stark and Dapples, 1946). This formation is exposed on the east and west limbs of a syncline extending from the southern Los Pinos to the central Manzano Mountains (sheet 1). Because of faulting along the Paloma thrust, the thickness of the formation on the eastern limb of the syncline ranges from 100 to 1,500 m (Stark and Dapples, 1946; Stark, 1956; Beers, 1976). The large thickness on the western limb in the central Manzanos probably results from tectonic thickening during folding.

The small exposure of fine-grained clastic sediments unconformably underlying the Bliss Sandstone along the Sacramento escarpment (Pray, 1961) is unique because the rocks are unmetamorphosed. Mud cracks are present; and sandy units are well sorted, often exhibiting crossbedding and containing very little detrital feldspar. This section is probably late Precambrian in age.

Mica-quartz schists and phyllites are composed chiefly of quartz and muscovite with minor and variable amounts of plagioclase, epidote, magnetite-hematite, chloritoid, and biotite (table 2 and fig. 19). In quartz content, they are gradational with quartz schists and quartzites. In thin section, the schists and phyllites generally exhibit well-developed penetrative foliation or

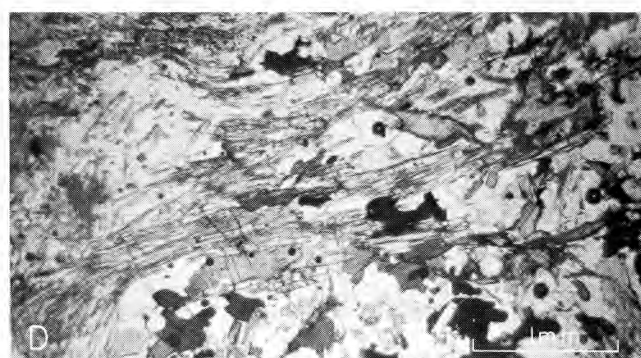
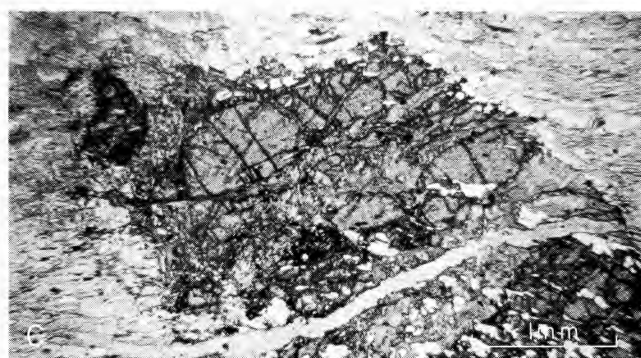
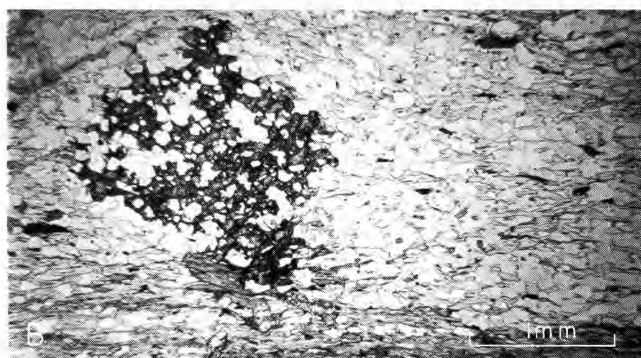
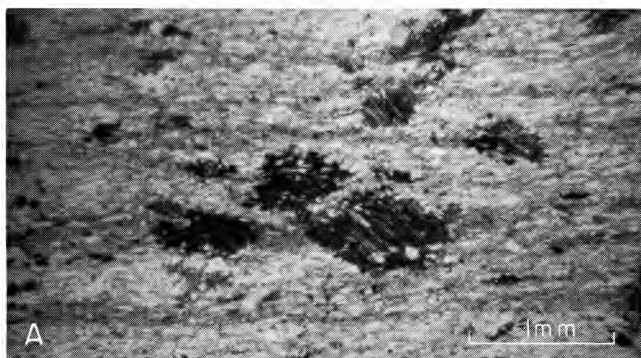


FIGURE 19—PHOTOMICROGRAPHS OF SCHISTS AND GNEISSES. A) Quartz-muscovite schist (NP-73, NP-74); from the Blue Springs Muscovite Schist near Parker Ranch, Los Pinos Mountains. Fine-grained quartz and muscovite with several large cross-biotite grains (dark); uncrossed polars. B) Garnet-muscovite schist (SANA-132); Sulphur Canyon, San Andres Mountains. Poikiloblastic garnet in a matrix of quartz and muscovite; uncrossed polars. C) Garnet-muscovite schist (SANA-132); Sulphur Canyon, San Andres Mountains. Partially chloritized garnet grain cut by quartz veinlet in matrix of quartz and muscovite; uncrossed polars. D) Sillimanite-biotite gneiss (SANA-145); inclusion in quartz monzonite, Cottonwood Canyon, San Andres Mountains. Elongated sillimanite needles with biotite (gray to black), quartz, and microcline; uncrossed polars.

TABLE 2-MODAL ESTIMATES IN PRINCIPAL PRECAMBRIAN METAMORPHIC ROCKS FROM CENTRAL AND SOUTH-CENTRAL NEW MEXICO; mean values given with ranges in parentheses.

	Gneiss	Quartzite	Feldspathic quartzite and arkosite	Mica-quartz schist and phyllite	Mafic meta-igneous rocks	Siliceous meta-igneous rocks
quartz	35 (20-50)	95 (90-100)	75 (50-90)	55 (50-80)	10 (2-30)	25 (10-40)
plagioclase	30 (5-35)	2 (0-5)	5 (5-20)	2 (0-10)	15 (2-50)	30 (25-40)
K-feldspar	20 (5-50)	2 (0-5)	15 (5-40)	tr (0-1)	0 (0-tr)	40 (20-50)
muscovite	5 (5-50)	1 (0-20)	5 (tr-10)	38 (10-80)	tr (tr-2)	1 (0-5)
biotite	3 (0-20)	tr (0-10)	tr (0-5)	1 (0-20)	1 (tr-5)	1 (0-5)
hornblende-actinolite	tr (0-5)	tr (0-40)	tr (0-10)	0	63 (60-95)	tr (0-5)
chlorite	tr	tr (0-tr)	tr (0-tr)	tr (0-20)	3 (tr-20)	tr (tr-1)
epidote	tr (0-5)	tr (0-3)	tr (0-3)	1 (0-10)	5 (0-50)	1 (tr-5)
magnetite-hematite	1 (tr-3)	tr (tr-3)	1 (tr-3)	1 (tr-2)	2 (tr-10)	1 (tr-2)
carbonate	0 (0-tr)	0 (0-tr)	0 (0-tr)	0 (0-tr)	tr (tr-5)	tr
sillimanite	tr (0-20)	0 (0-tr)	tr (0-10)	tr (0-5)	0	0
kyanite	0 (0-10)	tr (0-2)	0 (0-tr)	tr (0-3)	0	0
andalusite	tr (0-5)	tr (0-1)	0 (0-1)	tr (0-10)	0	0
staurolite	0	tr (0-2)	0	0	0	0
sphene	tr (0-tr)	0	0	0 (0-tr)	tr (0-1)	0
zircon	tr	tr	tr	tr (0-tr)	0	0 (0-tr)
rutile	tr	tr	tr	tr	0	tr
apatite	tr	tr	tr	tr	tr (0-tr)	tr
prehnite	0	0	0	0	tr (0-2)	0
tourmaline	tr (tr-1)	tr (0-1)	tr	tr (0-tr)	tr (0-tr)	0 (0-tr)
garnet	0 (0-tr)	0 (0-tr)	0 (0-tr)	tr (0-2)	tr (0-tr)	0
pyrite	0 (0-tr)	0 (0-tr)	0 (0-tr)	0 (0-tr)	tr (0-tr)	0 (0-tr)
stilpnomelane (?)	0	0	0	0	0 (0-1)	0 (0-tr)
chloritoid	0	0	0	1 (0-5)	0	0
limonite	tr	tr	tr	tr	tr	tr

cleavage. Some specimens exhibit fracture cleavage developed at steep angles to flow cleavage; others exhibit microfolds. Minor veinlets of epidote and quartz occur in some samples. Quartz grains, usually 0.1 mm or less in size, are generally xenoblastic and show a range of fabrics from decussate to well foliated. Mortar and flaser structures occur in some samples, and most quartz exhibits undulatory extinction. Plagioclase (An₂₀ to An₃₀) has a similar occurrence and generally exhibits incipient saussuritization. Micas range from ≤ 0.1 to 1 mm in length and are generally subparallel to foliation. Rare porphyroblasts of biotite range up to 6 mm in size. Biotite crystals are often partially chloritized and probably reflect retrograde metamorphism. Cross-micas are found in some areas such as the central Manzano and Los Pinos Mountains (fig. 19), and their presence attests to more than one period of metamorphism. Some cross-micas possibly formed in contact metamorphic aureoles during emplacement of granitic plutons; however, a spatial relationship between cross-mica distribution and granitic plutons is not apparent from existing data. Chlorite occurs in veinlets and as irregularly shaped crystals intergrown with micas. Epidote and magnetite occur as small, randomly dispersed grains. In some samples, magnetite crystals crosscut foliation and so appear to be postkinematic. Chloritoid porphyroblasts ranging in size from 1 mm to 1 cm characterize many of the schists and phyllites in the Los Pinos, Manzano, and Ladron Mountains. Many of these crystals also crosscut foliation and so appear to be postkinematic. Almost all are poikiloblastic, and partial to complete sericitization is common. Very small garnet

porphyroblasts (≤ 0.5 mm) occur in a few schists in the Manzano and Los Pinos Mountains; larger, partially chloritized garnets occur in mica schists in the San Andres Mountains (fig. 19). Kyanite has been reported in the Blue Springs Muscovite Schist at one locality in the Los Pinos Mountains (Mallon, 1966). Zircon, rutile, and apatite are rare; when found, they seem to be of detrital origin. Limonite occurs around some magnetite-hematite grains. Needlelike crystals of tourmaline and fibrous sillimanite occur in schists ranging 150 to 350 m from the southern border of the Priest pluton (Stark and Dapples, 1946; Basham, 1951). These minerals have formed in a contact metamorphic aureole adjacent to the pluton.

Quartzite and related rocks

Quartz-rich metasedimentary rocks can be grouped as quartzite (≥ 5 percent feldspar), feldspathic quartzite (5-25 percent feldspar), and arkosite (> 25 percent feldspar) and fine-grained equivalents (siltite, feldspathic siltite, and arkosic siltite); conglomeratic quartzite (and arkosite); and associated quartz and quartz-mica schists. Rocks of this group, principally feldspathic quartzite and arkosite, compose from 20 to 40 percent of the metamorphic sections in central and south-central New Mexico (table 1). The principal occurrences, with corresponding estimates of cumulative thickness, are: Manzano and Los Pinos Mountains (0.5-1.2 km), central San Andres Mountains between Hembrillo Wash and Mayberry Canyon (~ 5 km), western Ladron Mountains (3 km), northern Pedernal Hills (2.5 km),

Rincon Ridge in the northern Sandia Mountains (≤ 2.1 km), and Coyote Canyon in the northern Manzanita Mountains (1.5 km). In addition, about 1 km or more of interbedded siltite and metatuff is exposed in the Water Canyon area of the Magdalena Mountains. Other exposures of quartzite and arkosite are found in the central San Andres Mountains 5 km north of Gunsight Peak, 2.5 km east of Black Top Mountain, and 4 km north-northeast of Goat Mountain; in the northern part of the Monte Largo Hills, where one massive white quartzite bed about 300 m thick strikes northeasterly; in the central part of the Lemitar Mountains (well exposed in Corkscrew Canyon); and in the Coyote Hills west of San Antonio.

Members of the quartzite group generally form ridges and hogbacks and for the most part are well exposed (fig. 20). The rocks are usually white to buff, although red, orange, gray, and purple beds are locally important. Most units are massive, and individual beds range from 2 cm to 1 m thick. Quartz and quartz-mica schists have well-developed foliation and are gradational with massive beds. Small seams and fracture fillings of specular hematite are common in some of the massive quartzites. These seams and fillings are particularly well developed in the northern Pedernal Hills (Gonzalez, 1968) and in the central Manzano Mountains. At these localities, seams ranging from a few millimeters to two centimeters thick can be followed along strike for many meters. Although the origin of the seams is poorly understood, they may represent recrystallized magnetite-rich sand formed by metamorphic differentiation (Barker, 1968). Crossbedding is well preserved in feldspathic quartzites and arkosites of the Ladron Mountains and the central San Andres Mountains (fig. 16B). Although rare and often difficult to recognize because of deformation, crossbedding has also been observed in the Manzano, Los Pinos, and Magdalena Mountains (Stark and Dapples, 1946; Stark, 1956; Beers, 1976). Planar crossbedding is most common and occurs in beds 10-50 cm thick. Some of the best exposures of festoon crossbedding occur in arkosites and feldspathic quartzites. Pull-apart structures gradational with intraformational conglomerate also occur on this ridge.

Poorly sorted to moderately well sorted arkosites and feldspathic quartzites dominate in the following areas: in the lower parts of the Ladron and central San Andres Mountain sections, in the Rincon Ridge section in the northern Sandia Mountains (Hayes, 1951), in the mixed metaclastic section beneath the unconformity at Comanche Canyon in the central Manzano Mountains (Reiche, 1949), in the upper part of the White Ridge Formation and lower part of the Sevilleta Formation in the southern Manzano and in the Los Pinos Mountains (Stark, 1956; Beers, 1976), in the northern Manzanita Mountains on the south side of Coyote Canyon, in Corkscrew Canyon in the central Lemitar Mountains (Woodward, 1973), and in the Magdalena Mountains. The Magdalena Mountains section is composed dominantly of interbedded feldspathic siltites and quartzitic argillites, which seem partly to represent metatuffs.

Conglomeratic quartzites are rare; when found they occur as thin layers (1-10 cm thick) within massive

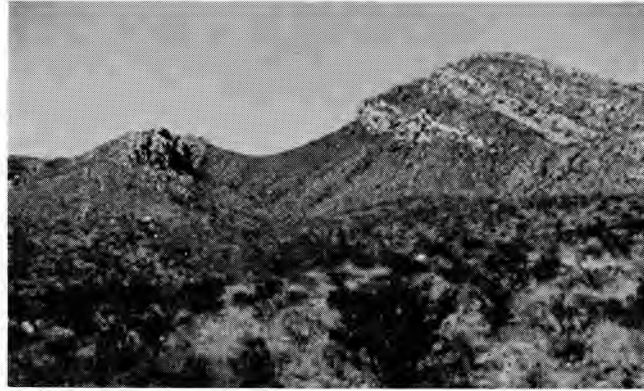


FIGURE 20—RIDGE ON NORTH SIDE OF HEMBRILLO CANYON, SAN ANDRES MOUNTAINS. Note quartzites (light rock) and metadiabase sill (in saddle).

quartzite or feldspathic quartzite beds. Clasts are usually well-rounded granules and pebbles of quartzite and quartz. In the middle part of the Ladron section, several stretched-pebble conglomeratic units occur. Clasts range in size up to 30 cm (averaging 2-5 cm) and are composed predominantly of quartzite with smaller amounts of orange granite, mica schist, amphibolite, and minor siliceous meta-igneous fragments. In the Magdalenas, several thin tuffaceous units contain small clasts (2 mm-1 cm in size) that may represent recrystallized and deformed pumice fragments.

Two massive white quartzite units extending from the southern Los Pinos to the central Manzano Mountains are the Sais Quartzite and the White Ridge Formation (Stark and Dapples, 1946, and sheet 1). The Sais Quartzite, the oldest exposed unit on the eastern limb of the southern Manzano syncline, ranges from 200 to 600 m thick and is bordered on the east by the steeply dipping Montosa fault. This unit is well exposed in Sais Quarry, located about 3 km northeast of the intersection of US-60 and NM-6 in the southern Manzano Mountains. The Sais Quartzite is composed of beds 1-2 m thick and is gradational with the overlying Blue Springs Muscovite Schist. The White Ridge Formation overlies the the Blue Springs Muscovite Schist and is characterized by a lower massive white quartzite (200-600 m thick) overlain by feldspathic quartzites and mica-quartz schists grading upwards into the Sevilleta Formation (Stark, 1956). The feldspathic quartzite section changes from 600 m to 100 m in thickness going from the Capilla Peak area to south of Manzano Peak (Stark, 1956). Although similar in appearance to the Sais Quartzite, the lower quartzite unit contains individual beds more variable in thickness (2 cm to 1 m). Except that detrital feldspar is rare in the quartzites of the Pedernal and Monte Largo Hills and of the northern Manzanita Mountains, the quartzites are lithologically similar to those of the Sais and White Ridge Formations.

Although quartzites are divided into two categories in table 2 (based chiefly on feldspar content), the divisions are somewhat arbitrary because a complete range in feldspar/quartz ratios exists between them. Most samples exhibit some preservation of original sand grains, which range typically from rounded to sub-rounded. Sorting is variable, ranging from typically moderate or fair to—less commonly—poor. Most

grains fall in the range of 0.1 mm to 1 mm in size; the siltites from the Magdalena Mountains, however, exhibit grain sizes ≤ 0.1 mm. Banding, which probably reflects original bedding, is observed in some thin sections. A distinctive feldspar-quartz matrix is present in some samples from the Ladron, San Andres, and northern Manzano Mountains. Foliation ranges from well developed to absent. Microfolding is locally present and is accentuated in the Pedernals by thin specular hematite bands (Gonzalez, 1968). Microboundins of quartzite as well as of quartzite augen occur in highly sheared samples from the Los Pinos-Manzano and Ladron Mountains. Some quartz grains are highly stretched ($\sim 10:1$) in the planes of foliation (fig. 21). Broken and cracked quartz and feldspar grains reflect late cataclastic deformation. Quartz and epidote veinlets reflect late-stage alteration.

Quartz is the most abundant mineral in most members of the quartzite group and occurs in both silt- and sand-size ranges. Subrounded to rounded sand grains are common; in detail, however, grain borders are usually sutured (fig. 21B). Suturing and grain deformation are locally intense—for example, in quartzites from the northern Manzanita Mountains. Undulatory extinction is pervasive, and flaser and mortar structures are locally developed.

Although both plagioclase and K-feldspar occur in most arkosites and feldspathic quartzites, one usually dominates. They occur as obvious clastic grains with subangular to subrounded borders (fig. 21C) and as crystalloblastic grains. Plagioclase grains are usually partly saussuritized and sometimes poikiloblastically enclose quartz. Rapidly tapering and bent albite twins in most samples reflect deformation. Compositions seem to be bimodal, grouping around An_{5-10} and An_{20-25} , and suggest that the rocks recrystallized below the peristerite solvus. Plagioclase forms up to 20 percent of some of the White Ridge Formation. Microcline with well-developed gridiron twinning is a major constituent in arkosites from the Ladron and northern Sandia Mountains (Juan Tabo sequence) and composes typically from 30 to 40 percent of the rock. Sieve textures are common in many of the large microcline grains, and micrographic and perthitic textures are common in samples from the Ladrons.

Muscovite and/or biotite, usually well oriented in foliation planes, are ubiquitous constituents of most members of the quartzite group (fig. 21D). Some samples in the Los Pinos-Manzano and Ladron Mountains contain cross-micas produced after the major regional metamorphism. Chlorite occurs in irregular patches and as pseudomorphs after biotite. Magnetite and specular hematite are common accessories and often form idioblastic crystals that crosscut foliation. Although hornblende is absent in most samples, it composes up to 40 percent of the rock in a few quartzites (≤ 5 percent) of the Los Pinos, Ladron, and Lemitar Mountains. These hornblende quartzites, which might be more appropriately referred to as para-amphibolites, exhibit prominent banding both in the field and in thin section (scale of one millimeter to several centimeters). This banding, together with the presence of subrounded quartz grains, attests to the sedimentary parentage of these rocks.

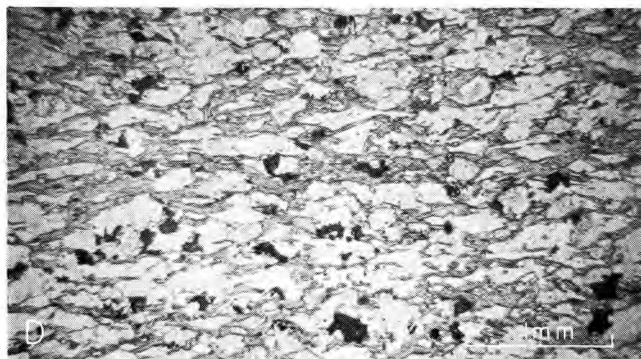
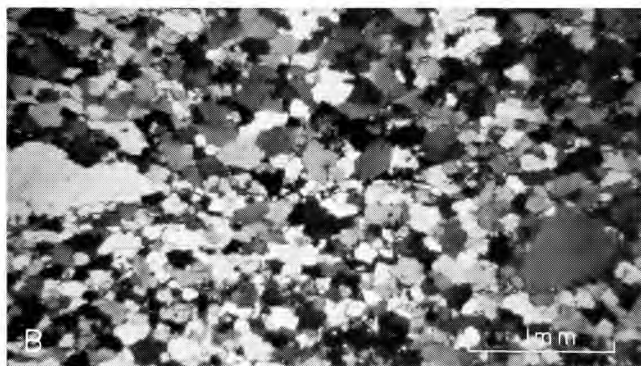
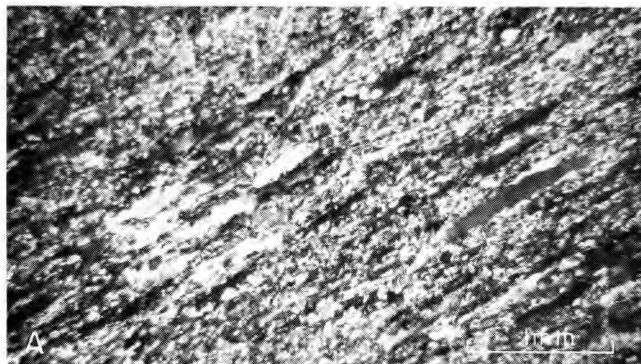


FIGURE 21—PHOTOMICROGRAPHS OF QUARTZITE, ARKOSITE, AND RELATED QUARTZ-RICH ROCKS. A) Quartzite tectonite (MZ-22); Monte Largo Canyon, Manzano Mountains. Note highly sheared and recrystallized quartz grains; crossed polars. B) Quartzite (SANA-99B); mouth of Hembrillo Canyon, San Andres Mountains. Note sutured boundaries of quartz grains; crossed polars. C) Arkosite (LD-19F); Ladron Mountains. Note subangular shapes of feldspar clasts and poor sorting; crossed polars. D) Quartz-muscovite schist (MZ-4); Cañon del Trigo, Manzano Mountains. Elongate quartz grains associated with muscovite and minor epidote (small dark grains); uncrossed polars.

In most members of the quartzite group, disseminated epidote grains commonly occur in trace amounts. Kyanite porphyroblasts (0.5-1 mm in size) are reported from quartzites in the Pedernal and central Manzano Mountains (Gonzalez, 1968; Stark, 1956; Anderson, 1948). Idioblastic staurolite grains, which crosscut foliation in quartz-muscovite schists in the Pedernals (Gonzalez, 1968), represent the only documented staurolite occurrence in the Precambrian terranes of central and southern New Mexico. Fibrous sillimanite and poikilo-blastic andalusite of contact metamorphic origin occur in the feldspathic quartzites of the Juan Tabo sequence adjacent to the North Sandia pluton in the northern Sandia Mountains. Zircon, tourmaline, and/or garnet grains (≤ 0.1 mm in size), some of probable detrital origin, occur in most quartzites. Rutile and apatite occur within detrital quartz grains. Pyrite is rare and forms idioblastic crystals. Some tourmaline occurs as needles (0.05-0.1 mm long), suggesting a metamorphic origin. Traces of carbonate and quartz cement occur in some samples from the Manzanita and San Andres Mountains.

Rock fragments vary in abundance in members of the quartzite group. In thin section, they are chiefly siltite and quartzite with traces of fine-grained schist and metavolcanic (?) fragments. Siltite and quartzite rock fragments are particularly abundant in the feldspathic quartzites of the Ladron Mountains, where they compose up to 35 percent of the rocks. In these samples, the quartzite grains are typically subrounded and associated with coarse detrital microcline and microcline-quartz grains that probably represent granitic rock fragments.

Mafic meta-igneous rocks

Included in this category are orthoamphibolite, chlorite schist, metadiabase, and metagabbro. Orthoamphibolites here include all mafic rocks of probable igneous parentage where hornblende and plagioclase are major constituents and where relict igneous textures are lacking. If chlorite (\pm epidote, \pm actinolite) is the major mafic phase, the rocks are called chlorite schists. Metadiabase and metagabbro exhibit relict ophitic to subophitic textures; metadiabase usually occurs as dikes or sills. The term greenstone is used here in a very general sense to include some combination of the four rock types described above. All of the textural and mineralogical varieties are closely associated and gradational with each other in the greenstone complexes of the Manzanita Mountains.

Four major occurrences of dominantly orthoamphibolite are found in the Precambrian terranes of central and south-central New Mexico. The most extensive exposure occurs east of Salinas Peak in the central San Andres Mountains, where a minimum of 3 km of massive to foliated amphibolite is exposed (sheet 3). This section is also characterized by quartzo-feldspathic migmatitic and pegmatitic components that crosscut the amphibolites and by quartz-feldspar-biotite gneisses interlayered with the amphibolites. The original section is tentatively interpreted as a succession of mafic sills and/or flows with some interlayered granitic sills. The second occurrence is found in the southern Caballo Mountains between Longbottom and Burbank Canyons

(fig. 11 on sheet 2). The overall character of this occurrence is strikingly similar to the Salinas Peak exposure. The third exposure, the Tijeras Greenstone, forms a northeasterly striking belt about 1.7 km wide by 9 km long in and south of Tijeras Canyon in the northern Manzanita Mountains (sheet 1). This formation is composed of intimately associated amphibolites and chlorite schists and greenstones interlayered, in part, with minor amounts of quartzite, mica schist, marble, and siliceous meta-igneous rocks (Bruns, 1959). Amphibolites dominate in the section, which is about 2 km thick. The fourth major occurrence is found in the Hell Canyon area in the southern Manzanita Mountains and is similar in many respects to the Tijeras Greenstone. The major difference is a larger proportion of interlayered mica schists and phyllites in the Hell Canyon section.

Amphibolite interlayers ranging from 1 to 100 m thick also occur in the quartzites and siliceous meta-igneous rocks in the Manzano, Los Pinos, Lemitar, and Ladron Mountains and in the central San Andres Mountains from Grapevine to Mayberry Canyon. Amphibolites continue southward from Mayberry Canyon to San Andres Peak as inclusions of varying sizes in the granitic rocks (fig. 16C). An amphibolite unit also occurs on the south side of the Monte Largo Hills (sheet 1), and minor amphibolite units occur interlayered with quartzite and/or schist in the Pedernal Hills and in the Manzanita Mountains. Amphibolite and chlorite-epidote schist units compose up to 10 percent of the Juan Tabo sequence in the northern Sandia Mountains (Hayes, 1951). Amphibolites are also a minor component in the quartzo-feldspathic gneiss terranes discussed later.

Individual amphibolite and chlorite-schist beds are typically 1-10 m thick, ranging to 100 m. They are broadly lensoid in shape, tapering laterally over a few hundred meters. Most units are concordant with surrounding beds. Some, however, are distinctly discordant or have discordant apophyses indicating an origin as mafic dikes and sills. Contacts are often sharp, but may be gradational with siliceous meta-igneous rock units over a few centimeters. Megascopically, the rocks are black to dark green with textures ranging from massive to very schistose, sometimes within the same amphibolite unit. In some places, such as the southern Manzano Mountains (Stark, 1956), they contain inclusions of siliceous meta-igneous rock and diorite, again suggesting an igneous origin. In a few units, lens-shaped plagioclase crystals 2-5 mm in size occur in a fine-grained hornblende-rich matrix; the crystals are reminiscent of relict phenocrysts. Pillow structures, obvious relict amygdules and vesicles, flow breccias, or other structures indicative of an extrusive origin were not found by the authors. In the Tijeras Greenstone and in the greenstones of the Hell Canyon area, epidote patches and veins, quartz veins, and occasional carbonate veins are found. In some of the amphibolites, such as those in the south-central Ladron Mountains, the rocks are uniformly banded over distances of tens of meters. Light-colored, fine-grained quartzo-feldspathic bands, probably representing recrystallized siliceous meta-igneous rock as indicated by relict phenocrysts, are intimately interlayered with these amphibolite bands.

Metadiabase has two common occurrences: 1) units within greenstone complexes ranging from concordant to locally discordant and 2) mafic dikes, sills, and plugs that crosscut various metamorphic and granitic rocks. Crosscutting mafic dikes occur in all of the major Precambrian exposures shown in fig. 2. Although some of the dikes may be Phanerozoic, most are slightly metamorphosed and hence appear to be Precambrian. Excellent examples of dikes that do not penetrate the Phanerozoic unconformity occur on the east side of Capitol Peak and in the Salinas Peak amphibolite complex in the northern San Andres Mountains. Precambrian metadiabase sills 50-250 m thick occur in the Hembrillo-Grandview Canyon area in the San Andres Mountains (sheet 3 and fig. 20) and in and north of Water Canyon in the Magdalena Mountains (fig. 6 on sheet 2). Diabase sills also intrude the unmetamorphosed clastic sediments in the Sacramento escarpment exposure (Pray, 1961).

Two major metagabbro bodies have been reported in the Precambrian terrane of central New Mexico. One occurs in the Magdalena Mountains between Garcia and Jordan Canyons (fig. β on sheet 2) and the other in the central Lemitar Mountains (fig. 7 on sheet 2). The Magdalena body exhibits an intrusive contact with quartzitic argillites and siltites and is intruded by the Magdalena pluton. Smaller satellite bodies occur north of Jordan Canyon, north of North Fork, and east of Kelly. The Lemitar body is intrusive into an amphibolite-quartzite sequence exposed in Corkscrew Canyon and intruded by the Polvadera pluton. Inclusions of older metasedimentary rocks occur in both bodies.

Mafic meta-igneous and associated rocks range from dark green to black and from coarse to fine grained. Foliation varies from well developed in chlorite and chlorite-amphibole schists to completely absent in some of the metadiabases and in the metagabbros. The rocks commonly weather into rounded slopes or valleys with the only good exposures often restricted to arroyo bottoms or steep cliffs. In the Tijeras Greenstone, the rocks are typically cut by small epidote and quartz veins and sometimes by carbonate veins.

Mafic meta-igneous rocks show a considerable range in mineral proportions as indicated in table 2. Hornblende or actinolite are dominant in all samples with the proportions of quartz, sodic plagioclase and epidote varying considerably (fig. 22). Relict subophitic to ophitic textures occur in the coarse-grained metagabbro bodies in the Magdalena and Lemitar Mountains and in metadiabase sills in the Hembrillo Canyon area of the central San Andres Mountains. At these locations pseudomorphs of hornblende after clinopyroxene are penetrated by small saussuritized sodic plagioclase crystals (fig. 22). Relict porphyritic textures characterized by partially saussuritized plagioclase phenocrysts (3-5 mm long) in a hornblende-plagioclase-quartz groundmass occur in the San Andres Mountains on the south side of Capitol Peak and in the Ladron Mountains. Phenocrysts of clinopyroxene now completely replaced by hornblende occur in one sample of greenstone from the Hell Canyon area in the Manzanita Mountains. Metamorphic textures and structures characterize most of the mafic meta-igneous rocks. Textures range from decussate to well foliated. Metamorphic

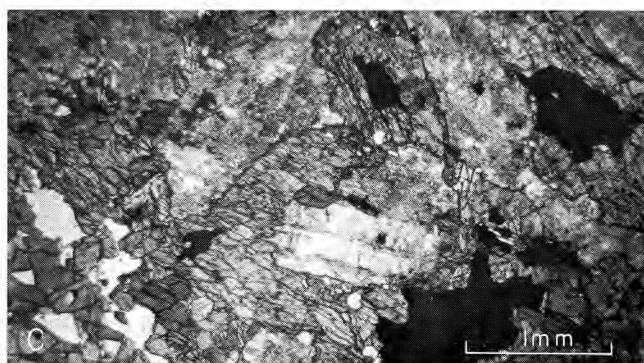
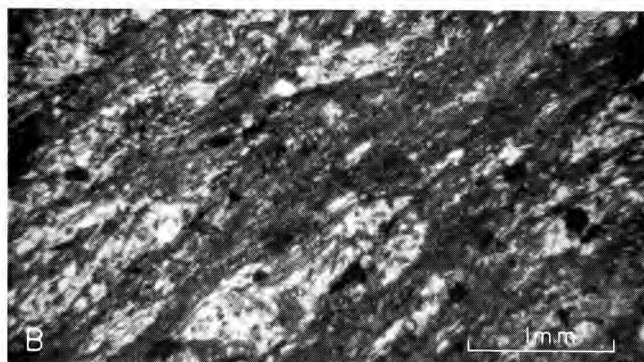
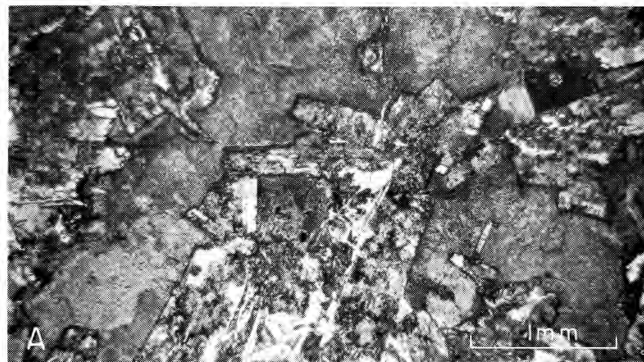


FIGURE 22--PHOTOMICROGRAPHS OF MAFIC META-IGNEOUS ROCKS. A) Metadiabase (SANA-120); from sill in Hembrillo Canyon, San Andres Mountains. Small saussuritized plagioclase crystals and amphibole pseudomorphs after pyroxene. Note preservation of subophitic texture; uncrossed polars. B) Amphibolite (MZ-6); Monte Largo Canyon, Manzano Mountains. Acicular actinolite crystals and sodic plagioclase; uncrossed polars. C) Amphibolite (SANA-17); from amphibolite complex east of Salinas Peak, San Andres Mountains. Green hornblende (gray with cleavage), sodic plagioclase partially saussuritized, ilmenite (black), and quartz (lower left); uncrossed polars. D) Amphibolite (SANA-69); from inclusion in San Andres pluton, San Andres Mountains. Well-crystallized hornblende (gray), plagioclase (white with alteration), quartz (white), and magnetite (black); uncrossed polars.

minerals range from poikiloblastic and poorly recrystallized to granoblastic and completely recrystallized. This range of textures seems to have developed in response to increasing grades of regional metamorphism (from upper-greenschist to middle-amphibolite facies). Locally, flaser and mortar structures are developed in the mafic rocks. Irregular patches and veinlets of epidote, quartz, chlorite, and sometimes carbonate characterize the low-grade varieties of greenstone.

The habit of amphibole varies considerably (fig. 22). It ranges from short stubby crystals (≤ 0.1 mm long) to long acicular crystals (≥ 1 mm long) and is sometimes partially chloritized. In metagabbro and metadiabase samples, the shape of hornblende seems to be controlled by original clinopyroxene. Remnants of pyroxene, however, have not been found. Much of the hornblende does not show preferred orientation in lower grade rocks but is usually aligned in the foliation in higher grade rocks. The hornblende is sometimes poikiloblastic. Its pleochroism ranges from X = light brown, Y = light green, Z = dark green, to X = light green, Y = dark green, Z = blue-green.

Plagioclase occurs as small, usually poorly twinned crystals showing varying degrees of saussuritization (fig. 22). The degree of saussuritization appears to decrease with increasing metamorphic grade. Compositions range from An₅₋₁₀ to An₂₅ with both albite and oligoclase present in the lower grade rocks. Quartz occurs as xenoblastic crystals intergrown with plagioclase; it is enclosed in crystals of hornblende in some samples from the south side of Sheep Mountain in the northern San Andres Mountains. In one sample from the Hell Canyon area (Manzanita Mountains), subrounded quartz grains (< 1 mm in size) may represent vesicle fillings in a mafic flow.

Epidote varies in abundance even within the same greenstone unit; it occurs as disseminated grains (0.05-0.5 mm in size) and as irregular patches and veinlets. Biotite often occurs associated with and probably replacing hornblende. Chlorite occurs in irregular patches and shows anomalous blue interference colors. Because it often appears to partially replace amphibole, it seems to be a retrograde mineral. Magnetite (\pm hematite) and ilmenite occur as small, often idioblastic grains that commonly crosscut foliation. Traces of tourmaline, apatite, sphene, garnet, pyrrhotite, pyrite, prehnite, and stilpnomelane(?) are present in some of the lower-grade greenstones. Sphene generally occurs around magnetite grains, and stilpnomelane(?) has been reported by Gonzalez (1968) around the edges of epidote grains in samples from the Pederal Hills. Minor carbonate is common in the lower grade varieties as irregular patches and in small veinlets. Small amounts of microcline is found in some of the amphibolites in the Monte Largo Hills (Huzarski, 1971).

Siliceous meta-igneous rocks

Siliceous meta-igneous rocks include fine-grained (typically porphyritic) sills and various rocks of probable volcanic origin that have overall granitic compositions. The major occurrences are in the southern Manzano, Los Pinos, and Ladron Mountains, where corresponding minimum thicknesses are 1.5 km, 1 km, and

1.8 km, respectively (Stark, 1956; Beers, 1976; Condie, 1976a). Several very minor rhyodacite sills (< 10 m thick) occur in the Manzanita Mountains on the ridge south of Coyote Canyon and in the North Canyon area. Minor tuffaceous units occur in the northern Magdalena Mountains (fig. 6 on sheet 2) and in the Coyote Hills. Two thin (< 5 m thick) red metavolcanic units occur just beneath the Phanerozoic unconformity in Hembrillo Canyon in the central San Andres Mountains. These represent the only siliceous meta-igneous rocks recognized south of the Coyote Hills.

The siliceous meta-igneous rocks in the Manzano and Los Pinos Mountains compose most of the Sevilleta Formation (Stark and Dapples, 1946), which extends from Capilla Peak in the Manzanos to the southern end of the Los Pinos Mountains (sheet 1). The spelling Sevilleta (rather than Sevillita) is used in this report. This formation occupies the axial zone of a southerly plunging syncline whose eastern limb only is exposed in the Los Pinos Mountains (Beers, 1976). The lower 500-800 m of the formation is composed dominantly of interbedded feldspathic quartzites and mica-quartz schists that grade into the underlying White Ridge Formation. The upper contact of the formation is not exposed because overlying units are eroded. In the Ladron Mountains, the siliceous meta-igneous rocks compose much of the northwestern part of the Precambrian core (Condie, 1976a). They extend discontinuously as inclusions in the Capirote pluton around the northeastern, eastern, and southern parts of the range (fig. 5 on sheet 2). The lower and upper contact of the Ladron meta-igneous section is not preserved because of granitic intrusion and subsequent erosion.

Siliceous meta-igneous rocks vary considerably in color, texture, and outcrop habit. Brown, buff, and orange are common, although white, purple, and black units are also found. The rocks range from massive and blocky (most common) to locally sheared and foliated. The massive varieties commonly form bold angular outcrops; the more foliated varieties form subdued outcrops. Sections of siliceous meta-igneous rocks contain from 5-percent (the Los Pinos and northwest Ladrons) to 30-percent (the southern Manzanos) amphibolite beds, which taper laterally over distances of tens to hundreds of meters. Some of the amphibolites are discordant.

Individual units within the massive portions of the siliceous meta-igneous sections appear to range from many tens to hundreds of meters in thickness. A relict porphyritic texture characterizes many of the rocks. Well-formed, relict plagioclase and/or quartz phenocrysts, typically 1-5 mm in size, occur in most outcrops. Even in the more foliated rocks, remnants of these phenocrysts are preserved. Some units (< 25 percent of the total) are distinctly banded with individual bands ranging from 1 to 5 cm thick. Whether this banding is primary or metamorphic in origin cannot be determined from field relationships. A few units, such as those in Hembrillo Canyon, also contain flattened and stretched volcanic rock fragments reminiscent of those found in young ash-flow tuffs (fig. 23). These rock fragments, however, may have been flattened and stretched during metamorphism. Rounded granitic inclusions are reported at one locality in the southern Manzanos (Stark,

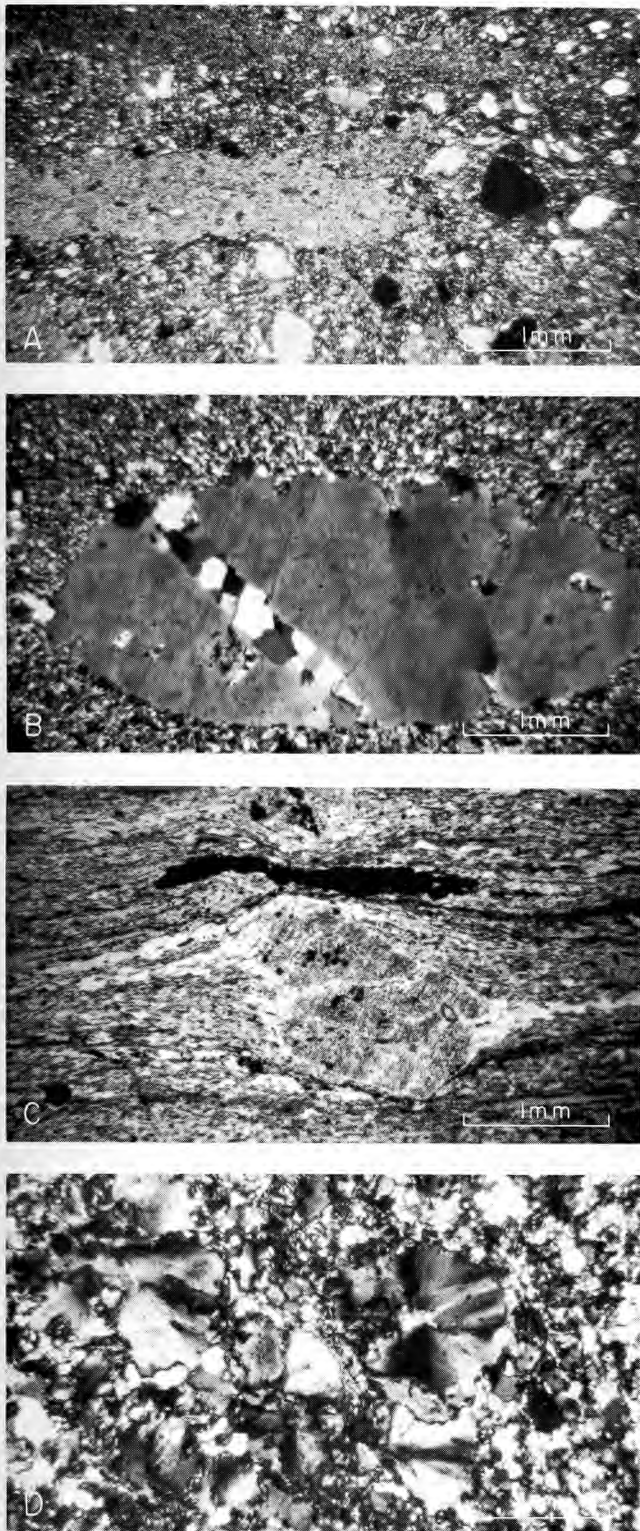


FIGURE 23—PHOTOMICROGRAPHS OF SILICEOUS META-IGNEOUS ROCKS. A) Metatuff (SANA-117); Hembrillo Canyon, San Andres Mountains. Angular quartz and feldspar fragments in fine-grained matrix of feldspar, quartz, and sericite. Large fragment in center may represent a flattened pumice fragment; crossed polars. B) Metarhyolite (LPSI-7); Bootleg Canyon, Los Pinos Mountains. Strained and partially resorbed quartz phenocryst in groundmass of quartz, feldspar, and epidote; crossed polars. C) Metarhyolite (LP73-9); Sevilleta Formation, west of upper Montosa well, Los Pinos Mountains. Albite phenocryst with quartz pressure shadows in groundmass of feldspar and quartz; uncrossed polars. D) Metarhyolite (SANA-144); Hembrillo Canyon, San Andres Mountains. Spherulitic aggregates of orthoclase in a quartz-feldspar groundmass; crossed polars.

1956). Flow structure and chilled borders reported by Stark and Dapples (1946) in the Sevilleta Formation in the Los Pinos Mountains, however, have not been found by later investigators (Mallon, 1966; Beers, 1976) nor by the authors. Epidote and quartz veins are locally abundant in the meta-igneous sections.

Siliceous meta-igneous rocks are composed chiefly of plagioclase and/or quartz phenocrysts in a fine-grained quartz-feldspar groundmass (fig. 23). The mineral proportions given in table 2 should be considered as approximations because of the fine-grained nature of the groundmasses. The most widespread igneous texture preserved is a porphyritic texture (fig. 23). Quartz and plagioclase phenocrysts (0.5-5 mm in size) compose 10-20 percent of most samples. Glomeroporphyritic textures are also common. Both plagioclase and quartz phenocrysts are partially resorbed (fig. 23). Micrographic intergrowths of quartz and K-feldspar occur in the groundmasses of some samples. With the exception of the two thin units from Hembrillo Canyon, textures characteristic of ash-flow tuffs—such as broken phenocrysts, imbricate structures, flattened rock fragments, and accretionary lapilli—were not found in any of the approximately 75 thin sections examined. Most of the rocks are massive; fabrics, when present, appear to represent metamorphic foliation produced along shear zones. In these sheared rocks, phenocrysts are partially aligned parallel to the fabric (fig. 23) and sometimes are bent and fractured. Albite twins often taper rapidly in these samples, and flaser structure is common in the groundmass.

Quartz phenocrysts exhibit undulatory extinction, partial resorption, and fracturing (fig. 23). Plagioclase phenocrysts are partly resorbed and sometimes partly replaced with recrystallized quartz and plagioclase. The latter texture increases in degree of development with increasing deformation. Twinning in plagioclase phenocrysts ranges from well developed to poorly developed. Varying degrees of saussuritization are common. Zoning is preserved in plagioclase phenocrysts in one sample from a rhyodacite sill in the central Manzanita Mountains. Matrices are composed of very fine grained feldspar-quartz intergrowths exhibiting decussate textures except when sheared. The proportion of matrix K-feldspar is difficult to estimate. The K_2O and normative Or contents of these rocks (appendix 2), however, suggest that 20-50 percent of the rocks are composed of K-feldspar. Magnetite (\pm hematite) occurs as disseminated grains (< 0.5 mm across) often showing idiomorphic outlines that crosscut foliation. Biotite or muscovite are ubiquitous minor constituents of most samples. Cross-muscovite is common in samples from the central Manzano and Los Pinos Mountains. Spherulitic patches of K-feldspar occur in the Hembrillo Canyon metavolcanic units (fig. 23) and indicate devitrification of an original glassy groundmass.

Of the secondary minerals found in the siliceous meta-igneous rocks, epidote, quartz, chlorite, and limonite are most widespread. Epidote occurs as irregularly distributed patches, as disseminated grains, and in veinlets. Secondary quartz, in part representing primary quartz recrystallized in situ, occurs as veinlets and irregular patches. Some biotite grains are partially chloritized. Limonite occurs as an alteration product in fractures and around magnetite grains.

Although evidence is not completely definitive, existing data favor an origin for most of the siliceous metaigneous rocks as thick sills. The glomeroporphyritic textures are particularly suggestive in this regard. The relatively great lateral extents of individual massive units (many kilometers in the Manzanos) suggests that these are not rhyolite flows. Up to 25 percent of some of the sections may represent some combination of air-fall and ash-flow tuffs as indicated by the banding and flattened rock fragments. With exception of the Hembrillo Canyon and Magdalena rocks, however, primary tuffaceous textures are not preserved in thin section.

Gneiss

Only two major occurrences of quartzo-feldspathic gneiss occur in the Precambrian of central and south-central New Mexico. The largest composes most of the Monte Largo Hills east of the Sandia Mountains (sheet 1). The second is the Cibola Gneiss (Kelley and Northrop, 1975), which occurs in a northeasterly trending belt, 1.3 km wide and 8 km long, in fault contact with the Tijeras Greenstone. Minor occurrences are found in the San Andres Mountains at the following locations (sheet 3): along the southern and eastern sides of Sheep Mountain between the Salinas Peak road and Camels Hump Ridge southwest of Salinas Peak, between Ash and Grapevine Canyons east of Black Top Mountain, 3 km northeast of San Andres Peak, and in a belt extending east from Little San Nicholas Canyon for about 2.5 km. One very minor outcrop in the northern Pederal Hills (fig. 4 on sheet 2) may represent a gneissic portion of an intrusive granite (Gonzalez and Woodward, 1972). Small outcrops composed dominantly of layered gneiss also occur in the Coyote Hills west of San Antonio (fig. 9 on sheet 2) and in the southern Organ Mountains, where the outcrop is ≤ 300 m in size (Dunham, 1935).

Gneiss complexes generally form poor, rubble-strewn outcrops. The rocks are medium to coarse grained and often contain microcline augen like that so well developed in the Cibola Gneiss (Lodewick, 1960; Kelley and Northrop, 1975). Gneissic foliation is commonly well developed and the rocks are often layered and banded. Local hornfelsic textures occur in gneisses of the Monte Largo area. Biotite is usually the most important dark mineral, although hornblende gneisses are found in the Monte Largo area and in some of the San Andres exposures. All gneiss terranes contain remnants of quartzite and amphibolite or chlorite schist. Several quartzite beds are continuous for long distances along strike in the Cibola Gneiss (Lodewick, 1960), and one prominent quartzite unit occurs in the northern part of the Monte Largo exposure. The gneisses are locally cut by pegmatites, light-colored migmatites, and quartz veins that become more abundant as the contacts with engulfing granitic rocks are approached. Both grain size and the amount of K-feldspar porphyroblasts increase in abundance in the Cibola Gneiss as the contact with

the South Sandia pluton is approached. These features seem to record progressive metasomatism around the southern edge of the pluton contact that extends into the gneiss for 20-50 m.

A summary of the average mineral proportions in gneisses from the Sandia Mountains, Monte Largo Hills, and San Andres Mountains is given in table 2. Quartz, sodic plagioclase (An_{10} to An_{25}), and K-feldspar (microcline) compose most of the rocks, and biotite is the dominant mafic mineral. The gneisses are granoblastic and range from rocks exhibiting only incipient foliation to well-banded rocks with prominent biotite-rich layers. They vary in average grain size from about 2 mm to nearly 10 mm. Samples adjacent to the South Sandia pluton contain microcline porphyroblasts up to 3 cm long. Except for these porphyroblasts, the major minerals typically exhibit xenoblastic textures. Mortar and flaser structures are developed along zones of intense shearing, and augen gneisses are locally important in some parts of the Cibola Gneiss (Lodewick, 1960). Many accessory minerals such as zircon, tourmaline, apatite, rutile, and garnet are commonly idioblastic. Typical alteration products are sericite (in feldspars), chlorite, hematite-limonite, and epidote. The latter three minerals occur as irregular patches and veinlets. Some chlorite replaces biotite, and some hematite-limonite appears to be an alteration product of primary magnetite.

Sillimanite occurs in the gneisses of the Monte Largo Hills area (Huzarski, 1971), in the Cibola Gneiss just north of Coyote Canyon adjacent to the South Sandia pluton (Lodewick, 1960), and in large gneiss inclusions in the granitic rocks near the mouth of Cottonwood Canyon in the San Andres Mountains. It occurs as patches of acicular crystals (fig. 19D) and as randomly oriented needles in quartz and muscovite. Sillimanite appears to coexist with K-feldspar in the Cibola Gneiss. Its close proximity to a granitic contact in the Cibola Gneiss and probably in the Monte Largo Hills area and its occurrence in gneissic inclusions in the Cottonwood Canyon area suggest that it is the product of contact metamorphism. Kyanite has been reported in gneisses in only one small outcrop in the southeastern Monte Largo Hills (Huzarski, 1971). Andalusite, which crosscuts gneissic foliation, composes up to a few percent of some of the gneisses in the northern Monte Largo Hills. Although the andalusite appears to postdate the major period of metamorphism in the Monte Largo Hills, the age relationships between the kyanite and sillimanite are not known. The sillimanite in the Cibola Gneiss and in gneisses of the Monte Largo area is interpreted to reflect contact metamorphism.

Although the composition of the parent rocks of the Precambrian gneisses in central and south-central New Mexico are unknown, the close association of quartzite, the common presence of layering, and the presence of rounded (detrital) zircons in the Cibola Gneiss (Lodewick, 1960) suggest a dominant clastic sedimentary parent—probably shales and siltstones.

Stratigraphy

Nine composite stratigraphic sections in the Precambrian terranes of central and south-central New Mexico have been measured or estimated from existing literature (table 1 and appendix 1). Locations of the sections are given in fig. 2 and on individual area geologic maps. Sections are shown diagrammatically with possible correlations in the SMP block in figs. 24 and 25. Pray (1961) gives an additional section in the Sacramento escarpment exposure. The detail in each section varies depending on the adequacy of exposure and accessibility. Sections are reported in the literature from the central Manzano and Los Pinos Mountains (Stark, 1956; Stark and Dapples, 1946). Condie has also measured sections in these mountain ranges and in the Ladron and northern Manzanita Mountains; those sections given in appendix 1 represent averages of all available data for these areas. Due to limited accessibility, the sections in the northern Manzano and Manzanita Mountains and in the central San Andres Mountains are more generalized representations. The least amount of detail is given in the Pederal and Magdalena sections, where poor exposure makes detailed measurements difficult. How representative the sections are of the original rock distributions and thicknesses is a function of the degree of deformation. The schist-phyllite units are probably overestimated in most sections because of drag folding and structural thickening. Although local faulting may have duplicated small parts of some of the sections, major duplication probably does not exist. An unknown portion of the section is missing in the northern Manzano and in the Ladron Mountains because of intrusion of granitic plutons. Faulting appears to have eliminated parts of the section in the northern Manzanita, central Manzano, and Los Pinos Mountains.

Crossbedding and channel-fill deposits in quartzites, minor fold distributions, and cleavage-bedding relationships were used to determine bed attitudes. The attitude of the beds beneath the unconformity at the base of the central Manzano section indicates that the synformal structure in the south-central Manzanos is a syncline. The tops of the Precambrian sections are either unconformities or intrusive contacts; and, with exception of the western synclinal limb of the central Manzano section (fig. 24, section 3), the bases of the sections are not exposed. The maximum exposed thicknesses occur in the northern Manzano (approximately 12.5 km) and San Andres (approximately 9.5 km) sections. A small amount of the northern Manzano section may be missing owing to intrusion of the Ojita pluton. The age relations between the Manzano and Manzanita sections (fig. 24, sections 1 and 2) are uncertain because the sections are separated by the intrusive Manzanita pluton. The similar strike and dip of both sections, however, suggest that the Manzanita section is older (fig. 24). Stratigraphic relations between the SMP sections and sections 6-9 (fig. 25) are presently unknown. Also, age relations among sections 6-9 are unknown.

The nine stratigraphic sections shown in figs. 24 and 25 may represent at least two lithologic associations. A summary of rock-type abundances in each section is given in table 1 to emphasize differences and similar

ities. It is clear that the two sections beneath the central Manzano unconformity have more mafic meta-igneous rock, less quartzite, and much less siliceous meta-igneous rock than do the overlying sections. The two older sections contain rock distributions very similar to those found in Precambrian rocks of the southern Sangre de Cristo Mountains (Miller and others, 1963; Mathewson, in preparation) and may represent part of the same association. With the exception of obvious correlations between the central Manzano and Los Pinos Mountains, sections 3-9 cannot be correlated; however, these sections tend to record similar stratigraphic changes. The evolution from a feldspathic quartzite and arkosite association to a mica-schist and clean quartzite association (followed by intrusion of voluminous, siliceous, near-surface igneous rocks) is evident in the Manzano-Los Pinos and Ladron sections. The first two stages of this evolution are also recorded in the Pederal and San Andres sections. Lack of exposure of the upper parts of these sections may be responsible for the near absence of siliceous meta-igneous rocks. Although the relationship between the Magdalena section and this lithostratigraphic succession is not yet clear, the presence of siliceous metatuffs suggests that the Magdalena section corresponds to a late stage. Minor mafic rocks, chiefly diabase sills and dikes, occur throughout the younger sections and become locally abundant in the siliceous meta-igneous portion of the Manzano-Los Pinos section.

The thin exposed section along the Sacramento escarpment (Pray, 1961) is one of the few exposures of the apparently widespread De Baca terrane in the basement of east-central New Mexico (fig. 3). This terrane has been mapped from well data (Muehlberger and Denison, 1964; Muehlberger and others, 1967; Denison and Hetherington, 1969) and is composed principally of fine-grained clastic sedimentary rocks and some carbonates intruded with diabase sills and minor amounts of high-alkali granitic rocks.

Preservation of primary structures in clastic meta-sedimentary rocks is not common in the Precambrian rocks of central and south-central New Mexico because of the degree of deformation and metamorphism. Crossbedding sufficiently well exposed and preserved for use in determining current directions occurs in some parts of the Ladron, Magdalena, and San Andres sections and rarely in the Manzano-Los Pinos section. After structural correction, transport directions deduced from crossbedding in these areas are towards the south or southeast. Because clear crossbedding measurements are sparse, these current directions may not be representative of the entire region.

Because only fragmentary exposures of the New Mexico Precambrian basement exist, reconstruction of sedimentary basin sizes and shapes and probable water depths is difficult. The outcrops, however, clearly show that sedimentary units taper laterally over distances of hundreds of meters to a few tens of kilometers. Even the White Ridge Formation and Sais Quartzite in the central Manzano-Los Pinos area seem to be composed of individual tapering units. The relative abundance of feld-

spar-rich sediments in the lower parts of sections 3-9 (table 1) suggest that nearby source terranes were uplifted rapidly. Local conglomeratic units also attest to nearby sources. The increasing abundance of mica-schist (shale) and feldspar-poor quartzite at higher stratigraphic levels seems to record more tectonically stable (and perhaps more distant) sources as well as some reworking. Existing evidence does not favor the presence of widespread (many hundreds to thousands of kilometers) stable-shelf deposits. Although not completely definitive, most evidence is compatible with a model involving small, isolated or partially connected basins (tens to a few hundred kilometers across), which undergo similar tectonic-sedimentary histories. The major source areas for these basins during their early stages of development would be nearby uplifted blocks between the basins. During the later stages of evolution, source areas may have been more distant, chiefly to the north. Various basins may have reached the same stage of development at different times in response to changing thermal-tectonic regimes.

Constraints on the composition of the source rocks can be deduced from estimates of clastic mineral and cobble proportions. The QFL (quartz and quartzite, total feldspar, lithic fragments) model parameters of McBride (1963) and Dickinson (1970) for medium- to coarse-grained clastic metasedimentary rocks from several Precambrian sections in central New Mexico are given in table 3. Included also in the table are the C/Q (chert/quartz and quartzite) and P/F (plagioclase/total feldspar) ratios. According to the interpretations of QFL data suggested by Dickinson (1970), the Precambrian sandstones in New Mexico seem to be derived chiefly from granitic source terranes. Q also includes some reworked quartzite fragments, indicating a contribution also from quartzite. The only clear evidence for volcanic provenance is the presence of volcanic rock fragments in a few fine-grained metasediments from the Magdalena Mountains. The model data show that the most immature sediments in terms of feldspar content occur in the Ladron and lower San Andres sections. The chemical composition of the metamorphosed sandstones and siltstones also reflects a dominantly granitic source. There is no evidence for a different source-area composition for the older sections (1 and 2) in the Manzanita and northern Manzano Mountains. Estimates of the average distribution of clast lithologies in conglomeratic units in the Ladron Mountains are as follows.

quartzite and feldspathic quartzite	45%
quartz	20 ⁰ 10
mica schist	7%
amphibolite	5 ⁰ 10
granitic rock (K-feldspar rich)	20%
siliceous meta-igneous rock	3%

These lithologies are the same as those exposed in the New Mexico Precambrian basement although the ratio of quartzite to granite is significantly greater in the cobbles. In general, this result is consistent with the results

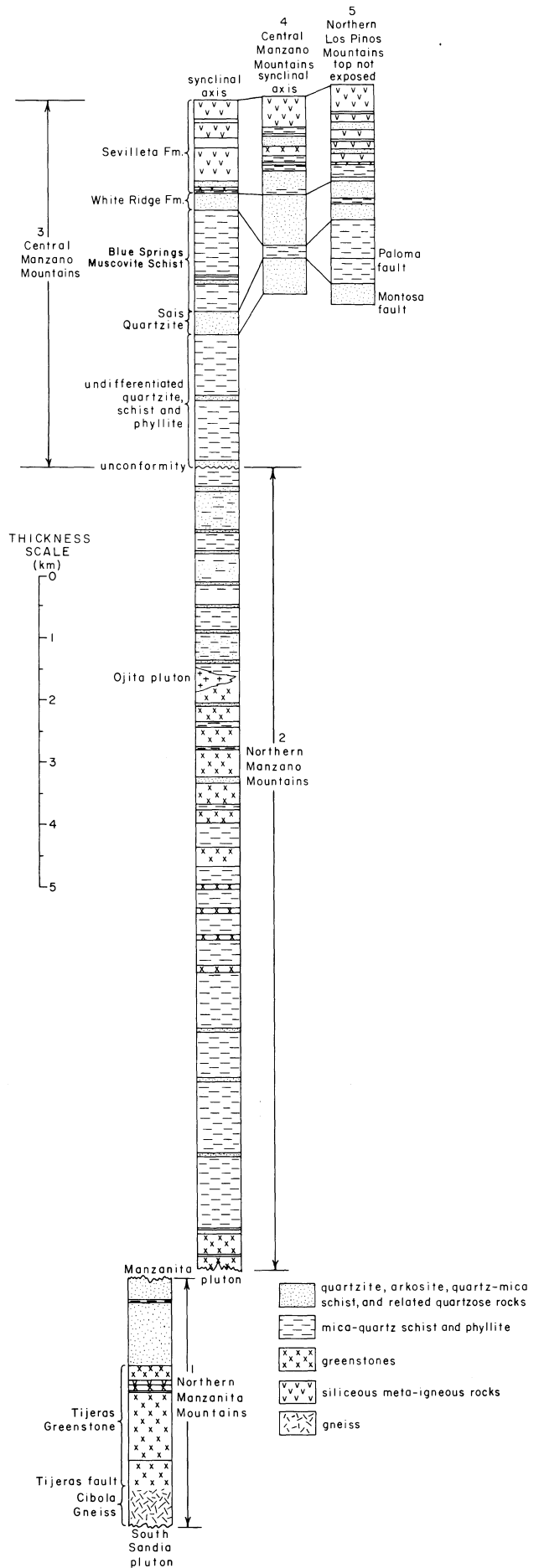


FIGURE 24—COMPOSITE STRATIGRAPHIC SECTIONS OF PRECAMBRIAN ROCKS IN THE SMP BLOCK showing possible correlations and age relationships between sections (measured sections and references given in appendix 1 and locations in fig. 2 and sheet 1). Column 3 shows west side of syncline; column 4 shows east side of syncline.

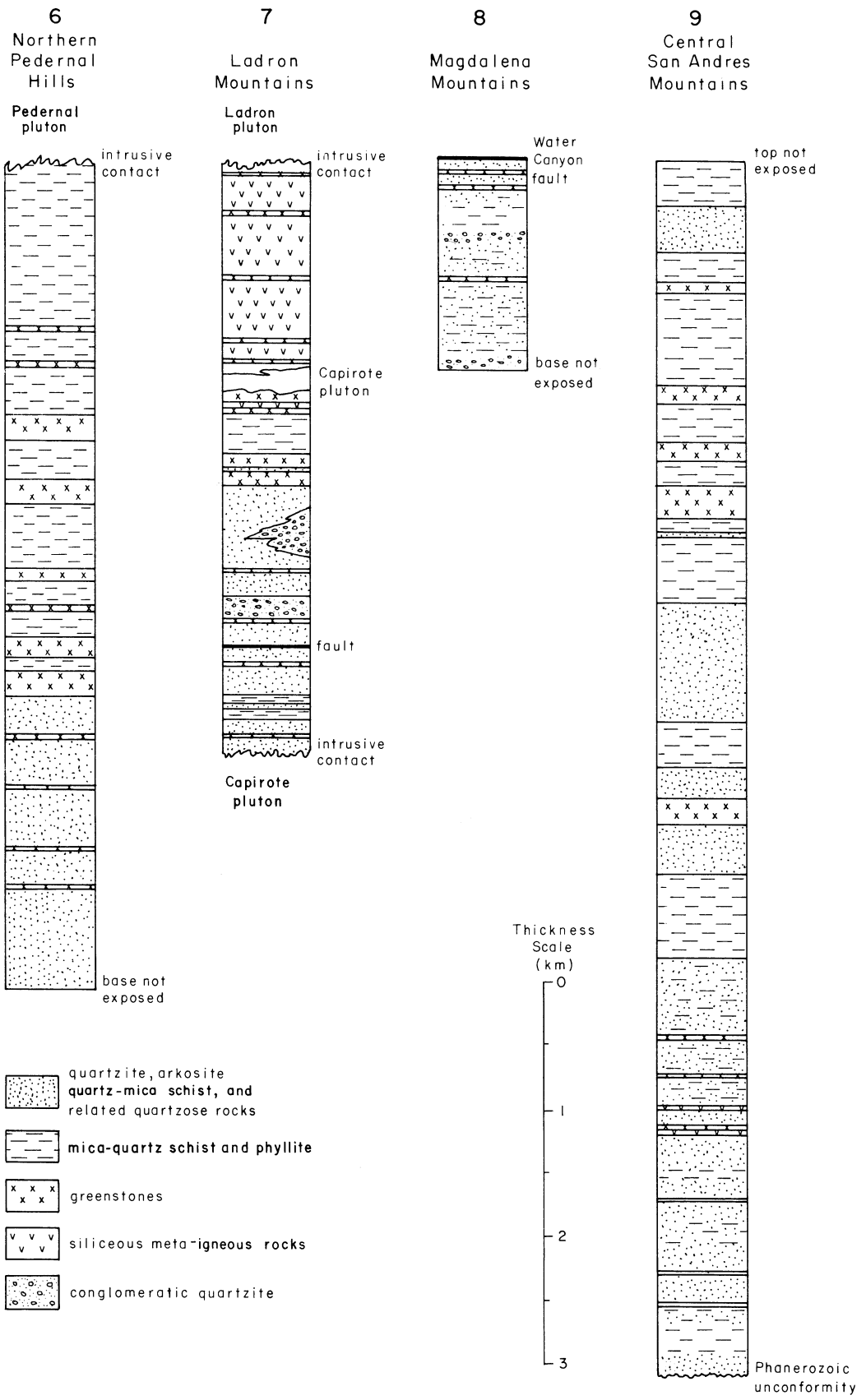


FIGURE 25—MISCELLANEOUS COMPOSITE STRATIGRAPHIC SECTIONS OF PRECAMBRIAN ROCKS IN CENTRAL AND SOUTH-CENTRAL NEW MEXICO (measured sections and references given in appendix 1 and locations of sections given in fig. 2 and on corresponding geologic maps, sheet 2). Correlations are not implied.

TABLE 3-DETRITAL-GRAIN MODAL PARAMETERS OF MEDIUM TO COARSE CLASTIC AND METASEDIMENTARY ROCKS FROM THE PRECAMBRIAN OF CENTRAL AND SOUTH-CENTRAL NEW MEXICO; mean values given with ranges in parentheses. Abbreviations: Q = quartz + quartzite; F = total feldspar; L = lithic fragments; P = plagioclase; C = chert.

Mountain range	Q	F	L	C/Q	P/F	No. of samples
northern Manzanita	94 (50-100)	6 (0-50)	tr	~ 0	~ 0.3	8
northern Manzano-Manzanita	83 (60-98)	16 (2-40)	1 (0-2)	~ 0	~ 1	3
central Manzano ¹	91 (70-100)	9 (0-30)	tr	~ 0	0.6 (0.1-1)	10
Los Pinos ²	93 (85-100)	7 (0-15)	tr	~ 0	~ 1	8
Ladron	67 (50-96)	32 (4-50)	1 (0-2)	~ 0	0.1 (0.01-0.7)	9
San Andres A ³	78 (68-87)	22 (12-32)	tr	~ 0	~ 1	3
San Andres B ⁴	99 (92-100)	3 (0-8)	tr	~ 0	~ 1	10

¹Sais Quartzite and White Ridge Formation

²metasedimentary rocks in the Sevilleta Formation

³lower part of the section in central San Andres Mountains

⁴middle and upper parts of the section in central San Andres Mountains

of the QFL parameters and suggests that much of the detrital material in the Precambrian sections from central and south-central New Mexico was derived from the reworking of a rock association similar to that exposed today.

Little is known of the provenance of the clastic sediments in the De Baca terrane although they probably represent reworked portions of the granitic-metasedimentary terrane underlying most of central and northern New Mexico (fig. 3).

Granitic rocks

Surface exposures and Precambrian basement samples from oil tests suggest that granitic rocks compose approximately two-thirds of the total Precambrian terrane in central and south-central New Mexico (Foster and Stipp, 1961). These rocks, which range from granodiorite to granite and syenite in composition, represent partial exposures of a minimum of 31 individual plutons (summarized in table 4). Pluton locations are shown in fig. 26, and average compositions are plotted on a quartz-K-feldspar-plagioclase classification diagram in fig. 27. A representative suite of average modal analyses is given in table 5. From existing field and petrographic data, the following conclusions may be drawn:

1) All plutons average quartz monzonite or granite in mineralogical composition, with four exceptions. Biotite is the principal mafic mineral and exhibits a large range in concentration.

2) Textural variations exist both within and between plutons.

3) Textural data in most of the quartz monzonites and granites suggest that the sodic plagioclase and biotite began to crystallize early followed by K-feldspar and quartz. Plagioclase is sometimes partially resorbed by later albite.

4) Small mafic inclusions of unknown parentage occur in the North and South Sandia, Ojita, Monte Largo, and Priest plutons. Inclusions of quartzite, siliceous meta-igneous rock, gneiss, and amphibolite of varying sizes and degrees of digestion and granitization are found in most of the granites and quartz monzonites.

5) Clearly defined contact metamorphic aureoles occur adjacent to the North Sandia, Monte Largo Hills, Pedernal, and Priest plutons.

6) Pegmatites and aplites are not numerous in most of the granites and quartz monzonites.

TABLE 4-MAJOR PRECAMBRIAN GRANITIC PLUTONS IN CENTRAL AND SOUTH-CENTRAL NEW MEXICO. Abbreviations: G = granite; QM = quartz monzonite; S = syenite; Gd = granodiorite.

Pluton	Minimum exposure area (sq km)	Average composition
1. North Sandia	50	QM
2. South Sandia	70	Gd
3. Ojita	60	Gd
4. Monte Largo	3	Gd
5. Priest	25	QM
6. Manzanita	30	QM
7. Los Pinos	17	G
8. Sepultura	10	G
9. Ladron	20	QM
10. Capiroto	30	QM
11. Magdalena	20	G
12. Oscura	40	QM
13. Mockingbird Gap	15	QM
14. Capitol Peak	75	QM
15. Strawberry Peak	9	G
16. Mayberry	30	G
17. San Andres	25	QM
18. Mineral Hill	50	QM
19. White Sands	10	QM
20. Organ	15	QM (?)
21. Fra Cristobal	40	QM
22. Caballo	17	QM
23. Polvadera	8	G
24. La Joyita	4	G
25. Pedernal	150	G
26. Rattlesnake Hill	30	G (?)
27. Pajarito Mountain	5	S
28. San Diego Mountain	2	QM
29. Tajo	~2	QM
30. Gallinas	~8	G (?)
31. Monte Largo Hills	~3	QM

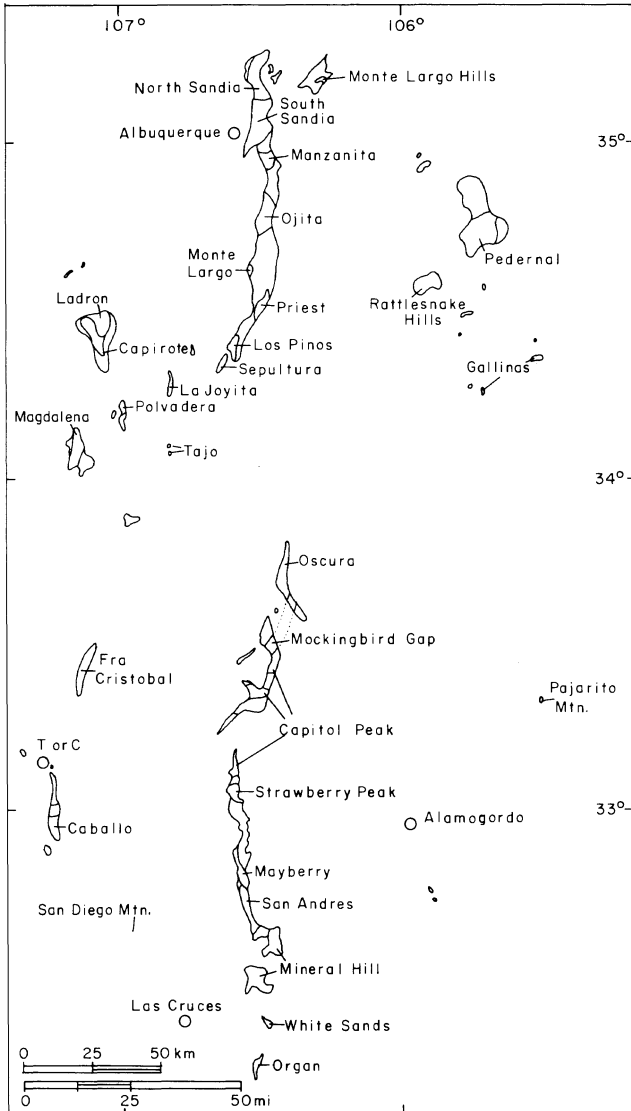


FIGURE 26—GEOGRAPHIC DISTRIBUTION OF PRECAMBRIAN GRANITIC PLUTONS IN CENTRAL AND SOUTH-CENTRAL NEW MEXICO.

Sandia plutons. Both plutons crop out along the western escarpment of the Sandia Mountains and in a few inliers on the eastern side of the range (sheet 1). They form a continuous belt 3-5 km wide and about 30 km long. On the whole, granitic rocks composing the plutons are mostly uniform, ranging from gray to pink and from medium to coarse grained. They commonly contain 5-15 percent of large microcline megacrysts (≤ 5 cm long). In thin section the rocks exhibit typical hypidiomorphic-granular textures. A very small outcrop of orbicular granite occurs in the North Sandia pluton near the base of La Luz Trail (Thompson and Giles, 1974). The contact of the North pluton is exposed in Juan Tabo Canyon and the contact of the South pluton in Tijeras Canyon. Both contacts are concordant with surrounding metamorphic foliation. The contact of the North pluton with adjacent metamorphic rocks is rather sharp and a distinct contact metamorphic aureole occurs adjacent to the pluton (Green and Callender, 1973). The contact of the South pluton exposed in Tijeras Canyon is gradational with the Cibola Gneiss, where large microcline megacrysts decrease in abundance over a few meters going into the gneiss. Lodewick (1960) has related this change to peripheral alkali metasomatism. No evidence for contact metamorphism exists for the South pluton. These differences in contacts support the geochemical data (discussed later), which indicate that the Sandia "granite" is composed of two distinct plutons. The North pluton seems to have been emplaced at a higher temperature than the South pluton.

Modal analyses by the authors (table 5) indicate that the average composition of the North and South plutons are quartz monzonite and granodiorite, respectively (fig. 27). Four types of inclusions occur in the plutons (Shomaker, 1965). Mafic inclusions, which are most abundant, seem to represent xenoliths of a rock not exposed in surrounding metamorphic terranes. Alteration in the form of hematite, epidote, and chlorite is concentrated along fractures and shear zones and increases in intensity in the northern part of the South pluton (Shomaker, 1965; Feinbert, 1969).

7) Epidote, sericite, albite, and secondary quartz are minor (but widespread) alteration products in most plutons.

8) Pluton contacts range from concordant to locally discordant, suggesting syntectonic to post-tectonic emplacement.

9) Field, petrographic, and compositional data are consistent with depths of emplacement for most plutons of 5-10 km.

Brief descriptions of most of the major plutons, with references to pertinent literature, follow.

North and South Sandia plutons

Descriptions of the field relationships, mineralogy, and textures and structures of the Sandia plutons are available in Hayes (1951), Shomaker (1965), Feinberg (1969), and Kelley and Northrop (1975). Although earlier investigators did not recognize more than one pluton composing the Sandia "granite," modal and compositional data reported in this study suggest at least two plutons, named the North Sandia and South

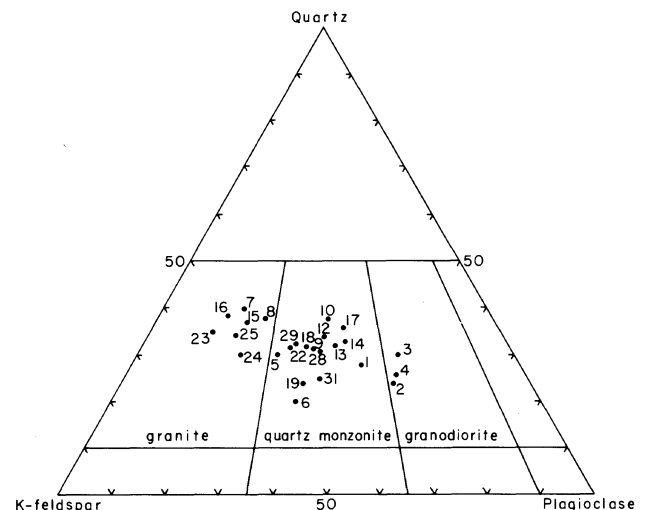


FIGURE 27—QUARTZ-K-FELDSPAR-PLAGIOCLASE CLASSIFICATION TRIANGLE showing average compositions of Precambrian granitic plutons from central and south-central New Mexico. Numbers correspond to listing in table 4 (after Bateman, and others, 1963).

TABLE 5—AVERAGE MODES OF PRECAMBRIAN GRANITIC PLUTONS FROM CENTRAL AND SOUTH-CENTRAL NEW MEXICO compiled from numerous sources cited in the text and from modal analyses by the authors. Common accessory minerals are zircon, apatite, rutile, epidote, chlorite, hematite, sericite; uncommon trace minerals are tourmaline, calcite, garnet, allanite, monazite, fluorite, garnet; tr = trace.

Pluton	K-feldspar	Plagioclase	Quartz	Biotite	Hornblende	Magnetite	Sphene	Muscovite	Accessory minerals
North Sandia	25	36	28	6	—	2.0	1.0	tr	2
South Sandia	20	39	25	10	tr	2.5	1.5	tr	2
Ojita	18	42	30	4	3	2	tr	tr	1
Monte Largo	21	40	25	6	5	2	tr	tr	1
Priest	38	23	30	7	—	1	tr	tr	1
Manzanita	42	32	20	2	—	2	tr	1	1
Polvadera	45	10	35	8	tr	1	—	tr	1
La Joyita	45	17	30	5	tr	1	—	1	1
Capirote	31	32	35	1	—	0.4	tr	tr	1
Ladron	29	33	31	2	—	0.3	tr	4	1
Los Pinos	39	13	40	5	—	1.5	tr	1	0.5
Sepultura	41	18	37	2	—	0.5	—	1	0.5
Monte Largo Hills	35	34	25	1	—	1	—	3	1
Pedernal	45	15	33	5	—	1	tr	tr	1.5
Oscura	31	30	31	4	tr	1	tr	2	1
Capitol Peak	38	33	31	4	—	1	tr	2	1
Mayberry	45	12	37	3	—	1	—	1	1
San Andres	28	33	33	3	—	1	tr	1	1
Strawberry Peak	42	16	35	4	—	1	tr	1	1
Mineral Hill	34	29	29	4	—	1.5	tr	1	1
White Sands	38	30	21	8	—	2	1	—	tr
Tajo	34	25	32	4	—	1	tr	4	tr
San Diego Mtn.	33	31	31	3	—	1	—	1	tr
Caballo	39	27	31	2	—	1	—	tr	tr

Aplitic dikes and pods are common in the South pluton (Shomaker, 1965). Pegmatitic phases are common in the aplites, the largest concentration occurring south of Pino Canyon. The abrupt change in dike density just south of this canyon (Kelley and Northrop, 1975, map 1) possibly marks the boundary between the North and South plutons. Except for having trace amounts of garnet or tourmaline, the aplites and pegmatites are similar mineralogically to the granitic rocks. The most extensive pegmatites intrude the Juan Tabo sequence (sheet 1). Over 225 bodies ranging in length from a few meters to 1 km were mapped by Hayes (1951) in this area. These pegmatites are often zoned and contain quartz (30-60 percent), K-feldspar (30-70 percent), sodic plagioclase (15-30 percent), muscovite (0-8 percent) and—occasionally—traces of black tourmaline and garnet. Quartz veins are of minor importance in the Sandia plutons.

Manzanita pluton

The Manzanita pluton (new name) was originally mapped as metarhyolite by Reiche (1949) and Myers and McKay (1970). However, field and petrographic studies by Condie indicate that the area is underlain by a coarse-grained gneissic granitic rock. Only a small portion of the pluton is exposed in the central part of the Manzanita Mountains along their western escarpment (sheet 1). Almost all of the exposure lies within the Sandia Military Reservation and is not readily accessible. The rock is characterized as an orange to red, coarse-grained, foliated granitic rock. Foliation strikes north

easterly and is parallel to that in surrounding metamorphic rocks; the foliation suggests syntectonic to pre-tectonic emplacement of the pluton. The northern and southern contacts of the pluton are well exposed. The northern contact, exposed about 1.5 km east of Coyote Springs, is concordant with adjacent feldspathic quartzites; the southern contact, exposed 1.5 km east-south-east of the USGS seismic station, is concordant with adjacent greenstones. Inclusions of surrounding rocks occurring in the granite near the contacts document the intrusive character of the pluton. Aplites and pegmatites are rare in the pluton, but epidote, quartz, and carbonate veinlets are locally abundant.

The average composition of the pluton is that of a quartz monzonite (table 5). K-feldspar is perthitic, exhibits microcline gridiron twinning, and often contains small inclusions of sodic plagioclase. The average grain size is 0.5-1 cm. Sodic plagioclase (0.1-1 mm) is partially saussuritized and is characterized by fractured and bent albite twins. Quartz occurs as small anhedral crystals (0.1-0.5 mm), commonly broken and crushed, and exhibits flaser and mortar textures. Biotite is almost completely chloritized; and epidote, sericite, and carbonate occur in veinlets and as irregular patches.

Ojita and Monte Largo plutons

Because the Ojita and Monte Largo plutons are similar in composition, they are considered together. The granitic rocks composing the plutons vary from gray to tan and are generally medium grained. The northern and southern contacts of the Ojita pluton are

well exposed and range from concordant to discordant with the surrounding metamorphic rocks. With the exception of silicification, contact effects of the pluton on surrounding rocks are minimal (Reiche, 1949). The exposed contacts of the Monte Largo pluton also vary from discordant to concordant and are commonly sheared (Stark, 1956). Existing data suggest that the plutons were emplaced during the late stages of tectonic activity or that they are post-tectonic.

The rocks composing the plutons are quite variable in terms of mineralogy; they range from granodiorite to quartz monzonite. Average modes suggest that both bodies are K-rich granodiorites (table 5 and fig. 27). A small zone of quartz gabbro is preserved in the Ojita pluton just south of Ojita Canyon. Mafic inclusions and aplites are prominent in both bodies. Pegmatites, however, are rare. Detailed textural relationships are described by Reiche (1949) and Stark (1956). Granitic rocks in the plutons are composed chiefly of highly saussuritized sodic plagioclase. K-feldspar is chiefly perthitic microcline, although clear orthoclase rims occur around some of the plagioclase grains. Hornblende appears to have been the principal mafic phase but is now partly altered to biotite and/or chlorite. Augite relicts are reported by Reiche (1949) in the quartz gabbro. Samples are sometimes partially altered to epidote, sericite, and carbonate.

Priest pluton

The Priest pluton crops out as a lens-shaped area in the southern Manzano Mountains (sheet 1). The contact of the pluton is well exposed on the northwest and south. Although generally concordant with surrounding schists and quartzites, the pluton clearly intrudes the rocks (Stark, 1956). A distinct contact metamorphic aureole surrounds the pluton on the southern border (Staatz and Norton, 1942; Stark and Dapples, 1946; Basham, 1951). Dorman (1951) gives a detailed study of fracture patterns in the pluton. The granitic rocks in the pluton range from gray to pink with a dark-red facies on the east. They are medium to coarse grained and contain from 5 to 10 percent large microcline megacrysts (up to 7 cm long). Epidote veinlets are common, and locally small pegmatites (30-50 cm wide and 3-5 m long) are gradational with the granitic rocks. Mafic inclusions are ubiquitous and have a distinct preferred orientation of about N. 5° E. Inclusions of schist and quartzite derived from surrounding rocks are common in the border zones of the pluton.

The pluton is composed chiefly of K-feldspar, saussuritized sodic plagioclase, and quartz (table 5). Biotite is the major mafic mineral and is usually partially chloritized and epidotized. Mineralogy and textures are further described by Stark (1956).

Los Pinos pluton

The Los Pinos pluton crops out in the central part of the Los Pinos Mountains (sheet 1). The field and petrographic relationships are described in Stark and Dapples (1946), Mallon (1966), and Beers (1976). The contact of the pluton is concordant with the Sevilleta Formation on the east and locally discordant with this formation

around the northern tip. Definitive evidence for contact metamorphism is lacking. Inclusions of meta-igneous rock and quartzite, exhibiting varying degrees of digestion by the granitic rock, are common in parts of the pluton. One large amphibolite septum occurs near the crest of the range in the upper part of Bootleg Canyon (Beers, 1976). Pegmatites are rare, but quartz veins are locally abundant. Granitic rocks of the Los Pinos pluton are pink to orange and range from fine to medium grained. Locally they contain small amounts of secondary epidote and quartz. Quartz and K-feldspar, often showing micrographic intergrowths (fig. 28), compose most of the rock—appropriately classified as a granite. Plagioclase (~An₃₄) is partially saussuritized and biotite is commonly partially chloritized. A facies in which miarolitic cavities abound occurs about 1 km north of the summit of Whiteface Mountain.

Sepultura pluton

The Sepultura pluton was defined by Beers (1976) at the southwestern end of the Los Pinos Mountains (sheet 1). This pluton is separated from the Los Pinos pluton by a long narrow septum of meta-igneous rocks, well exposed at the mouth of Bootleg Canyon. Both granites exhibit concordant contacts with this septum. The Sepultura looks much like the Los Pinos in the field. The chief differences in the Sepultura are 1) smaller biotite and magnetite content (table 5), 2) a greater abundance of quartzite and meta-igneous inclusions, and 3) a larger proportion of aplitic rocks (particularly abundant along the southeastern margin of the pluton). Like the Los Pinos granite, the Sepultura contains few pegmatites. Although the Sepultura granite may represent an apophysis of the Los Pinos granite, it is distinct in composition from the latter.

Pederal pluton

Although poorly exposed for the most part, the Pederal pluton underlies a large area in the central and southern part of the Pederal Hills (fig. 4 on sheet 2). Contacts of the pluton with the metamorphic terrane on the north are sharp and range from concordant to locally discordant. The metamorphic rocks have also been subjected to contact metamorphism adjacent to the pluton (Gonzalez, 1968). The granitic rocks contain both mafic inclusions of unknown source and fragments of schist and quartzite that seem to have been derived from surrounding metamorphic terranes. Small pegmatite-aplite dikes cut the pluton. Portions of the granitic terrane are highly sheared; such shearing may have accompanied emplacement (Gonzalez and Woodward, 1972).

Most of the Pederal pluton is composed of granite with small portions of alkali granite and quartz monzonite. The rock varies from pink to orange and from fine grained to coarse grained. Microcline occurs as large crystals engulfing plagioclase; it is locally perthitic and exhibits micrographic intergrowths. Plagioclase is partially saussuritized, and biotite is partially chloritized.

Ladron pluton

The Ladron pluton underlies part of the northern Ladron Mountains. The contact of the pluton is well exposed along the southern boundary where it is discordant to the foliation in surrounding metamorphic rocks. It is interpreted as post-tectonic. Adjacent rocks show no evidence of contact metamorphism; a large roof pendant of meta-igneous rocks is preserved in the northern part of the pluton (fig. 5 on sheet 2). Most of the Ladron pluton is composed of coarse-grained granitic rock ranging from buff to orange in color. A late-stage facies, gradational with earlier phases, is generally white and locally aplitic or pegmatitic. With exception of the roof pendant, the pluton contains only a relatively small number of inclusions of surrounding metamorphic rocks. Although locally epidotized, the rocks are fresh compared to most samples of the adjacent Capirote pluton. Mineralogically, the pluton differs from the Capirote by the presence of both biotite and muscovite. More detailed descriptions of the pluton are given in Black (1964) and Cookro (1978).

Capirote pluton

The Capirote pluton crops out in several areas in the Ladron Mountains (fig. 5 on sheet 2) and is described in Black (1964), Condie (1976a), and Cookro (1978); it underlies most of the range. The contacts are structurally complex and poorly exposed. The pluton intrudes siliceous meta-igneous rocks in the northwestern and southern parts of the range and is intruded by the Ladron pluton along the eastern side of the range. Evidence of contact metamorphism is absent. Contacts with the meta-igneous rocks are generally concordant, although locally discordant. Most evidence favors syntectonic to post-tectonic emplacement. Constituent rocks range from buff to orange and from medium to coarse grained. The pluton is relatively free of pegmatites and aplites, but quartz veins are locally important. A granophyre occurring about 1 km east of Ladron Peak is tentatively included as a facies of the Capirote pluton. Although the granophyre is isolated from the pluton proper, its composition and degree of alteration are similar.

Inclusions of amphibolite, siliceous meta-igneous rock, and quartzite occur throughout the pluton and are particularly abundant in the Cerro Colorado area and along the eastern margin of the mountains. A zone containing up to 80 percent inclusions wraps around the northern edge of Cerro Colorado (Condie, 1976a). Quartzite and siliceous meta-igneous inclusions are texturally and mineralogically gradational with granitic rocks suggesting varying degrees of digestion and granitization by the pluton. An altered facies that occurs along the eastern side of the range is highly fractured and contains varying amounts of epidote, albite, and secondary quartz. The average composition of unaltered samples of the Capirote pluton is that of a quartz monzonite (table 5). Details of the mineralogy and textural relationships are further described by Black (1964) and Cookro (1978).

La Joyita pluton

The La Joyita pluton comprises most of the core of the La Joyita Hills, east of San Acacia, New Mexico (fig. 8 on sheet 2). The northern two-thirds of the exposure is composed of orange to red coarse-grained granite, often exhibiting a relict foliation that apparently was inherited from partially digested inclusions of schist and quartzite. The southern one-third of the area is composed of a medium- to coarse-grained biotite gneiss with minor amphibolite units and small exposures of intrusive foliated granite. The granite and gneiss are often imperceptibly gradational. Existing evidence suggests that the biotite gneiss represents a large inclusion composed dominantly of biotite schist, partially granitized and recrystallized during emplacement of the granite. The La Joyita granite differs from other Precambrian granitic plutons in central and south-central New Mexico by the relative abundance of small pegmatites and, locally, aplites. These pegmatites rarely extend for more than 50 m, range typically from a few centimeters to 30 cm in width, and often occur in swarms. Some of the major swarms are indicated on the geologic map (fig. 8 on sheet 2).

Polvadera pluton

The Polvadera pluton comprises most of the Precambrian exposure in the Lemitar Mountains (fig. 7 on sheet 2). The contact is exposed at two locations along the southern border. The pluton intrudes a metagabbro body north of the mouth of Corkscrew Canyon and amphibolites and quartzites in the small exposure southwest of Polvadera Peak (Woodward, 1973). The granitic rocks composing the pluton range in color from pink to tan and brown in more altered exposures. A few minor pegmatites and quartz veins with northeasterly strike cut the pluton. The dominant rock in the pluton is medium- to coarse-grained granite and is characterized by an unusually low amount of sodic plagioclase (table 5). Plagioclase is highly saussuritized, and biotite is partially replaced by chlorite. Mortar textures are common and reflect cataclastic deformation.

Magdalena pluton

The Magdalena pluton forms most of the east slope of the Magdalena Mountains (fig. 6 on sheet 2). The pluton intrudes fine-grained metaclastic rocks and metagabbro and is in turn crosscut by later metadiabase dikes. Inclusions of the country rocks are common near the pluton contacts. The pluton is composed of pink or orange granite and varies from fine grained to coarse grained. The grain size appears to increase from north to south. Major minerals are quartz, perthitic K-feldspar, sodic plagioclase, and biotite. Detailed descriptions of field relations and petrography are given in Loughlin and Koschmann (1942).

Oscura and Capitol Peak plutons

The Oscura pluton forms most of the core of the Oscura Mountains, and the Capitol Peak pluton forms most of the core of the northern San Andres Mountains

(sheet 3). Their similarity in mineralogy and composition suggests that they may be part of the same body. Contacts of the Oscura pluton are not exposed. The Capitol Peak pluton intrudes the amphibolite complex and gneisses east of Salinas Peak and quartzites and gneisses north and south of Cottonwood Canyon (sheet 3). Both plutons are composed of red to gray, medium- to coarse-grained quartz monzonite. Locally, the rocks are porphyritic. Biotite segregations locally impart a gneissic texture with a northwest trend and near-vertical dip. Gneiss and amphibolite inclusions (fig. 16) are also of minor importance in both bodies. Aplite dikes and narrow pegmatites occur in the plutons at several places, but are not numerous. The granitic rocks at the northern tip of the San Andres Range are fractured, pervasively altered, and locally mineralized with barite, galena, and sphalerite. The amphibolite-gneiss complex east of Salinas Peak may represent a roof pendant in the Capitol Peak pluton.

In thin section, the granitic rocks of these plutons are composed chiefly of feldspars and quartz (table 5 and fig. 28). Plagioclase forms twinned euhedral crystals with a compositional range of An₂₃ to An₃₄. Oscillatory zoning occurs in some plagioclase from the Oscura pluton. In contrast with the clear K-feldspar, the plagioclase is clouded with fine-grained alteration products such as sericite. Where in contact with K-feldspar, plagioclase has a clear albitic border zone, optically continuous with the core. Myrmekitic intergrowths of quartz and albite locally replace K-feldspar (fig. 28). Quartz occurs between feldspar grains and commonly exhibits undulatory extinction. K-feldspar is perthitic microcline or orthoclase. The dominant mafic constituent in both plutons is biotite, usually partly or completely altered to chlorite. Muscovite is prominent in some samples and forms large poikilitic crystals; it probably formed after most other minerals crystallized. Accessory constituents include sphene, zircon, apatite, and opaque minerals. Small garnets occur in some of the aplitic varieties (fig. 28). Epidote is a rare secondary mineral. Sphene forms up to two percent of some samples from the Oscura pluton. Pale reddish-brown, lozenge-shaped crystals show idiomorphic overgrowths on rounded cores (fig. 28). The boundary between the two zones is outlined by opaque mineral grains.

Oscillatory zoning in the plagioclase indicates derivation of the Oscura quartz monzonite from a melt. Refractory minerals such as sphene may have been present in the melt as rounded grains that developed their overgrowths during later crystallization. After the main stage of crystallization, and upon reaching solvus temperatures, K-feldspar separated into K-rich and Na-rich phases, now in perthitic intergrowth. The albite component had sufficient mobility to form oriented overgrowths on plagioclase (An₂₆) crystals formed earlier. Ordering of the K-feldspar converted orthoclase to microcline; that this process is not complete is indicated by K-feldspar in a wide range of structural states (Budding and Condie, 1975).

Mockingbird Gap pluton

The Mockingbird Gap pluton is exposed in a small area in the south-central Oscura Mountains and again in

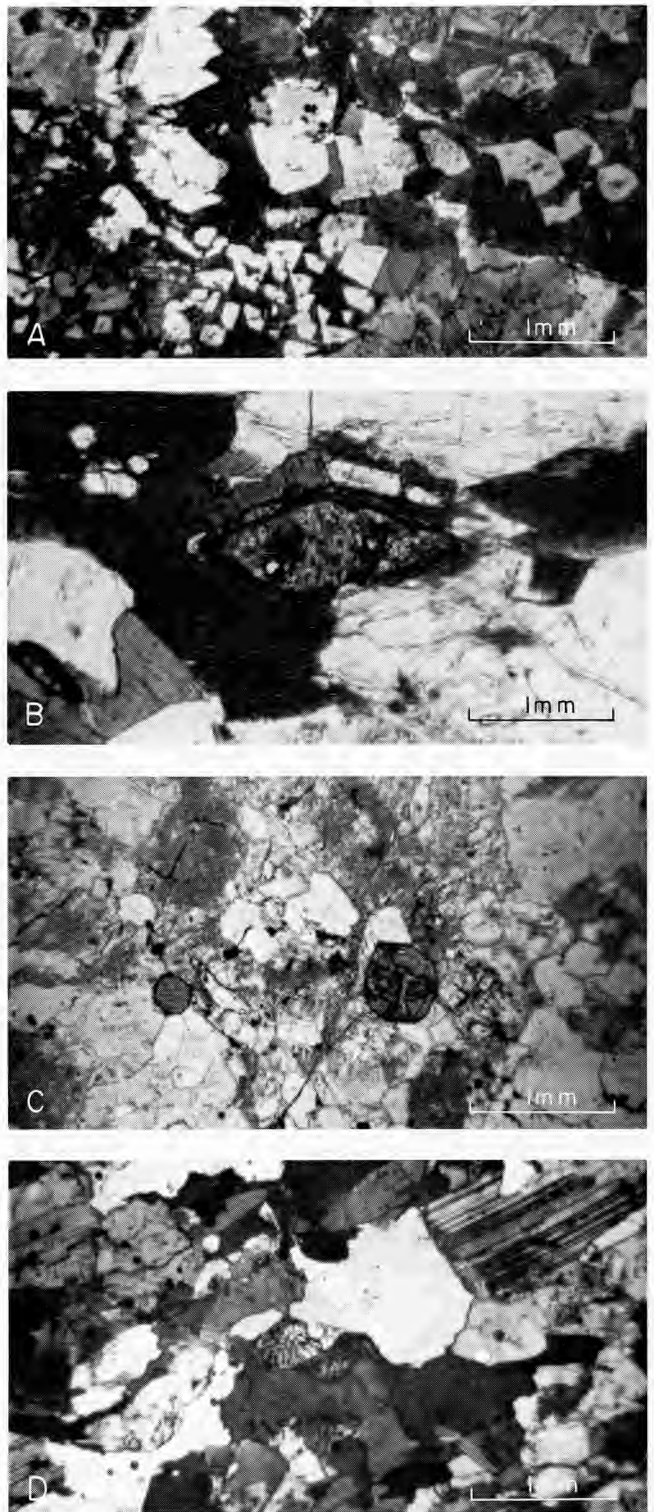


FIGURE 28—PHOTOMICROGRAPHS OF GRANITIC ROCKS. A) Granite (NP-82); Los Pinos pluton. Micrographic intergrowth of quartz and K-feldspar; crossed polars. B) Quartz monzonite (OSC-26); Oscura pluton. Quartz, oligoclase, K-feldspar (partly replaced by myrmekite in center), and biotite (gray); crossed polars. C) Aplitic quartz monzonite (OSC-29); Oscura pluton. Quartz and feldspar with two small garnet crystals (partly replaced with chlorite); uncrossed polars. D) Quartz monzonite (OSC-26); Oscura pluton. Overgrowth on sphene; dark mineral is biotite; uncrossed polars.

the northern San Andres Mountains (sheet 3). Except for the fault contact with the Capitol Peak pluton in the San Andres Mountains (north of Johnson Park Can-

yon), the contact relationships with the Oscura and Capitol Peak plutons are unknown. It is probable, however, that the Mockingbird Gap pluton intrudes these other bodies. The pluton is composed of gray to buff, medium-grained, locally porphyritic quartz monzonite. It differs from other Precambrian plutons in the White Sands Missile Range because it contains small amounts of hornblende in addition to biotite.

Strawberry Peak and Mayberry plutons

The Strawberry Peak pluton underlies a small area in the vicinity of Sulphur Canyon in the southern San Andres Mountains; the Mayberry pluton occurs between Lost Man and San Andres Canyons farther south in the range (sheet 3). The Strawberry Peak pluton is intrusive into the upper part of the phyllite-quartzite succession dominating the central part of the southern San Andres Mountains. Its contacts are generally concordant. The Mayberry pluton intrudes the lower part of this succession and contains numerous inclusions of the surrounding rocks. Amphibolite inclusions are particularly abundant, the largest occurring in the Mayberry pluton in San Andres Canyon.

The average modes indicate that white to buff, medium- to coarse-grained granite is the chief rock type in both plutons (table 5). Perthitic microcline exceeds plagioclase (An_{25}) in abundance. Biotite, partly or entirely altered to chlorite, is the principal mafic constituent. Allanite, apatite, zircon, and sphene are accessory minerals.

San Andres pluton

The San Andres pluton is exposed between San Andres and Little San Nicholas Canyons in the southern San Andres Mountains (sheet 3). It contains numerous inclusions of amphibolite and quartzite and is intrusive into the gneiss complex just north of the mouth of Little San Nicholas Canyon. The pluton is altered and exposures are poor in the vicinity of Salt Canyon. It is composed of white to red, medium-grained quartz monzonite and contains a wide range of dark minerals (0-5 percent). Myrmekitic replacement of microcline is widespread, and epidote and calcite were observed as secondary minerals.

Mineral Hill pluton

The Mineral Hill pluton underlies a large part of the southern San Andres Mountains (sheet 3). The only contact exposed is on the north where the pluton intrudes quartzite. Much of the pluton north of Black Mountain seems highly fractured and altered. The dominant rock type is white to buff, fine- to coarse-grained quartz monzonite. Biotite-rich schlieren and amphibolite inclusions are locally important, and they seem to represent partially digested fragments of country rock. Principally because of alteration, the dark mineral content ranges from nearly 0 to 8 percent. Secondary albite may be abundant.

Granitic rocks of the Caballo Mountains and Red Hills

Three different types of granitic rock have been distinguished in the Caballo Mountains and Red Hills (fig. 11 on sheet 2). At the northern end of the range (poorly exposed for the most part) is a gneissic granite pluton. This pluton is characterized by an abundance of gneiss and mica-schist inclusions exhibiting varying degrees of granitization, deformation, and alteration (Mason, 1976). Intruded into this complex terrane and composing most of the central part of the Caballos are bodies of brick-red syenite and granite. The southern part of the range and the Red Hills are composed chiefly of the Caballo pluton. This pluton forms subdued outcrops ranging from orange to buff in color; it is in fault contact with the red granite in Longbottom Canyon and intrudes the amphibolite complex between Longbottom and Burbank Canyons.

The original mineralogical composition of the gneissic pluton on the north is difficult to ascertain because of the large volume of partially to completely digested inclusions; the pluton is probably a granite or quartz monzonite. The syenites are composed of as much as 90 percent microcline with only minor sodic plagioclase (5 percent) and quartz (≤ 5 percent). Staatz and others (1965) have pointed out that these rocks are similar to fenites and have suggested a metasomatic origin for them. The Caballo pluton is composed of orange to buff, medium- to coarse-grained quartz monzonite and is locally gneissic.

Miscellaneous plutons

The Tajo pluton is exposed in several fault-bounded blocks about 8 km east of Socorro (fig. 10 on sheet 2). The similarity of the granitic rocks in all of the exposures suggests that they are part of the same pluton. Although some fresh exposures exist in incised canyons, most exposures are weathered and altered. Tertiary veins of fluorite-barite are common in some areas. Granitic rocks range from medium- to coarse-grained and from orange to buff in color. Preliminary examination of thin sections indicates that quartz monzonite is the common rock type.

Precambrian granitic rocks are exposed in the fault-bounded Tonuco uplift at San Diego Mountain south of Hatch (Seager and others, 1971; fig. 13 on sheet 2). These rocks are highly altered and weathered and poorly exposed. They are locally gneissic and contain amphibolite and schist inclusions. Thin-section analysis indicates that quartz monzonite is the chief rock type.

Several small exposures of granitic rock, probably representing apophyses of a larger pluton at depth, are exposed in the Monte Largo Hills (Lambert, 1961; Huzarski, 1971; sheet 1). These occurrences have both gradational and crosscutting relationships with surrounding rocks. Aplites and pegmatites (sometimes tourmaline-bearing) are moderately abundant both in the granitic rocks and in the metamorphic terranes. The average composition of the granitic rocks is that of a muscovite-bearing quartz monzonite (table 5).

The Precambrian exposure along the western side of the Fra Cristobal Mountains (fig. 12 on sheet 2) is composed of heterogeneous medium- to coarse-grained, pink to white granitic rocks that contain varying amounts of partially digested metamorphic rocks (Jacobs, 1956; McCleary, 1960). Quartz veins are abundant.

Precambrian hornblende-syenite and syenite crop out at Pajarito Mountain southwest of Hondo, New Mexico (fig. 18 on sheet 2). The syenite is intruded into the hornblende-syenite, which is often broken and brecciated. Pegmatitic phases are common in syenite. The rocks are composed principally of K-feldspar, sodic amphibole, and clinopyroxene.

The White Sands pluton (new name) crops out on the extreme eastern tip of the eastern ridge of the Organ Mountains about 5 km south of White Sands, New Mexico (fig. 17 on sheet 2). The contacts of the pluton

with older rocks are not exposed; the pluton is intruded on the west by a Tertiary pluton. Dunham (1935) gives a generalized geologic description of the area. The Precambrian granitic rock is a coarse-grained, porphyritic quartz monzonite containing large K-feldspar mega

(≤ 3 cm long). These crystals are partly replaced by myrmekite. Pegmatites and aplites are minor. At least two periods of aplite injection are recorded (fig. 16). In general, the rock is relatively free from the effects of alternation.

The Organ pluton crops out along Rattlesnake Ridge in the southern Organ Mountains. This pluton is similar to the White Sands pluton except for the presence of a medium-grained facies (Dunham, 1935). It contains a large inclusion of gneiss, but contacts with country rocks are not exposed. The area lies in a target range of the Fort Bliss Military Reservation and is inaccessible for study.

Structural geology

SMP block

The SMP block includes the Sandia, Manzanita, Manzano, and Los Pinos Mountains (sheet 1). Cleavage or foliation is developed to varying degrees in most of the meta-igneous and metasedimentary rocks in the SMP block. Fine-grained, clastic sedimentary rocks are generally phyllites or schists. Amphibolites range from massive to schistose. Siliceous meta-igneous rocks and many quartzites are massive and lack penetrative foliation. Locally, however, both rock types are intensely sheared. Slip- and flow-cleavage are well developed in most of the phyllites and schists; fracture cleavage is well developed in most of the phyllites and schists, but may occur in all rock types. Although granitic plutons are generally concordant, all but the Manzanita are locally discordant to the foliation in surrounding rocks. Occasional foliation in the granitic rocks seems to be relict from partially digested inclusions and roof pendants.

The overall trend of foliation ranges from N. 20-30° E. in the southern Manzano and Los Pinos Mountains to N. 40-50° E. in the Manzanita Mountains and Monte Largo Hills (sheet 1). Foliation trends are variable in the rocks surrounding the Ojita pluton and in Rincon Ridge in the northern Sandias. Foliation dips are variable, generally southeastward north of the unconformity in the central Manzanos and vertical or westward south of this unconformity. In general, foliation and slaty cleavage approximately parallel bedding; the maximum divergence between the two is ≤ 15 degrees. The Manzanita pluton exhibits a strong foliation parallel to that in surrounding metasedimentary and meta-igneous rocks.

A break in the stratigraphy of the SMP block occurs at the angular unconformity northwest of Comanche Canyon (sheet 1). At this point, a massive white quartz

ite striking N. 30° E. and dipping about 50° SE. unconformably overlies a section composed dominantly of fine-grained clastic metasediments striking almost east-west and exhibiting variable but steep dips. Assuming the overlying section was deposited horizontally, the underlying beds would have dipped about 20° SW. at the time of deposition (Reiche, 1949). Very little relief is evident on the unconformity. The unconformity is important because it divides the Precambrian section in the SMP block into two associations (table 1). The older section characterizing the northern Manzano, Manzanita, Sandia, and Monte Largo areas is composed chiefly of phyllites and schists. Above the unconformity, siliceous meta-igneous rocks are associated with phyllites, schists, and quartzites; mafic meta-igneous rocks are less important.

The only large fold recognized in the SMP block is described by Stark (1956) in the southern Manzano Mountains and seems to be a syncline. It trends about N. 30° E. , with the axis nearly horizontal to slightly plunging south-southwest (sheet 1). The trace of the axial plane approximately follows the center of the exposure of Sevilleta Formation. Four features suggest that it is a syncline (Stark and Dapples, 1946; Stark, 1956; Beers, 1976) : 1) the presence of the unconformity at the base of the west limb; 2) rare crossbedding in the quartzites, indicating a younging towards the fold axis; 3) minor folds especially well developed in the eastern limb, also suggesting a younging towards the fold axis; and 4) foliation steeper than bedding in the eastern limb. The syncline becomes progressively overturned from south to north. In the Los Pinos Mountains, dips are about 45° W., changing to vertical in the vicinity of Manzano Peak and finally to about 60° E. in the Comanche Canyon area. The White Ridge Formation is much thinner on the western than on the eastern limb;

which quartzite unit on the western limb represents the Sais Quartzite is difficult to determine. Because of the large thickness of schists and phyllites on the western limb, however, the basal quartzite above the unconformity probably does not represent the Sais (as suggested by Reiche, 1949).

Whether the section is right-side up is not entirely clear from evidence in the northern Manzano and Manzanita Mountains. Minor fold orientations are variable. However, the relationships of foliation to bedding and the rare preservation of crossbedding (Reiche, 1949) suggest that the section is upright. If this conclusion is correct, the oldest preserved rocks in the SMP block are the Tijeras Greenstone and Cibola Gneiss (fig. 24) and their possible equivalents along strike in the Monte Largo Hills. The age relation of the sections north and south of the Sandia plutons, however, is unknown.

Drag folds are common in the SMP block, ranging in size from a few centimeters to—rarely—10 m. Beers (1976) recognizes at least four sets of drag folds in the Los Pinos Mountains. The most prominent drag folds in the area have axial planes paralleling the foliation. Some of the largest are shown on geologic map (sheet 1) south of Manzano Peak and in the Coyote Canyon area. Drag folds in the Cibola Gneiss suggest that it represents the overturned limb of a syncline where the axial plane has the same strike as the foliation (Lodewick, 1960). Drag folds in the Tijeras Greenstone suggest that it represents the eastern upright limb of an anticline (Bruns, 1959).

Only one major fault of Precambrian age, the Tijeras fault, is recognized in the SMP block. This fault, which strikes N. 45° E. and dips 70° NW., separates the Cibola Gneiss and the Tijeras Greenstone in the northern Manzanita Mountains. Although the Tijeras fault was also active during early Cenozoic time (Kelley and Northrop, 1975), the large amount of altered and silicified fault breccia found only in the Precambrian rocks adjacent to the fault suggests Precambrian movement (Kelley, 1959). The Precambrian motion appears to have been high-angle reverse faulting from the northwest (Bruns, 1959). A second fault, the Moore fault, has been suggested between the Tijeras Greenstone and overlying quartzites (Kelley and Northrop, 1975). The contact between these units, however, is not exposed. Remnants of metasedimentary rock and metatuff in the greenstone complex, which seems to be composed primarily of diabase sills, are equally consistent with an intrusive contact between these units. Many small faults of probable Precambrian age, mostly high-angle normal or reverse faults, occur throughout the area. They are generally characterized by breccia and mylonite zones, which are often highly silicified. The pegmatites in the Rincon Ridge area seem to have been emplaced along Precambrian fracture systems.

Existing data suggest the existence of at least two periods of Precambrian deformation in the SMP block and Monte Largo Hills. The first period, involving only the rocks beneath the Comanche Canyon unconformity, is characterized by northwest-southeast compression and is accompanied by regional low-grade metamorphism. This deformation resulted in isoclinal folding about northeast-trending axes and the production of drag folds and various types of cleavage. During the

final stages of this deformation, the Tijeras thrust fault formed. A second period of regional metamorphism (recognized in the southern SMP block) and compression also directed in a northwest-southeast direction occurred after formation of the younger rocks above the unconformity. This period—equivalent to the first period of deformation described by Mallon (1966) in the Los Pinos Mountains—is characterized by isoclinal folding and the development of penetrative cleavage and foliation. Most granitic plutons were emplaced during the late stages of this deformation. The effects of the second deformation have not yet been defined in the section beneath the unconformity. The late stages of this period of deformation are characterized by cataclastic structures and the development of nonpenetrative flexure slip and cleavage folds and of fracture cleavage (deformations 2 and 3 of Mallon, 1966). Finally, the existence of southeast-striking open folds in the Manzanita Mountains (Reiche, 1949) seems to require a late, minor east-west compression in this area.

San Andres Mountains

East of Salinas Peak in the northern San Andres Mountains, the curved belt of amphibolite and associated gneiss and quartzite has a northeasterly trend with variable, steep dips of foliation (sheet 3). This complex seems to represent a large roof pendant within the Capitol Peak pluton. The synformal shape of the belt plunging to the southeast may be the result of deformation during forceful intrusion of the pluton. The thick sequence of supracrustal rocks between Sulphur and Lost Man Canyons (sheet 3) exhibits a predominant north-northwest strike with steep easterly dips. Crossbedding preserved in quartzites and arkosites indicates that the section faces to the east. Foliation in this section, especially in the Hembrillo Canyon area, ranges from poorly developed to well developed. Many of the meta-igneous units in the section are massive and do not exhibit any foliation.

Several phyllite units well exposed in Sulphur Canyon contain subangular to subrounded quartzite fragments of pebble- to cobble-size around which the layering is disturbed. Such structures are commonly interpreted to have formed from intense deformation of interlayered quartzite-phyllite sequences (that is, the clasts represent boudins). However, this interpretation does not explain the origin of phyllites in Sulphur Canyon because adjacent beds in the canyon section are relatively undisturbed and some quartzites retain primary crossbedding. Instead, these structures may represent disrupted quartzite beds produced by gravitational gliding or slumping in the sedimentary basin.

Pederal Hills

The strike of foliation (approximately parallel to bedding) in metamorphic rocks of the Pederal Hills (fig. 4 on sheet 2) ranges from about N. 70° E. (dip ~ 30° SE.) in the quartzites at the northern end of the hills to east-west (dip ~ 70° S.) in the schists in the central and southeastern parts of the area. The schist and granitic rocks are highly sheared in portions of the area. The Pederal pluton intrudes the surrounding schists and

contains inclusions of them. The intense shearing may have occurred in response to forceful intrusion of the pluton (Gonzalez, 1968; Gonzalez and Woodward, 1972) or may have occurred after its emplacement.

The oldest structures recognized in the area are small isoclinal, nearly recumbent, folds (wave lengths of 5-10 cm) in the quartzites (Gonzalez and Woodward, 1972). The axial planes of these folds parallel foliation, dip about 65° S., and formed during regional metamorphism. A few large, tightly compressed folds (wave lengths about 150 m) occur in the quartzites (fig. 4 on sheet 2). Smaller, tightly compressed open folds (wave lengths 5-10 cm), generally trending parallel to foliation, also occur in the schists. Several high-angle faults of probable Precambrian age have been mapped in the quartzites, and one has been mapped in the central part of the schists. Such faults are generally characterized by silicified breccia zones ≤ 30 cm wide. Overall, the structural history fits within the framework described for the southern part of the SMP block.

Ladron Mountains

Well-preserved crossbedding in the quartzites and local dragfolding indicate that the quartzite-amphibolite-phyllite section south of Ladron Peak represents the eastern limb of a northeasterly trending anticline (Condie, 1976a). The siliceous meta-igneous sequence in the northeast part of the range strikes N. 45° W. and dips at angles of 40-60° SW. This sequence has been greatly disrupted by emplacement of the Capirote and Ladron plutons; it can be traced around the northeastern part of the range and then—by the presence of inclusions in the Capirote pluton in varying stages of digestion—south along the eastern side of the range and into the Cerro Colorado area (fig. 5 on sheet 2). Drag folds are common only in the phyllites, amphibolites, and meta-igneous rocks. High-angle faults of probable Precambrian age occur in some parts of the range. These are generally characterized by mylonitization and silicification. Some of the larger faults are shown on the geologic map (fig. 5 on sheet 2).

The similarity of rock associations and structural patterns in the Ladrons to those in the southern Manzano and Los Pinos Mountains suggests a similar structural history. The Capirote pluton seems to have been emplaced during the late stages of deformation. A late cataclastic deformation is recorded by fracture cleavage and local mylonitization. The emplacement of the Ladron pluton preceded or accompanied this deformation.

Other areas

Structural trends in the Magdalena Mountains north of Water Canyon are east-northeast and change to a

more northerly direction near the Magdalena pluton (fig. 6 on sheet 2). Dip of bedding and foliation is to the south, and primary structures in the metasedimentary rocks indicate that the sequence faces the same direction. In the Coyote Hills from southeast to northwest, gneissic foliation shows a gradual change from easterly strikes and northward dips to northerly strikes and near-vertical dips (fig. 9 on sheet 2). These attitudes define an overturned synform plunging west-northwest at about 40 degrees. Near the western edge of the Precambrian exposure, structural trends have been rotated to the north by Cenozoic faulting.

A northerly trend characterizes the granitic rocks in the La Joyita Hills, where partially digested inclusions in the granitic rocks define a pattern changing from northerly to northeasterly (fig. 8 on sheet 2). A northerly trend also characterizes the amphibolites and quartzites in the Lemitar Mountains to the west (fig. 7 on sheet 2). The amphibolite complex in the southern Caballo Mountains exhibits a general easterly trend with variable steep dips (fig. 11 on sheet 2). As with the amphibolite complex in the northern San Andres Mountains, this complex appears to represent a roof pendant in a granitic pluton.

Conclusions

The regions in central and south-central New Mexico having the most continuous exposures of supracrustal successions are the SMP block and the southern San Andres Mountains. With little deviation, these areas exhibit north-northeast and north-northwest trends, respectively; major fold axes seem to be subhorizontal in both areas. More complex structural patterns, often exhibiting significant deviations from these two trends, occur in the smaller Precambrian exposures (such as in the Caballo, northern San Andres, Ladron, Magdalena, and Coyote Hills exposures) and may have resulted from rotation and other deformation accompanying the forceful injection of surrounding granitic plutons.

Evidence for large-scale horizontal transport (such as recumbent folds or low-angle thrusts) is not present. The tectonic environment seems to have been one where vertical movements predominated, perhaps because of vertical basement-block motion. The formation of narrow synclinal folds or synclinoria may have been initiated by gravitational gliding of supracrustal rocks from uplifts into adjoining basins. Subsequent compression in an east-west direction (± 20 degrees) deformed these troughs into tightly compressed synclines with steep or overturned limbs. Contemporaneous or later forceful emplacement of granitic plutons modified the north-trending fold belts and produced local deviation from the main structural grain.

Metamorphism

The effects of both regional and contact metamorphism are recorded in Precambrian rocks from central and south-central New Mexico. Difficulties are often encountered in determining the stable mineral associations of these rocks. Many show evidence of retrograde metamorphism—such as chloritization of biotite and garnet, sericitization of aluminum silicates and feldspars, and saussuritization of plagioclase.

Another problem is the incomplete recrystallization of mafic rocks formed initially at high temperature and subsequently metamorphosed under greenschist-facies conditions. Such rocks may contain plagioclase of relatively high anorthite content (An_{30} - An_{50}) even though the surrounding metasedimentary rocks contain sodic plagioclase and other minerals characteristic of the greenschist facies. This phenomenon is particularly noticeable in the metadiabases and metagabbros that retain ophitic and subophitic textures and are composed of hornblende-actinolite, andesine or oligoclase, and varying amounts of epidote. Most of the amphibolites, however, are completely recrystallized, and their mineral associations are compatible with those of the surrounding metamorphic rocks.

Rocks that have undergone regional metamorphism are exposed in the SMP block, Monte Largo and Pederal Hills, and in the Ladron, Magdalena, and central San Andres Mountains; small exposures are also found in the Lemitar and southern Caballo Mountains and in the Coyote Hills. For the purpose of considering metamorphic mineral assemblages, the rocks can be grouped into four compositional categories: 1) mafic meta-igneous rocks (metadiabase, metagabbro, chlorite schist, amphibolite); 2) quartzose rocks (quartzite, arkosite, conglomeratic quartzites, siltite); 3) pelitic rocks (phyllites, mica schists, gneisses); and 4) siliceous meta-igneous rocks. A summary of the major metamorphic minerals in these rock types as a function of increasing metamorphic grade is given in table 6.

Nearly unmetamorphosed volcanic rocks are exposed in and near Hembrillo Canyon in the central San Andres Mountains. This sequence, composed largely of quartzite, arkosite, phyllite, schist, and metadiabase sills, contains two red siliceous metavolcanic units just east of the sub-Cambrian unconformity. The volcanic rocks seem to be tuffs and contain rounded phenocrysts of quartz, K-feldspar, and albite in a fine-grained groundmass of K-feldspar, chlorite, sericite, and sphene. Spherulitic texture is still preserved in some samples. Others contain lensoid fragments composed principally of sericite that may represent recrystallized, flattened pumice fragments.

Rocks of the greenschist facies or rocks transitional between the greenschist and amphibolite facies are widespread in the Precambrian terranes of central and south-central New Mexico. They are well exposed in the SMP block and in the Magdalena, Ladron, and central San Andres Mountains. Characteristic mineral assemblages are as follows:

- quartz-muscovite-chlorite
- quartz-muscovite-chloritoid
- quartz-muscovite-biotite-albite

- quartz-biotite-K-feldspar-albite
- quartz-muscovite-biotite-garnet-(K-feldspar)
- quartz-biotite-garnet-(K-feldspar)-(albite)
- actinolite-chlorite-epidote-albite-(prehnite)
- hornblende-chlorite-epidote-(albite)
- hornblende-epidote

Rocks of the amphibolite facies are characterized by the appearance of staurolite and sillimanite in the pelitic and quartzose members and by the disappearance of albite (table 6). Amphibolite-facies terranes occur in the Pederal and Monte Largo Hills, in the northern San Andres Mountains (Salinas Peak area), in the southern Caballo Mountains, and in the Coyote Hills exposure. Kyanite is preserved in only a few localities, generally in quartz-muscovite schist. The assemblages quartz-muscovite-staurolite and quartz-muscovite-kyanite characterize the schists in the Pederal Hills (Gonzalez, 1968). In mafic rocks, the assemblages hornblende-oligoclase-epidote- (quartz) and hornblende-andesine-(epidote)-(quartz) occur in many localities.

ACF and AKF values for rocks listed in appendix 2 are shown and defined in fig. 29. Because the total Fe content of the analyses is in the form of Fe_2O_3 , part of this amount was allocated for magnetite, which makes up about three percent in the mafic rocks and one percent in the siliceous rocks. The remaining iron-oxide was recalculated as FeO and added to the MgO to determine the F value. In the ACF diagram, the mafic rocks plot very close to the actinolite-epidote or hornblende-plagioclase joins. The distribution of siliceous meta-igneous rocks on the AKF diagram vary widely, but all fall within the subtriangle microcline-muscovite-biotite indicative of the common mineral association found in these rocks.

TABLE 6—PROGRESSIVE CHANGES IN METAMORPHIC MINERAL ASSEMBLAGES IN PRECAMBRIAN ROCKS OF CENTRAL AND SOUTH-CENTRAL NEW MEXICO; _____ = major phase, ---- = minor phase.

	Greenschist facies	Amphibolite facies
Mafic meta-igneous rocks	$An_{0-10} \pm An_{20-25}$	$An_{20}-An_{40}$
plagioclase	_____	_____
epidote	_____	-----
amphibole	_____	_____
chlorite	_____	-----
calcite	-----	-----
quartz	-----	-----
Quartzose, pelitic, and siliceous meta-igneous rocks		
chlorite	_____	-----
muscovite	-----	-----
biotite	-----	-----
garnet	-----	-----
kyanite	-----	-----
sillimanite	-----	-----
plagioclase	$An_{0-10} \pm An_{20-25}$	$An_{20}-An_{40}$
quartz	_____	_____
chloritoid	-----	-----
K-feldspar	_____	-----
staurolite	-----	-----

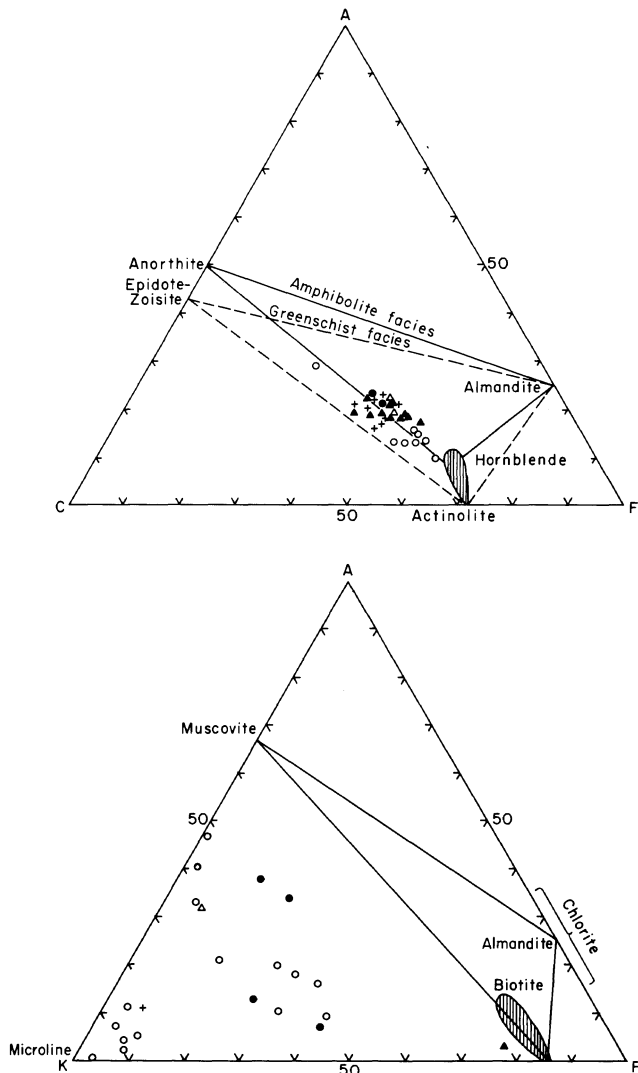


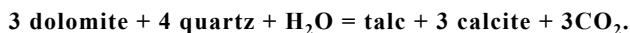
FIGURE 29—ACF AND AKF DIAGRAMS SHOWING DISTRIBUTION OF METAMORPHIC ROCKS FROM THE PRECAMBRIAN OF CENTRAL AND SOUTH-CENTRAL NEW MEXICO. ACF: A = Al₂O₃ + Fe₂O₃ - (Na₂O + K₂O); C = CaO; F = FeO + MgO + MnO. AKF: A = Al₂O₃ + Fe₂O₃ - (CaO + Na₂O); K = K₂O; F = FeO + MgO + MnO. Symbols: • = Ladron Mts., ° = Los Pinos-Manzano Mts., + = San Andres Mts., Δ = Magdalena Mts., ▲ = Manzanita Mts.

Obvious zones of contact metamorphism occur adjacent to only four plutons: North Sandia, Pederal, Priest, and Monte Largo Hills. Two zones representative of the hornblende-hornfels facies have been reported adjacent to the North Sandia pluton (Green and Callender, 1973). The inner zone is characterized by the assemblage quartz-K-feldspar-biotite-sillimanite and the outer zone by quartz-andalusite-muscovite. Intersecting univariant reaction curves suggest a temperature and P_{H_2O} at the contact of 600–650° C and 2 kb, respectively. The southern contact zone of the Pederal pluton is characterized by hornblende and tourmaline-bearing assemblages (Gonzalez, 1968). A description of mineral zonation in the contact aureole adjacent to the southern border of the Priest pluton is given by Staatz and Norton (1942), Basham (1951), and Stark (1956). In progressing outward from the pluton over 150–350 m, the following zones are recognized: 1) garnet-pseudosillimanite-muscovite, 2) sillimanite, 3)

epidote. The pseudosillimanite may represent muscovite pseudomorphs after andalusite. Andalusite (and possibly sillimanite) reported in gneisses and schists adjacent to the Monte Largo Hills pluton is of contact metamorphic origin. The sillimanite that occurs in the Cibola Gneiss adjacent to the South Sandia pluton and in gneissic inclusions in the Capitol Peak pluton (near the mouth of Cottonwood Canyon), as well as recently reported cordierite from gneissic inclusions in granitic rocks of the northern Caballo Mountains (Mason, 1976), may also be of contact metamorphic origin.

The succession of regional metamorphic mineral associations observed in the Precambrian rocks of New Mexico are indicative of the Barrovian (kyanite-sillimanite) facies series (Miyashiro, 1961). The occurrence of chloritoid in the greenschist facies and the presence of staurolite, kyanite, and sillimanite are especially indicative of P-T (pressure-temperature) conditions of this facies series. Fig. 30 is a stability diagram of pertinent minerals, showing the proposed facies-series evolution.

An important aspect of the lower grades of metamorphism concerns the stability of talc occurring in Hembrillo Canyon. The stability and formation temperature of talc depends on the partial pressure of CO₂ if the mineral is produced from the reaction:



This reaction requires siliceous dolomite for the production of the talc; however, the reaction-product calcite is absent from the assemblage. A partial chemical analysis of the talc rock (L. Brandvold, personal communication, 1975) shows that MgO = 25.8 percent and Al₂O₃ = 0.06 percent; Ni and Zn are present in the 100-ppm range, and Cu, Pb, Co, Cr, Mo, and Cd are less than 20 ppm. A more plausible explanation for this talc occurrence is the metamorphism of a layer rich in magnesium-montmorillonite, possibly derived from a volcanic ash unit similar to those units found nearby in

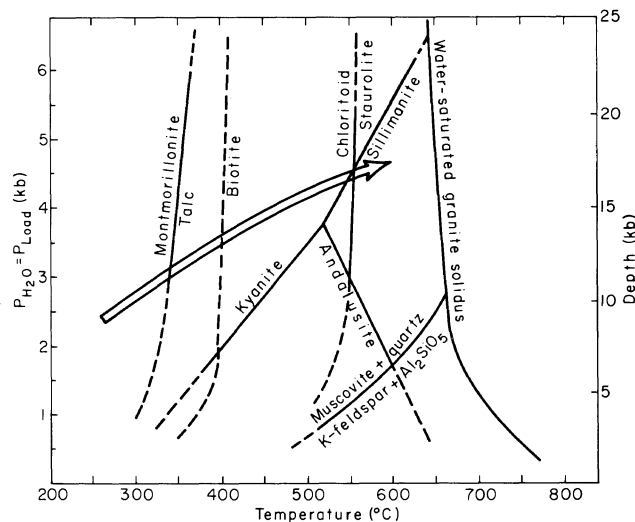


FIGURE 30—P-T (PRESSURE-TEMPERATURE) DIAGRAM OF PHASE RELATIONS AND PROBABLE COURSE OF PROGRESSIVE METAMORPHISM IN PRECAMBRIAN ROCKS OF CENTRAL AND SOUTH-CENTRAL NEW MEXICO. Equilibrium curves after Evans (1965), Holdaway (1971), Hoschek (1969), Metz and Puhan (1970, 1971), Metz and Winkler (1963), Turner (1968), and Winkler (1974).

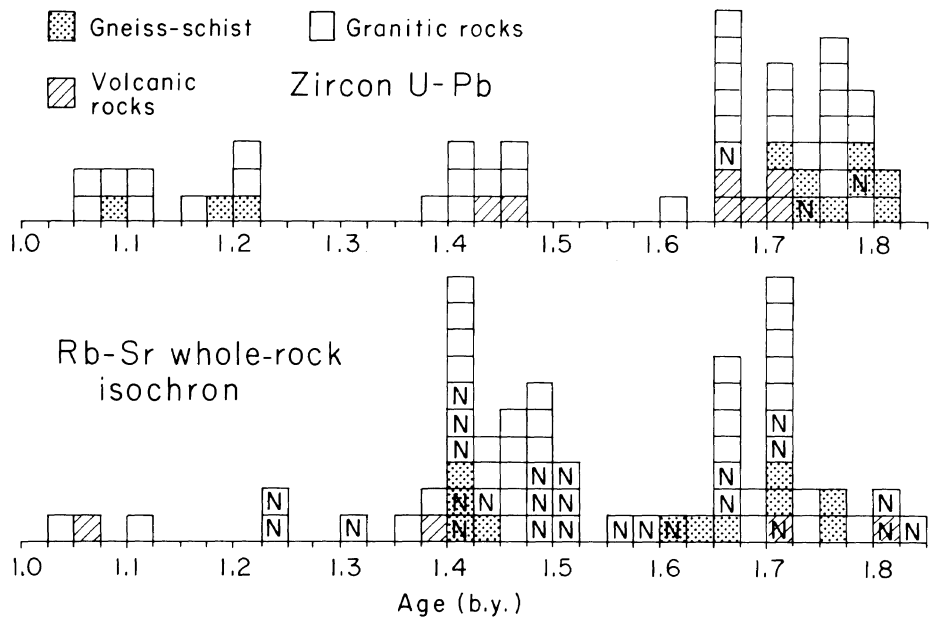


FIGURE 31—HISTOGRAMS OF U-Pb ZIRCON AND WHOLE-ROCK Rb-Sr ISOCHRON AGES FROM THE SOUTHWESTERN UNITED STATES compiled from many references. Dates from New Mexico are indicated with the letter N. Decay constants: $\lambda_{Rb^{87}} = 1.39 \times 10^{-11} \text{yr}^{-1}$; $\lambda_{U^{238}} = 1.54 \times 10^{-10} \text{yr}^{-1}$; $\lambda_{U^{235}} = 9.72 \times 10^{-10} \text{yr}^{-1}$.

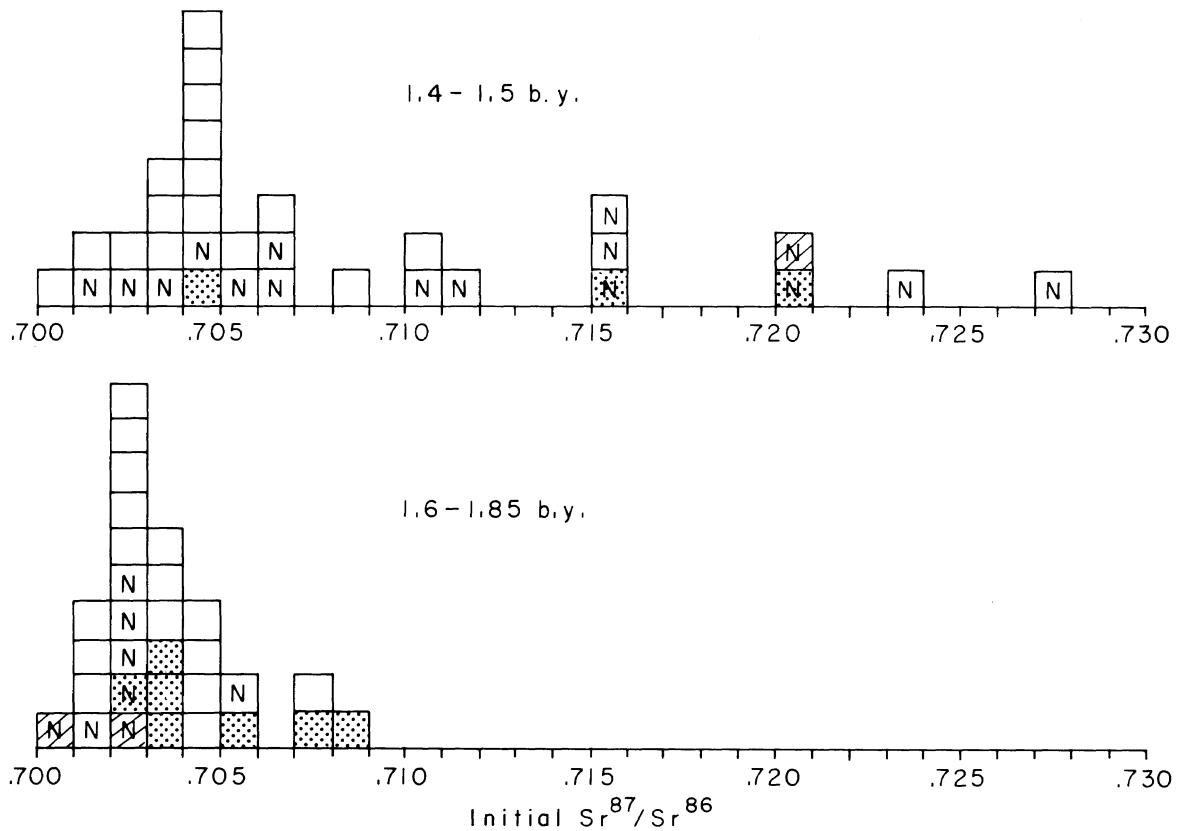


FIGURE 32—INITIAL Sr^{87}/Sr^{86} RATIOS OF WHOLE-ROCK ISOCHRONS FROM THE SOUTHWESTERN UNITED STATES. Symbols as in fig. 31; New Mexico ratios are indicated with the letter N.

Hembrillo Canyon. Metz and Winkler (1963) observed the formation of talc from magnesium-montmorillonite in the temperature range from 275° C to 300° C and in the pressure interval of 700 to 2,000 bars with a partial pressure of CO₂ near zero (fig. 30).

Amphibolite-facies metamorphism is characterized by the presence of staurolite and sillimanite and by the formation of calcic plagioclase at the expense of sodic plagioclase and epidote above the peristerite solvus 450-500° C. The proposed facies series implies a geothermal gradient of about 40° C per km depth. This steep gradient is important because it provides heat in the lower crust; this heat may cause partial melting and

produce granitic magmas. Most of the Precambrian rocks in central and south-central New Mexico were buried to depths of 10-12 km and heated to maximum temperatures of 400-500° C. In the northern San Andres and Caballo Mountains and in the Monte Largo, Coyote, and Pedernal Hills, rocks were buried to depths of 12-15 km and metamorphosed at temperatures of 500-550° C. In the Hembrillo Canyon area, the terrane was metamorphosed at a maximum temperature of 350° C and at a probable depth of 5-8 km. Contact metamorphism was superimposed on the regional metamorphism in central and south-central New Mexico, recording temperatures of 600-650° C.

Geochronology

Published Precambrian radiometric ages in central and south-central New Mexico have been compiled by Condie. When necessary ages were recalculated using $\lambda_{\text{Rb}}^{87} = 1.39 \times 10^{-11} \text{ yr}^{-1}$, $\lambda_{\text{U}}^{235} = 9.72 \times 10^{-10} \text{ yr}^{-1}$ and $\lambda_{\text{U}}^{238} = 1.54 \times 10^{-10} \text{ yr}^{-1}$. Histograms of U-Pb zircon ages and Rb-Sr whole-rock isochron ages from southern California, Sonora, Arizona, Colorado, New Mexico, and west Texas are given in fig. 31. Major periods of granitic plutonism are recorded at 1.7-1.8, 1.65, and 1.4-1.5 b.y., with a distinct minimum between the 1.65- and 1.7-b.y. events. Younger ages of 1.0-1.3 b.y. characterize the west Texas and southern New Mexico Precambrian; isolated ages in this range, however, are reported in other parts of the Southwest. New Mexico dates are noted in fig. 31.

A summary of the major Precambrian events in central and south-central New Mexico deduced from available geologic and geochronologic data is given in table 7. The oldest radiometric dates in New Mexico (1.75-1.85 b.y.) come from granitic and siliceous metavolcanic rocks in the Tusas and Nacimiento Mountains in the northern part of the state (Fullagar and Shiver, 1973; Barker and others, 1974; Brookins, 1974). The rock assemblages formed during this time interval are very similar to those in central and south-central New Mexico formed at a later time. The oldest isochron age from central and south-central New Mexico is about 1.7 b.y. from the siliceous meta-igneous rocks of the Sevilleta Formation in the Los Pinos-Manzano Mountains (Bolton, 1976). A 1.6-b.y. isochron comes from the Cibola Gneiss (Taggart and Brookins, 1975). If the age relationships suggested in fig. 24 are correct, the Cibola Gneiss is older than the Sevilleta Formation. The difference in the two radiometric ages, however, may not be real because of large error associated with both isochrons. A low initial Sr⁸⁷/Sr⁸⁶ ratio for the Cibola Gneiss (0.702) indicates that this unit had a very limited crustal history prior to regional metamorphism. A 1.57-b.y. isochron has been obtained from the Ojita pluton and a 1.52-b.y. isochron from the Magdalena metagabbro (White, 1977). Isochron ages from the North Sandia, Pedernal, and Priest plutons indicate emplacement

at about 1.5 b.y. (Taggart and Brookins, 1975; Mukhopadhyay and others, 1966; Bolton, 1976). Numerous mineral ages (Wasserburg and Towell, 1965; Muehlberger and others, 1966) as well as Rb-Sr isochron ages at about 1.4-1.45 b.y. seem to record widespread regional heating and sporadic plutonism in the Southwest at this time. Recent isochron ages from south-central New Mexico record the following ages of granitic plutons (White, 1977): Ladron, 1.4 b.y.; Oscura, 1.37 b.y.; Capitol Peak, 1.35 b.y.; Mineral Hill, 1.32 b.y.; Magdalena, 1.3 b.y.; and Mayberry 1.27 b.y. The 1.4- b.y. whole-rock isochrons from the Los Pinos and Sepultura plutons reported by Bolton (1976) have extremely high initial Sr⁸⁷/Sr⁸⁶ ratios (> 0.723). Mukhopadhyay and others (1975) interpret an anomalously young isochron age of about 1.4 b.y. from the metamorphic rocks into which the Pedernal pluton is intruded to reflect open-system conditions during cataclastic deformation.

TABLE 7—SUMMARY OF MAJOR PRECAMBRIAN EVENTS IN CENTRAL AND SOUTH-CENTRAL NEW MEXICO. Principal radiometric age references Muehlberger and others, 1966; Denison and Hetherington, 1969 Brookins, 1974; Mukhopadhyay and others, 1975; Bolton, 1976 White, 1977; Brookins and Della Valle, 1977.

Age (b.y.)	Events
1.0-1.1	Deposition of the DeBaca terrane
	Siliceous volcanism and granitic plutonism in the Franklin Mountains
1.2-1.4	Intrusion of the Mockingbird Gap pluton
	Intrusion of syenite complex at Pajarito Mountain
~ 1.5	Intrusion of Mayberry, Capitol Peak, Ladron, Magdalena, Mineral Hill, Oscura, Los Pinos, and Sepultura plutons ~
	Intrusion of North Sandia, Pedernal, and Priest plutons and plutons in the Zuni Mountains
~ 1.6	Intrusion of Magdalena gabbro
	Intrusion of Ojita pluton
1.65-1.7	Intrusion of hypabyssal siliceous igneous rocks (± volcanics) in the Los Pinos-Manzano Mountains

Granitic rocks and siliceous meta-igneous rocks from the Franklin Mountains near El Paso and other areas in west Texas and from the Mockingbird Gap pluton in the San Andres Mountains record ages of 1.0-1.1 b.y. (Wasserburg and others, 1962; Denison and Hetherington, 1969; White, 1977); mineral ages from the syenite at Pajarito Mountain suggest an emplacement age of about 1.2 b.y. (Denison and Hetherington, 1969). The age of sediments of the De Baca terrane is not known, but is probably about 1 b.y. (Denison and Hetherington, 1969).

Initial $\text{Sr}^{87}/\text{Sr}^{86}$ ratios determined from whole-rock

isochrons are important relative to magma origin. Available results from the Southwest are shown in fig. 32, grouped into two age categories; ratios from New Mexico are so designated. Most values in both age categories fall between 0.701 and 0.705. Rocks with 1.6-1.85-b.y. ages, however, average about 0.702-0.703; the average of the younger rocks is ≥ 0.705 . Also several anomalously high initial ratios occur in the younger age category. Livingston (1969) first suggested an increase in initial ratios with decreasing age in Precambrian rocks of the Southwest from his results on granitic rocks in southeastern Arizona.

Geochemistry

Over 250 complete or partial chemical analyses have been obtained from igneous and metamorphic rocks from Precambrian terranes in central and south-central New Mexico. Samples were analyzed for major elements (except Na) and Rb, Sr, Zr, Y, and Ni by nondestructive X-ray fluorescence, employing methods described by Condie (1967) and Reynolds (1963), using USGS and intralab rock standards. Na, Cr, Co, Ja, Cs, La, Ce, Sm, Eu, Tb, Yb, and Lu were determined by instrumental neutron activation using methods described in Gordon and others (1968) and in Condie and Lo (1971). Those samples for which complete major- and/or trace-element results are available are given in appendices 2 and 3. These data, together with results of partial chemical analysis, were used in constructing figs. 33-45. To evaluate the effects of alteration, both altered and unaltered samples were analyzed and are distinguished as such in figs. 33, 36, and 37. Altered samples were selected from their modal amounts of secondary minerals (such as chlorite and sericite). Sample locations are given in appendix 4.

Because volatile elements (H_2O , CO_2) were not determined, all major-element totals were recalculated based on the amounts of volatiles reported in the literature for rocks of similar composition and mineralogy. Mafic rocks were recalculated to 98 percent and siliceous rocks to 99.5 percent. Barth mesonorms (Barth, 1959) were calculated for siliceous meta-igneous and granitic rocks with the aid of a computer program. Because Fe^{+2} and Fe^{+3} were not distinguished analytically, the amount of total Fe as FeO necessary to account for modal iron oxides and sulfides was subtracted from total Fe and the remainder combined with MgO to make normative biotite. Eu anomalies are expressed as Eu/Eu^* ratios, where Eu is the observed Eu content and Eu^* is the interpolated Eu content determined by drawing a line from Tb to Sm on a chondrite-normalized plot. Chondrite REE (rare earth element) values used in normalization are from the nine-chondrite composite of Raskin and others (1968).

Perhaps the most striking feature of the meta-igneous and granitic rocks from the Precambrian in this region is their bimodal nature. The rocks define two distinct

compositional populations—one characterized by SiO_2 in the range of 60-78 percent and K_2O greater than or equal to 3 percent, the other with SiO_2 values of 45-52 percent and K_2O less than 1 percent (fig. 33). Only three unaltered samples fall in the gap between these populations. The siliceous population can be further divided into three groups based on a variety of geochemical parameters. These groups are here called the high-Ca, high-K, and high-Si groups (fig. 33) after some of their major-element characteristics. The bimodal character of the Precambrian igneous rocks from this part of New Mexico contrasts strikingly with typical calc-alkaline and alkaline series where a spectrum of compositions commonly exists from mafic to siliceous end members.

Up to 15 samples were analyzed from individual granitic plutons in order to evaluate compositional variability and to arrive at accurate estimates of mean composition. Samples for which complete analyses are available are listed in appendices 2 and 3. In general, the results suggest that compositional variation within individual plutons is less than that between plutons. The only exception is the Ojita pluton, which is quite heterogeneous for some elements (appendix 2, part B). The greatest intrapluton variations observed are for Mg, Ti, Cr, Cs, Ba, and sometimes Rb and Sr.

To aid understanding of the provenance of clastic metasedimentary rocks, a suite of samples of feldspathic quartzite and arkosite have also been analyzed for major and trace elements.

Mafic meta-igneous rocks

Average compositions of Precambrian mafic meta-igneous rocks from six areas in central and south-central New Mexico are given in table 8; these averages include a two-sample average from metadiabase dikes in the Black Range northwest of Kingston, New Mexico. The several samples with high K_2O contents (> 1.5 percent) shown in fig. 33 appear to have undergone alkali-metasomatism during regional metamorphism and are not included in the averages. Both the major- and trace-element data indicate that the New Mexico mafic rocks are tholeiites (classification schemes of Yoder and

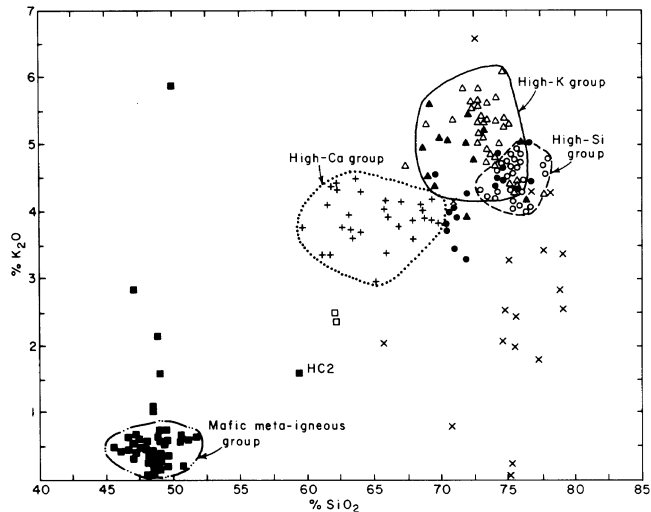


FIGURE 33— K_2O - SiO_2 VARIATION DIAGRAM FOR PRECAMBRIAN IGNEOUS ROCKS FROM CENTRAL AND SOUTH-CENTRAL NEW MEXICO. Symbols: ■ = mafic meta-igneous rocks, + = high-Ca group, ° = granitic rocks of the high-Si group, • = rhyolite and quartz latite, □ = rhyodacite from Manzanita Mountains (samples MZ-22 and MZ-23). Granitic rocks: Δ = high-K group, low-REE subgroup; ▲ = high-K group, high-REE subgroup; × = altered siliceous meta-igneous and granitic rocks.

Tilley, 1962; Miyashiro, 1975; and Pearce, 1976). The New Mexico rocks differ from Archean and most modern tholeiites (Condie, 1976b) by their low Al and K/Rb ratios and high Fe, Mg, and Co contents.

The large variabilities in Ba, Sr, Cs, Rb, and, to a smaller extent, K suggest that these elements have been mobilized during alteration or metamorphism. However, no systematic relationship occurs between the concentrations of these or any other elements and metamorphic grade. When the New Mexico rocks are classified in terms of various geochemical plots relating composition to tectonic setting of modern basalts, the New Mexico tholeiites fall into two groups in terms of the Ti-Y-Zr and F_1 - F_2 discriminant plots of Pearce and Cann (1973) and Pearce (1976). This is illustrated for Ti-Y-Zr in fig. 34. For comparison, amphibolite samples are also included from the upper Pecos River area east of Santa Fe (Mathewson, in preparation) and the Tusas Mountains in northern New Mexico; and metadiabase samples are included from the Black Range and Mimbres River localities in southwest New Mexico. The Tijeras Greenstone and upper Pecos samples fall in the plate-margin field, and most of the other samples fall in the within-plate field on both the Ti-Y-Zr and F_1 - F_2 plots. When Tijeras and Pecos samples are further considered in terms of the Ti-Zr, Ti-Zr-Sr, and F_2 - F_3 plots (not shown) for distinguishing various plate-margin settings, the samples fall into low-K or calc-alkaline basalt fields.

REE-distribution patterns have been shown to be relatively unaffected by regional metamorphism (Green and others, 1972; Gullers and others, 1974; Field and Elliott, 1974) and may be useful in classifying and studying the origin of the Precambrian mafic rocks from New Mexico. Average REE patterns from various geographic areas are shown in fig. 35. In general, the patterns define three groups. Group I includes the Tijeras Greenstone samples and samples from the lower

TABLE 8—AVERAGE COMPOSITIONS OF PRECAMBRIAN MAFIC METAGNEOUS ROCKS FROM CENTRAL AND SOUTH-CENTRAL NEW MEXICO (oxides in weight percent; trace elements in parts per million; total Fe as Fe203). 1 = average of six samples from Tijeras Greenstone; 2 = average of two samples from Magdalena metagabbro; 3 = average of ten amphibolite samples from Manzano Mountains; 4 = average of two metadiabase samples from Black Range; 5 = average of five amphibolite and metadiabase samples from San Andres Mountains; 6 = average of two amphibolite samples from Ladron Mountains.

	1	2	3	4	5	6
SiO ₂	49.4	46.4	48.2	48.2	48.2	48.6
TiO ₂	0.95	1.63	1.36	2.01	1.45	1.79
Al ₂ O ₃	12.0	13.4	13.3	13.4	13.0	12.8
Fe ₂ O ₃	14.4	15.5	14.3	14.3	13.9	14.8
MgO	8.86	8.43	8.44	7.35	8.48	7.64
CaO	9.80	9.16	9.41	9.34	9.90	9.60
Na ₂ O	2.32	3.14	2.55	2.64	2.35	2.43
K ₂ O	0.35	0.35	0.50	0.82	0.69	0.41
Cr	198	53	86	418	172	122
Co	57	65	52	45	52	56
Ni	59	51	53	51	64	59
Rb	13	11	12	57	39	15
Sr	149	191	213	244	208	223
Zr	184	135	123	144	123	131
Ba	77	108	190	202	370	134
Cs	0.5	1.0	1.5	5.5	3.0	4.3
Y	40	23	0	24	21	24
La	2.7	12	6.5	14	11	14
Ce	7.5	30	15	36	26	35
Sm	2.4	4.6	4.0	4.6	4.1	5.1
Eu	1.1	1.8	1.2	1.7	1.7	1.7
Tb	0.79	1.1	0.80	0.78	0.85	0.81
Yb	3.3	3.6	3.2	2.7	3.7	3.8
Lu	0.57	0.59	0.49	0.48	0.59	0.59
Σ7REE	18	54	31	60	48	61
K/Rb	223	264	346	119	147	227
Rb/Sr	0.087	0.057	0.056	0.23	0.19	0.067
K/Ba	38	27	22	34	16	25
Ba/Sr	0.52	0.57	0.89	0.83	1.8	0.60
La/Yb	0.82	3.3	2.0	5.2	3.0	3.7
Eu/Eu*	1.1	1.1	0.88	1.2	1.2	1.0

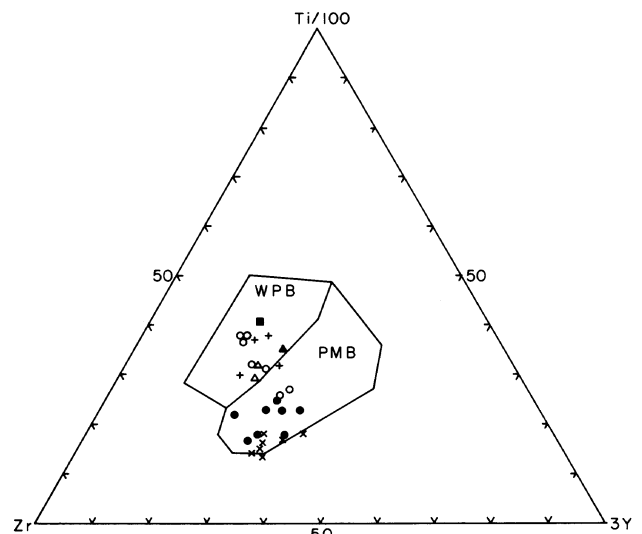


FIGURE 34—Ti-Zr-Y VARIATION DIAGRAM FOR PRECAMBRIAN IGNEOUS ROCKS FROM NEW MEXICO. Modern tholeiite fields after Pearce and Cann (1973). PMB = plate-margin basalts; WPB = within-plate basalts. Symbols: • = upper Pecos River succession; + = Ladron Mountains; ° = San Andres Mountains; × = Tijeras Greenstone; ■ = Black Range; ▲ = Mimbres River locality; Δ = Magdalena metagabbro.

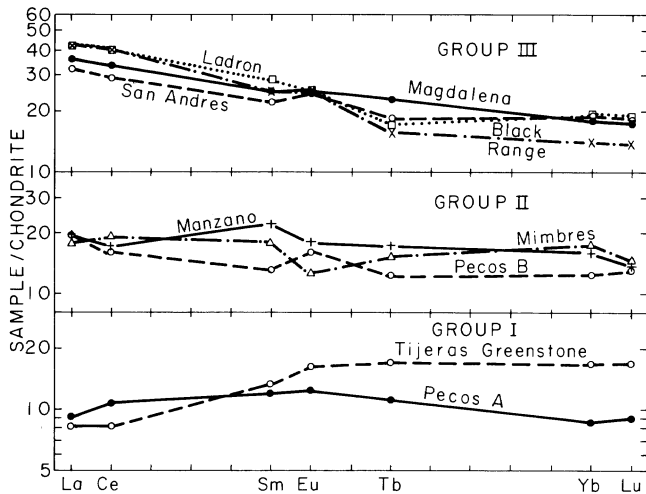


FIGURE 35—AVERAGE CHONDRITE-NORMALIZED REE DIAGRAM FOR PRECAMBRIAN IGNEOUS ROCKS FROM NEW MEXICO.

Mathewson, in preparation); it is characterized by light-REE depletion similar to that observed in some modern oceanic-rise tholeiites. Group II includes samples from the Manzano Mountains, Mimbres River locality, and middle part of the Pecos succession (Pecos B) and is characterized by flat REE patterns. Group III, defined by samples from the Ladron Mountains, Black Range, San Andres Mountains, and Magdalena metagabbro, is characterized by slightly enriched light-REE patterns. Heavy-REE concentrations are similar in all three groups. The progressive enrichment of light REE in going from Group I to Group III may have been produced by premetamorphic alteration, differences in degree of melting or crystallization, or differences in source compositions. This enrichment probably does not reflect metamorphic processes because of an absence of a correlation of metamorphic grade with the amount of light-REE enrichment.

Sample HC-2 from the greenstone complex in the Hell Canyon area is unique and, so far, is the only andesite found in the Precambrian terranes of central and south-central New Mexico. Except for its greater Mg, Cr, Ni, Ba, and light REE and lower Al (appendices 2 and 3), it is similar to young calc-alkaline andesite.

Siliceous meta-igneous rocks and granitic rocks

Existing geochemical data for unaltered Precambrian siliceous igneous rocks from central and south-central New Mexico suggest a threefold subdivision, summarized in table 9 (Condie, 1978). The concentrations of many major and trace elements, however, overlap among the three groups—especially between the high-Si and high-K groups. For the purpose of discussion, the high-K group is further subdivided into low-REE and high-REE subgroups. The high-Ca group occurs only in the northern part of the study area and may represent the southern extremity of a province of high-Ca granitic and gneissic rocks found in northern New Mexico and Colorado. Available radiometric dates indicate that this province contains granitic rocks ranging in age from <

TABLE 9—GEOCHEMICAL CLASSIFICATION OF SILICEOUS META-IGNEOUS ROCKS AND GRANITIC PLUTONS FROM THE PRECAMBRIAN OF CENTRAL AND SOUTH-CENTRAL NEW MEXICO.

High-Ca group

Ojita
Monte Largo
Priest
North Sandia
South Sandia
Manzanita rhyodacite sills

High-Si group

Sepultura
Los Pinos
Capirote
Magdalena
Pederal
Siliceous meta-igneous rocks (including rocks from the Sevilleta Formation)

High-K group

Low REE

Oscura
Capitol Peak
Ladron
San Andres
Manzanita

High REE

Mockingbird Gap
Mayberry
Mineral Hill
Strawberry Peak
White Sands

1.4 to 1.85 b.y. The high-K group dominates most of the study area; some plutons, however, occur, also within the high-Ca province (the Manzanita and other small high-K plutons in northern New Mexico). Although the high-Si group seems to dominate in the Socorro region, results from a study by Condie (1978) indicate that high-Si plutons also occur in other parts of the state. Average compositions of granitic and siliceous meta-igneous rocks from central and south-central New Mexico are compared to published igneous-rock averages in tables 10-12.

High-Ca group

With two very minor exceptions, only granitic rocks (granodiorites and calcic quartz monzonites) are represented in the high-Ca group (table 9). The exceptions are two very thin rhyodacite sills (2-3 m thick) occurring in the greenstone succession in the central Manzanita Mountains (samples MZ-22 and MZ-23). The high-Ca group is characterized by high CaO (2-3.5 percent), intermediate K₂O (3-4.5 percent) and SiO₂ (60-70 percent), and K₂O/Na₂O ratios in the range of 1 to 1.5 (table 10; figs. 33 and 36). On standard major-element diagrams (Miyashiro, 1975), members of this group fall in calc-alkaline fields. Except for being somewhat enriched in K, Rb, and Cs and depleted in Ca and Sr, this group is similar in composition to published averages in high-Ca granitic rocks (table 10). Normative An contents generally fall in the range of 10-20 percent and normative Bi values (10-15 percent) agree well with modal biotite contents. Although rocks of this group contain modal K-feldspar and quartz, their bulk normative compositions fall well within the plagioclase volume of the Ab-Or-An-Q system. The group is characterized by moderate-Rb and high-Sr contents and plots in a restricted area on an Rb-Sr diagram (fig. 37). If the crustal thickness grid proposed by Condie (1973) is applied to these rocks, it suggests that they were emplaced in continental crust that was ≥ 30 km thick. The rocks also exhibit a rather limited range in K/Rb ratio (175-200), which is below the crustal average of 250; and they contain unusually large amounts of Cs. These features sug-

TABLE 10—AVERAGE COMPOSITIONS OF PRECAMBRIAN ROCKS OF THE HIGH-CA GROUP FROM CENTRAL AND SOUTH-CENTRAL NEW MEXICO compared to other average granitic rocks (oxides in weight percent; trace elements in parts per million; total Fe as Fe₂O₃). 1 = North Sandia pluton; 2 = South Sandia pluton; 3 = Ojita-Monte Largo plutons; 4 = Priest pluton; 5 = average high-Ca granite (from Turekian and Wedepohl, 1961); 6 = average granodiorite (from Taylor and White, 1966).

	1	2	3	4	5	6
SiO ₂	69.2	66.3	65.9	68.5	67.2	66.9
TiO ₂	0.76	1.03	0.65	0.39	0.57	0.60
Al ₂ O ₃	13.7	13.9	16.1	15.4	15.5	15.7
Fe ₂ O ₃	4.81	6.85	5.15	2.92	4.23	4.22
MgO	1.00	1.33	1.74	1.60	1.56	1.6
CaO	2.75	3.73	2.93	2.58	3.54	3.6
Na ₂ O	3.29	3.11	3.10	4.00	3.83	3.8
K ₂ O	3.99	3.25	3.88	4.19	3.04	3.1
K ₂ O/Na ₂ O	1.2	1.1	1.3	1.1	0.79	0.82
Cr	9	10	18	22	22	30
Co	11	18	14	7	7	10
Rb	192	150	160	191	110	110
Sr	241	228	176	342	440	440
Zr	364	365	130	131	140	140
Ba	840	790	550	597	420	500
Cs	8.3	7.6	10	8.8	2	4
La	62	49	36	44	45	40
Ce	140	118	73	98	81	80
Sm	13	11	6.9	6.7	8.8	6.0
Eu	3.1	2.9	1.2	0.78	1.4	1.3
Tb	2.3	1.9	1.0	0.68	1.4	1.3
Yb	4.9	4.1	3.5	1.6	3.5	4.7
Lu	0.79	0.64	0.54	0.29	1.1	0.6
Σ7REE	226	188	122	152	142	134
K/Rb	173	180	201	182	229	234
Rb/Sr	0.80	0.66	0.91	0.56	0.25	0.25
K/Ba	48	34	59	58	60	52
Ba/Sr	3.5	3.5	3.1	1.8	0.95	1.1
La/Yb	13	12	10	28	13	8.5
Eu/Eu*	0.71	0.78	0.54	0.42	0.49	0.58

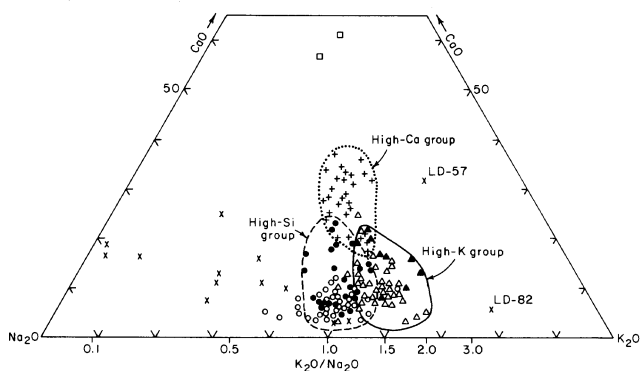


FIGURE 36—Na₂O-K₂O-CAO DIAGRAM FOR PRECAMBRIAN IGNEOUS ROCKS FROM CENTRAL AND SOUTH-CENTRAL NEW MEXICO. Symbols: + = high-Ca group, o = granitic rocks of the high-Si group, • = rhyolite and quartz latite, □ = rhyodacite from Manzanita Mountains (samples MZ-22 and MZ-23). Granitic rocks: Δ = high-K group, low-REE subgroup; ▲ = high-K group, high-REE subgroup; x = altered siliceous meta-igneous rocks.

gest that these rocks are more fractionated than most high-Ca granitic rocks. Their REE contents, however, are generally similar to other high-Ca granitic rocks (table 10), and they exhibit typical enriched REE patterns with small Eu anomalies (fig. 38).

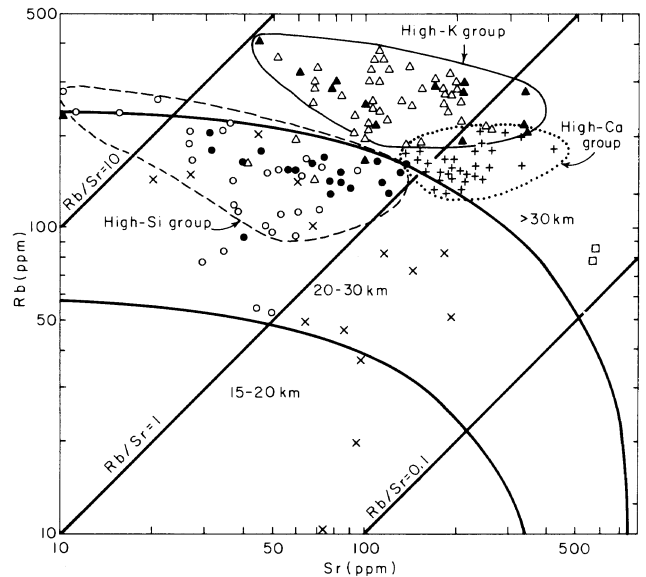


FIGURE 37—Rb-Sr DIAGRAM FOR PRECAMBRIAN IGNEOUS ROCKS FROM CENTRAL AND SOUTH-CENTRAL NEW MEXICO. Crustal thickness grid (dashed lines) from Condie (1973). Symbols: + = high-Ca group, o = granitic rocks of the high-Si group, • = rhyolite and quartz latite, □ = rhyodacite from Manzanita Mountains (samples MZ-22 and MZ-23). Granitic rocks: Δ = high-K group, low-REE subgroup; ▲ = high-K group, high-REE subgroup; x = altered siliceous meta-igneous rocks.

The similarity of both major- and trace-element concentrations in the Ojita and Monte Largo granodiorites (appendices 2 and 3) supports the suggestion by Stark (1956), based on field and hand-specimen observations, that these two bodies are part of the same intrusion. The Monte Largo pluton may represent an apophysis of the Ojita pluton, or both bodies may represent arms of an extensive batholith buried along the west side of the Manzano Mountains. Although only nine samples of Sandia granitic rocks were analyzed, both major- and trace-element data indicate the existence of at least two plutons (table 10; appendices 2 and 3). Although the nature of the contact between the plutons is unknown, it must lie between samples 5 and 6 (that is, between Embudito and Pino Canyons, sheet 1). The North Sandia pluton is more alkali-rich and less mafic; it contains more Rb and REE than the South Sandia pluton. The REE patterns of both plutons are similar (fig. 38) and exhibit the smallest Eu anomalies of any of the granitic

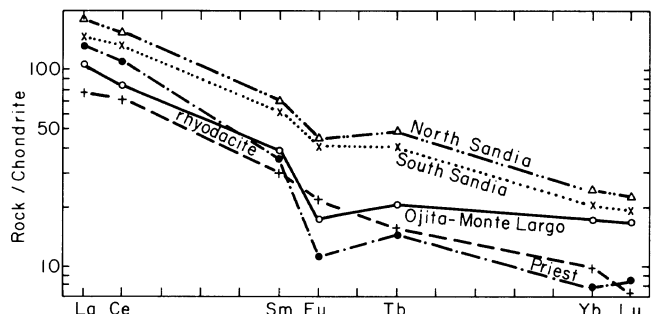


FIGURE 38—CHONDRITE-NORMALIZED AVERAGE REE DISTRIBUTIONS FOR MEMBERS OF THE HIGH-CA GROUP FROM THE PRECAMBRIAN OF CENTRAL NEW MEXICO. Rhyodacite from sills in the Manzanita Mountains is also shown.

rocks analyzed from central and south-central New Mexico. The Priest quartz monzonite is peculiar compared to the other high-Ca granitic rocks in New Mexico because it is low in Fe and heavy REE, is high in Sr, and exhibits a large Eu anomaly.

The rhyodacites from the two small sills in the Manzanita Mountains differ in composition from the plutonic members of the high-Ca group by their low SiO₂, Na₂O, K₂O, and Rb and relatively high MgO, Fe₂O₃, CaO, Sr, and Cr (table 12). These differences suggest that the sills do not represent part of the same magmas that produced the plutons.

High-K group

The high-K group is characterized by K₂O values chiefly in the range of 4.5-6 percent and K₂O/Na₂O ratios of 1.3-2 (figs. 33 and 36). On an AFM diagram (not shown) this group and the high-Si group define a steeply descending, Mg-poor limb with a large concentration of samples near the alkali corner. On the whole, members of this high-K group are similar in composition to average granite (table 11). Most samples of the

group are enriched in normative Or compared to many members of the high-Si group (fig. 39). The Mockingbird Gap quartz monzonite is also richer in An and Bi. Except for samples from the Mockingbird Gap pluton, which falls in the plagioclase volume, most samples from the high-K group cluster near the univariant cotectic at 500 b P_{H20} in the system Ab-An-Or-Q, only slightly above (more An-rich than) the high-Si group. Most members of the group, therefore, represent initial melts or highly fractionated magmas that crystallized at low water pressures. The high Rb content of this group distinguishes it from both the high-Ca group and from most members of the high-Si groups (fig. 37) and is also responsible for its comparatively low K/Rb ratios (140-160). Except for being high in Ca and Cs and low in Cr (appendices 2 and 3), the composition of the Oscura aplitic quartz monzonite is indistinguishable from the quartz monzonite proper. Also, the striking similarity in the composition of the Oscura and Capitol Peak plutons suggests that they are part of the same batholithic complex. The red and gray varieties of these bodies, which are so prominent in the field, do not exhibit significant chemical differences (appendices 2 and 3).

TABLE 11-AVERAGE COMPOSITION OF PRECAMBRIAN GRANITIC ROCKS OF THE HIGH-K AND HIGH-SI GROUPS FROM CENTRAL AND SOUTH-CENTRAL NEW MEXICO compared to other averages (oxides in weight percent; trace elements in parts per million; total Fe as Fe₂O₃). 1 = Capirote granophyre; 2 = unaltered Capirote quartz monzonite; 3 = Los Pinos granite; 4 = Sepultura granite; 5 = Magdalena granite; 6 = Pedernal granite; 7 = Oscura quartz monzonite; 8 = Capitol Peak quartz monzonite; 9 = Ladron quartz monzonite; 10 = San Andres quartz monzonite; 11 = Manzanita quartz monzonite; 12 = Mockingbird Gap quartz monzonite; 13 = Mayberry granite; 14 = Strawberry Peak quartz monzonite; 15 = Mineral Hill quartz monzonite; 16 = White Sands quartz monzonite; 17 = low-Ca granite (from Turekian and Wedepohl, 1961); 18 = granite (from Taylor and White, 1966).

	High-Si Group						High-K Group						High-K Group						Average Granites	
	1	2	3	4	5	6	7	8	9	10	11	12	13	14	15	16	17	18		
SiO ₂	78.1	76.6	74.9	75.1	76.0	76.6	73.9	72.9	75.3	73.7	74.2	69.5	72.0	71.8	72.7	67.4	74.2	71.2		
TiO ₂	0.17	0.22	0.24	0.22	0.31	0.07	0.23	0.28	0.19	0.26	0.29	0.48	0.56	0.44	0.28	0.79	0.20	0.5		
Al ₂ O ₃	12.4	13.0	12.0	13.4	11.5	12.6	14.5	14.7	13.4	14.0	13.8	15.1	12.8	13.4	15.3	14.8	13.6	14.7		
Fe ₂ O ₃	1.31	1.03	2.75	1.20	3.33	1.12	1.40	1.51	1.14	1.97	2.17	2.97	5.44	2.95	2.20	5.00	2.03	3.56		
MgO	0.20	0.11	0.08	0.07	0.10	0.11	0.37	0.47	0.44	0.15	0.30	1.40	0.31	0.16	0.17	0.91	0.27	0.60		
CaO	0.31	0.46	0.84	0.64	0.76	0.67	0.78	0.91	1.05	1.29	1.31	1.94	1.85	1.01	1.18	2.34	0.71	2.0		
Na ₂ O	3.98	3.79	4.37	4.19	2.77	4.20	3.21	3.40	3.44	3.31	2.73	3.25	2.64	4.70	2.54	3.46	3.48	3.5		
K ₂ O	3.06	4.30	4.27	4.72	4.75	4.14	5.09	5.30	4.51	4.81	4.69	4.93	3.89	5.02	5.13	4.68	5.06	4.2		
K ₂ O/Na ₂ O	0.77	1.1	0.98	1.1	1.7	1.0	1.6	1.6	1.3	1.5	1.7	1.5	1.5	1.1	2.0	1.4	1.5	1.2		
Cr	2	1	2	4	5	2	6	6	8	4	5	3	3	4	4	14	4	10		
Co	0.3	1	1	0.6	0.4	1.7	4	5	3	3	6	7	2	7	4	12	1	2		
Rb	54	127	135	223	151	177	272	302	269	183	204	289	204	418	278	231	170	145		
Sr	50	46	63	24	48	≤10	187	145	87	135	100	194	86	45	82	200	100	285		
Zr	104	167	—	—	402	123	127	147	82	208	191	251	427	304	187	424	175	180		
Ba	1030	539	1035	631	1020	190	687	820	380	840	610	—	291	420	586	1040	840	600		
Cs	1.0	2.2	2.6	3.0	1.6	5.9	5.9	6.2	0.8	2.3	10	2.1	5.0	7.6	2.7	2.7	4	5		
La	37	25	70	52	87	36	33	44	28	44	40	52	35	74	72	82	55	50		
Ce	84	76	170	141	197	73	82	98	61	98	99	146	93	166	174	222	92	100		
Sm	7.8	7.8	21	18	21	10	6.4	7.7	6.5	9.2	9.0	17	10	14	18	22	10	5		
Eu	0.85	0.63	3.1	2.4	2.1	0.55	0.90	1.1	0.85	1.5	1.3	0.63	0.73	1.2	1.2	2.4	1.6	0.47		
Tb	2.0	1.7	4.0	2.8	3.4	1.7	0.97	0.88	1.1	0.89	1.4	2.4	2.2	2.6	3.6	2.9	1.6	0.15		
Yb	7.0	7.3	12	11	12	7.8	3.1	2.5	2.9	1.5	5.0	6.7	6.2	8.0	8.4	6.6	4.0	0.18		
Lu	1.0	1.2	1.9	1.8	1.9	1.5	0.45	0.39	0.43	0.24	0.83	0.99	1.1	1.2	1.3	1.1	1.2	0.04		
Σ7REE	140	120	282	229	324	131	127	155	101	155	157	226	148	267	279	339	165	156		
K/Rb	470	281	263	176	261	194	155	146	139	481	191	142	158	100	153	168	247	240		
Rb/Sr	1.1	2.8	2.1	9.3	3.1	≥18	1.5	2.1	3.1	0.82	2.0	1.5	2.4	9.3	3.4	1.2	1.7	0.51		
K/Ba	25	66	34	62	39	181	66	54	99	105	64	—	111	99	73	33	50	50		
Ba/Sr	21	12	16	26	21	≤19	3.4	5.7	4.4	6.2	6.1	—	3.7	2.5	7.8	5.2	8.4	2.1		
La/Yb	5.3	3.4	6.3	4.9	1.3	4.6	12	18	9.7	29	8.0	7.8	5.7	9.3	8.6	12	14	278		
Eu/Eu*	0.28	0.23	0.43	0.44	0.32	0.17	0.45	0.50	0.39	0.61	0.45	0.11	0.20	0.25	0.19	0.37	0.48	0.50		

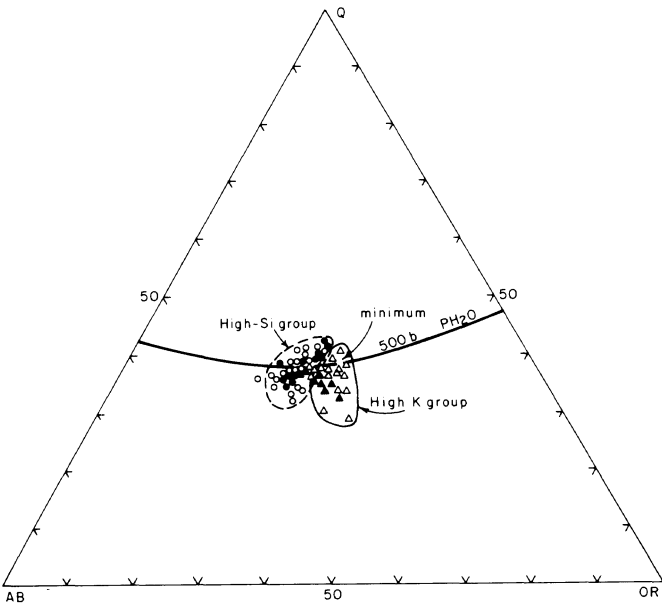


FIGURE 39—NORMATIVE COMPOSITIONS OF IGNEOUS ROCKS FROM THE HIGH-K AND HIGH-SI GROUPS PROJECTED FROM AN ONTO THE AB-OR-Q SYSTEM. Quartz-feldspar cotectic shown at 500 b P_{H_2O} from Tuttle and Bowen (1958). Symbols: \circ = granitic rocks of the high-Si group, \bullet = rhyolite and quartz latite. Granitic rocks: Δ = high-K group, low-REE subgroup; \blacktriangle = high-K group, high-REE subgroup.

In terms of REE distributions, the high-K group can be roughly divided into low-REE ($\Sigma 7\text{REE} \leq 150$ ppm) and high-REE ($\Sigma 7\text{REE} \geq 150$ ppm) subgroups, which are gradational with each other (table 11). These subgroups are not paralleled by a geographic subdivision. The low-REE subgroup is characterized by moderate Eu anomalies ($\text{Eu}/\text{Eu}^* > 0.35$) and the high-REE subgroup by large anomalies ($\text{Eu}/\text{Eu}^* \leq 0.35$) (figs. 40 and 41). The former subgroup also exhibits more fractionated REE patterns ($\text{La}/\text{Yb} = 8\text{-}30$) than the latter ($\text{La}/\text{Yb} = 6\text{-}12$). The REE patterns of the red, gray, and aplitic varieties of the Oscura and Capitol Peak plutons are essentially indistinguishable.

High-Si group

The high-Si group, besides exhibiting high SiO_2 (73-78 percent) and unusually low Mg contents (mostly ≤ 0.2 percent MgO), is characterized by moderate K_2O (3.5-5 percent), low CaO (0.5-1.0 percent), and $\text{K}_2\text{O}/\text{Na}_2\text{O}$ ratios in the range of 0.7-1.5 (figs. 33 and 36; table 12). Except for their low Sr and Mg contents, rocks of this group are similar to published average granite compositions (table 11). The group exhibits low normative An (2-4 percent) and Bi (mostly 2-5 percent). In the Ab-An-Or-Q system, most rock compositions cluster near the lower end of the two feldspar-quartz cotectic, not quite over the minimum in the Ab-Or-Q system at 500 b P_{H_2O} (fig. 39). As with the high-K group, this distribution is consistent with these rocks representing cotectic melts crystallized at low water pressures. On the Rb-Sr diagram (fig. 37), this group defines a field of increasing Rb with decreasing Sr. Sr contents vary by over an order of magnitude. The lower Rb content of most members of the high-Si group (< 200 ppm) distinguishes them from most members of the high-K group. Because this lower Rb content probably reflects fractional crystallization (Condie, 1977), the crustal thickness grid of

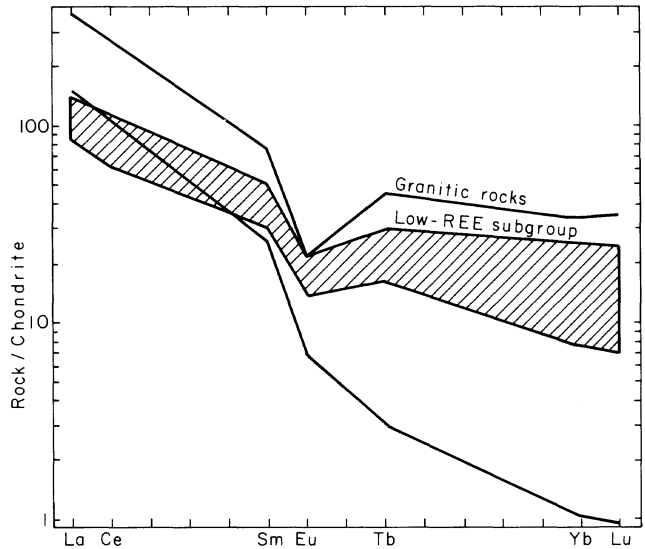


FIGURE 40—CHONDRITE-NORMALIZED ENVELOPE OF VARIATION OF AVERAGE REE DISTRIBUTIONS FOR MEMBERS OF THE LOW-REE SUBGROUP OF THE HIGH-K GROUP FROM NEW MEXICO compared to the envelope of variation of granitic rocks.

Condie (1973) is probably not applicable to these rocks. The high-Si group is characterized by only slightly increasing K with increasing Rb; this factor explains the large range in K/Rb ratios (table 11). Ba and REE ($\Sigma 7\text{REE} = 200\text{-}300$ ppm, excluding the Capirote pluton) are high, but Cs is low. REE patterns are relatively enriched in heavy REE ($\text{La}/\text{Yb} \leq 10$) and in this respect the high-Si group differs from many granites and siliceous volcanics reported in the literature (tables 11 and 12; fig. 42). All members of the high-Si group show negative Eu anomalies ($\text{Eu}/\text{Eu}^* = 0.2\text{-}0.45$). No apparent relationship exists, however, between Eu/Eu^* (or La/Yb) and Rb, Sr, K, Ba, Cs, or SiO_2 contents.

Excepting the two minor rhyolite sills from the Manzanita Mountains, all of the siliceous meta-igneous

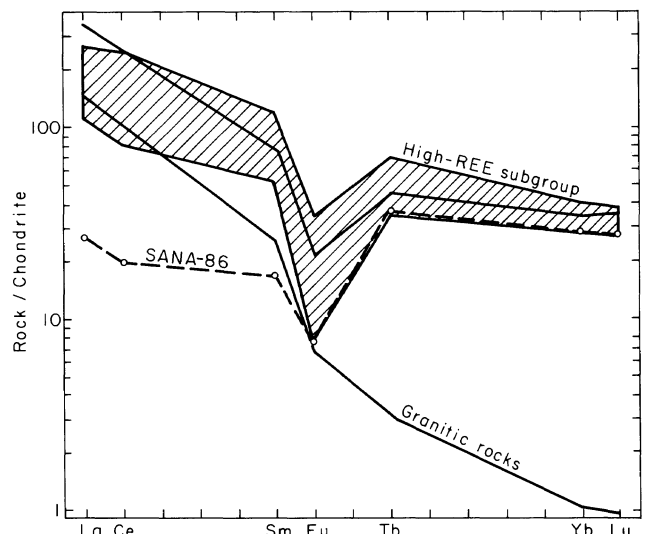


FIGURE 41—CHONDRITE-NORMALIZED ENVELOPE OF VARIATION OF AVERAGE REE DISTRIBUTIONS FOR MEMBERS OF THE HIGH-REE SUBGROUP OF THE HIGH-K GROUP FROM NEW MEXICO compared to the envelope of variation of granitic rocks. Albitized sample (SANA-86) shown separately.

TABLE 12-AVERAGE COMPOSITIONS OF PRECAMBRIAN SILICEOUS META-IGNEOUS ROCKS FROM CENTRAL AND SOUTH-CENTRAL NEW MEXICO and of the Taupo rhyolite from New Zealand (oxides in weight percent; trace elements in parts per millions; total Fe as Fe₂O₃). 1 = rhyodacite from Manzanita Mountains (MZ-22, 23); 2 = rhyolite composite from Los Pinos-Manzano Mountains (average of NP-46, 47, 49, 58, 62); 3 = Quartz-latite composite from Los Pinos-Manzano Mountains (average of LD-57; N-32, 36; NP-22, 24, 32, 36, 53, 64, 68, 81; MAN-D, E, K); 4 = rhyolite from Hembrillo Canyon, San Andres Mountains (SANA-144); 5 = average Taupo rhyolite, New Zealand (from Ewart and others, 1968).

	1	2	3	4	5
SiO ₂	62.2	75.2	72.0	76.5	74.2
TiO ₂	0.65	0.22	0.33	0.17	0.28
Al ₂ O ₃	14.5	13.3	13.4	12.1	13.3
Fe ₂ O ₃	7.42	1.97	4.32	1.80	1.90
MgO	3.66	0.05	0.34	0.18	0.28
CaO	6.39	0.65	1.86	0.79	1.59
Na ₂ O	2.23	3.74	3.49	2.96	4.24
K ₂ O	2.41	4.85	3.92	5.02	3.18
K ₂ O/Na ₂ O	1.1	1.3	1.1	1.7	0.75
Cr	29	2	3	9	2
Co	20	1	3	4	---
Rb	83	183	1.43	95	108
Sr	531	46	79	41	125
Zr	186	---	277	203	160
Ba	683	1160	820	1850	870
Cs	8.4	4.1	4.1	1.6	3
La	25	77	68	72	28
Ce	64	162	138	144	44
Sm	5.6	23	18	15	5.5
Eu	1.5	3.0	2.7	1.2	1.0
Tb	0.72	3.4	3.1	3.0	1.2
Yb	2.0	11	10	10	3.6
Lu	0.24	2.0	1.5	1.6	---
Σ7REE	99	281	241	247	84
K/Rb	241	220	228	439	250
Rb/Sr	0.16	4.0	1.8	2.3	0.87
K/Ba	2.9	35	40	23	30
Ba/Sr	1.3	25	10	45	7.0
La/Yb	13	7.0	6.8	7.2	7.8
Eu/Eu*	1.0	0.44	0.46	0.23	0.52

rocks analyzed (including those from the Sevilleta Formation) can most appropriately be classified in the high-Si group. Using the normative classifications of Rittmann (1952) and O'Conner (1965), most samples fall into two categories: rhyolite and quartz latite. The quartz latites contain plagioclase phenocrysts, and their bulk compositions fall in the plagioclase volume of the Ab-An-Or-Q system; the rhyolites usually contain quartz phenocrysts (\pm minor plagioclase) and plot near the quartz-plagioclase two-phase surface or a small distance into it in the quartz volume. The average compositions of the siliceous meta-igneous rocks are given in table 12 together with an average young rhyolite from the Taupo area in New Zealand. The rhyolites are similar in composition to plutonic members of the high-Si group, and the quartz latites differ from the high-Si group by having higher Ca, Mg, and Fe contents. The rhyolites differ from the Taupo rhyolite in their low Mg, Ca, Sr, and high K, Ba, and REE. Although containing more REE, the relative distribution of REE in the siliceous meta-igneous rocks is similar to that observed in the Taupo rhyolite; however, the latter has slightly more fractionated REE patterns. A suite of 15 siliceous meta-igneous samples was collected in stratigraphic succession from the Sevilleta Formation in the Los Pinos Mountains (the Piñon section, appendices 2, 3, and 4) to evaluate stratigraphic compositional variations. The results indicate that rhyolite and quartz latite are intimately mixed and that secular compositional variations in major or trace elements are not present.

The Capirote quartz monzonite and granophyre are lower in REE and exhibit larger Eu anomalies than do other members of the high-Si group (fig. 42). The origin of this difference is presently unknown. Three possible causes merit consideration: 1) REE were lost during alteration of the Capirote; 2) the Capirote is highly contaminated with inclusions of metasedimentary and meta-igneous rock, and these may have affected the REE patterns; or 3) a volatile phase rich in REE escaped from the Capirote magma just prior to its final emplacement and solidification. K, Rb, and Cs are also low in the granophyre; this fact is consistent with alteration of the rock because these elements seem to have been lost during alteration. We have difficulty explaining how only the REE were disturbed in the Capirote, however, if either of the first two processes are responsible for the peculiar REE patterns.

Effects of alteration

Altered samples of siliceous meta-igneous and granitic rock were analyzed to evaluate the effects of alteration on chemical composition. These samples are designated as such on figs. 33, 36, and 37. The meta-igneous samples collected from the Ladrón Mountains all contain varying amounts of epidote, albite, quartz, sericite, chlorite, limonite and carbonate. The occurrence of these minerals as irregular patches, as pseudomorphs after primary minerals, and as veinlets attests to their secondary origin. The series of samples analyzed from the altered facies of the Capirote pluton (including LD-106 from the unaltered facies; appendix 2) contains varying amounts of these minerals, the most important being albite (Cookro, 1978). Sample

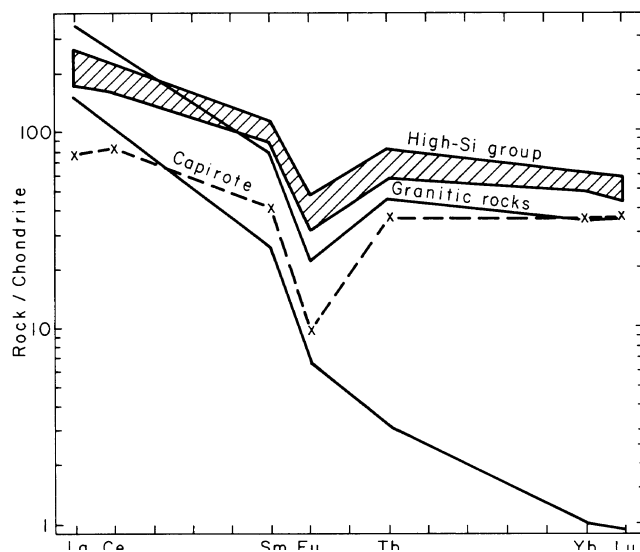


FIGURE 42-CHONDRITE-NORMALIZED ENVELOPE OF VARIATION OF AVERAGE REE DISTRIBUTIONS FOR MEMBERS OF THE HIGH-SI GROUP FROM NEW MEXICO compared to the envelope of variation of granitic rocks. Capirote pluton shown separately.

SANA-86 from the Mineral Hill pluton (appendix 2) also seems to have been albitized.

The most striking effect of alteration is the loss of K, Rb, Cr (and sometimes of Sr and Co) and the enrichment of Na (and sometimes of Ca and Fe). Depletion in K and Rb in most albitized samples is shown graphically in figs. 33 and 37. In fig. 36 a rough progressive alteration trend can be defined extending away from the high-Si group towards the Na₂O-CaO join. Samples exhibit progressively decreasing K₂O/Na₂O ratios (from 0.7 to < 0.1) with increasing amounts of albitization. The small increase in CaO results primarily from epidotization with a minor contribution from carbonate formation. Sample LD-57 does not seem to be albitized in thin section but contains moderate amounts of epidote and sericite, which account for its high CaO and K₂O. Sample LD-82 is strongly enriched in secondary biotite, accounting for its high K₂O content. Three samples from the altered facies of the Capirote pluton (4, 97, 117) also have lost significant Sr during albitization. Most albitized samples have lost varying amounts of Fe, Mg, Ti, Cr, Co, and Al. Cs behaves erratically and shows no systematic relationship to any type of alteration. Losses of alkalis and transition metals have also been reported from albitized or spilitized rocks from other areas (Melson and Van Andel, 1966; Murray and Condie, 1973) and characterize Na metasomatism. This behavior is in contrast to that observed during progressive deep-sea alteration of modern volcanics, which involves alkali-element enrichments and little or no change in transition metals (Hart, 1969; Christensen and others, 1973; Hart and others, 1974; Condie, 1976b).

Although the study by Hermann and others (1974) suggests that spilitization does not appreciably affect REE distributions in mafic rocks, little is known of the effects of progressive albitization and epidotization in siliceous igneous rocks. Siliceous meta-igneous samples LD-52, LD-57, and LD-83 from the Ladron Mountains were selected for REE analysis because they exhibit varying degrees of these types of alteration. The resulting REE patterns are shown relative to the envelope of variation of unaltered siliceous meta-igneous rocks in fig. 43. The REE pattern of the moderately epidotized sample (LD-57) is little affected by this process; the two albitized samples (LD-52, LD-83) have lost REE. Except for the smaller Eu anomalies, the overall REE patterns have not changed. On the other hand, a partially albitized sample (SANA-86) from the Mineral Hill pluton exhibits significant light REE losses (fig. 41). No evidence for relative enrichment of heavy REE during albitization was found, despite proposals by Mineyev (1963) and other Russian workers. Our results suggest that albitization of siliceous igneous rocks can result in significant REE losses and sometimes preferential losses of light REE.

Feldspathic quartzites and arkosites

In order to aid in understanding the provenance of the rocks, a representative suite of feldspathic quartzites and arkosites from the Los Pinos and Manzano Mountains was analyzed for major and trace elements (appendices 2 and 3). In comparison to the siliceous meta-igneous rocks with which many of the quartzites and

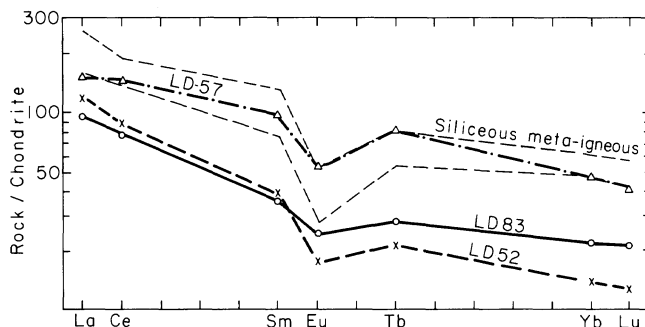


FIGURE 43—CHONDRITE-NORMALIZED AVERAGE REE DISTRIBUTIONS FOR ALTERED SILICEOUS META-IGNEOUS ROCKS FROM THE LADRON MOUNTAINS compared to the envelope of variation of unaltered siliceous meta-igneous rocks of the high-Si group.

TABLE 13—AVERAGE COMPOSITION OF PRECAMBRIAN FELDSPATHIC QUARTZITE-ARKOSITE FROM CENTRAL NEW MEXICO compared to other sandstone averages (oxides in weight percent; trace elements in parts per million; total Fe as Fe₂O₃). 1 = average feldspathic quartzite-arkosite from the Precambrian of central New Mexico (13 major elements and six trace elements included in average); 2 = average arkose (major elements from Pettijohn, 1963; trace elements from miscellaneous compilations by Condie); 3 = hornblende-bearing feldspathic quartzite (NP-70) from Los Pinos Mountains; 4 = average lithic arenite (subgraywacke), from Pettijohn (1963); 5 = graywacke, from Pettijohn (1963).

	1	2	3	4	5
SiO ₂	77.5	77.1	62.4	66.1	66.7
TiO ₂	0.63	0.3	0.65	0.3	0.6
Al ₂ O ₃	12.8	8.7	12.1	8.1	13.5
Fe ₂ O ₃	2.71	2.28	7.88	5.4	5.5
MgO	0.34	0.5	4.44	2.4	2.1
CaO	0.96	2.7	8.52	6.2	2.5
Na ₂ O	1.71	1.5	2.91	0.9	2.9
K ₂ O	3.14	2.8	0.59	1.3	2.0
Cr	20	35			
Co	5	1			
Rb	113	80			
Sr	52	100			
Zr	276	300			
Ba	530	500			
Cs	3.9	3			
La	36	30			
Ce	72	92			
Sm	8.4	10			
Eu	1.2	1.6			
Tb	1.4	1.6			
Yb	5.3	4			
Lu	0.91	1.2			
Σ7REE	125	140			
K/Rb	231	291			
Rb/Sr	2.2	0.80			
K/Ba	49	47			
Ba/Sr	10	5.0			
La/Yb	6.8	7.5			
Eu/Eu*	0.45	0.47			

arkosites are interbedded or closely associated, the quartzites and arkosites are higher in SiO₂, lower in K₂O and Na₂O; most samples have K₂O/Na₂O ratios greater than 1.5 (appendix 2; tables 12 and 13). They are also enriched in Cr and Co and depleted in Rb, Ba, and (in most cases) REE, compared to the siliceous meta-igneous rocks. The REE distribution patterns, however,

of three of the six samples analyzed for REE (MAN-F, MAN-30, MAN-33) are similar to those of the high-Si igneous group; NP-33 has a smaller Eu anomaly (fig. 44). The other three samples MAN-72, MAN-J, MAN-C show greater depletion in heavy REE. The average arkosite-feldspathic quartzite is grossly similar to a younger arkose average (table 13). The chief differences are the relatively high Al and K and low Ca and Sr in the Precambrian rocks. The differences reflect, in part, the presence of carbonate (at the expense of feldspar) in many younger arkoses.

The results clearly show that the feldspathic quartzites and arkosites cannot simply represent reworked volcanic or volcanic-plutonic rock from the high-Si group of igneous rocks—or, for that matter, from either of the other igneous-rock groups. Most of the major- and trace-element distributions, however, can be explained by a combination of reworking high-Si igneous rocks and quartzite. The mineralogical and textural immaturity of the sediments suggests that changes in chemical composition during weathering and erosion should have been minimal. The high SiO₂ in the quartzite-arkosite (compared to high-Si igneous rocks) reflects enrichment of granite-derived quartz and quartzite during weathering and erosion. As previously discussed, petrographic observations support this interpretation. The high Cr, Co, and Fe reflect enrichment in magnetite during sedimentary processes. The lower alkali and related-element contents probably reflect a dilution effect caused by the quartz enrichment. The

cause of the relative depletion in heavy REE in some of the rocks, however, is not understood.

The one sample of a hornblende-bearing feldspathic quartzite that was analyzed is compared to the average composition of graywacke and lithic arenite (subgraywacke) in table 13. Although some similarities exist between this quartzite and the two wacke averages, the rock cannot be classified in either category or as an arkose. Perhaps these unusual quartzites are best accounted for by a minor contribution of mafic material (amphibolite and/or mafic igneous rock) in the source area to the more typical quartz-feldspar detritus.

A comparison of the compositions of the quartzites and arkosites to the composition of younger sandstone of known tectonic setting may be helpful. Schwab (1975) has suggested that K₂O-Na₂O-SiO₂ may distinguish between some tectonic settings. Compositions of many sandstones of known tectonic setting were employed to delineate the miogeoclinal, eugeoclinal, and continental-rift fields in fig. 45. Most of the New Mexico Precambrian feldspathic quartzites and arkosites fall in the field of overlap between miogeoclinal and rift sandstones, and none fall in the eugeoclinal field. If Precambrian quartzites from New Mexico in which feldspars were not important constituents were plotted on this figure, they would undoubtedly fall closer to the SiO₂ apex. Caution should be used, however, in employing this geochemical similarity along to draw a parallel between the Precambrian sedimentary environment in New Mexico and Phanerozoic environments.

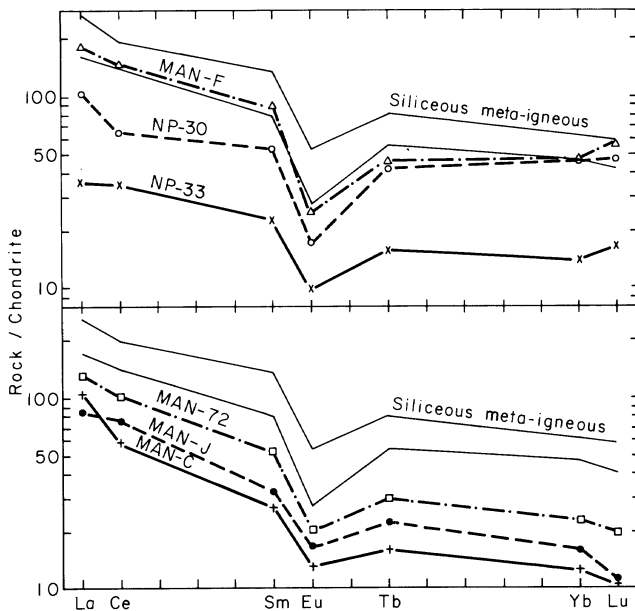


FIGURE 44—CHONDRITE-NORMALIZED REE DISTRIBUTIONS IN PRECAMBRIAN FELDSPATHIC QUARTZITES AND ARKOSITES FROM NEW MEXICO. Envelope of variation of siliceous meta-igneous rocks shown for comparison.

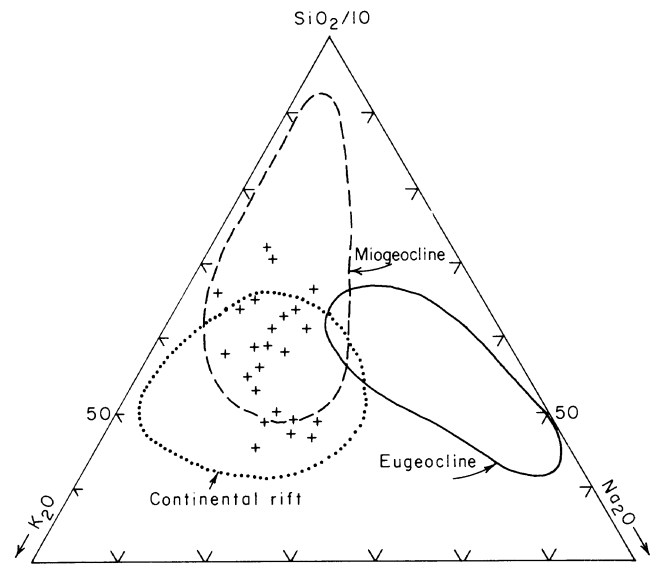


FIGURE 45—K₂O-NA₂O-SiO₂ VARIATION DIAGRAM FOR PRECAMBRIAN FELDSPATHIC QUARTZITES AND ARKOSITES (+) FROM THE LOS PINOS AND MANZANO MOUNTAINS. Sandstone tectonic settings from Schwab (1975) and miscellaneous compilations for this report by Condie.

Magma origin

Two aspects of magma origin will be considered: 1) temperature, depth of emplacement, and water content of granitic (and siliceous meta-igneous) magmas and 2) origin and source of siliceous and mafic magmas. Recent experimental studies indicate that granitic magmas are emplaced at temperatures of 700-800° C and erupted at temperatures of 800-900° C (Carmichael, 1963; Brown and Fyfe, 1970; Whitney, 1975). Experimental data and detailed studies of other granites similar in composition to those in the Precambrian of New Mexico (for instance, Barker and others, 1975) suggest that the voluminous granites and quartz monzonites of New Mexico were emplaced at about 700° C and the granodiorites at 750-800° C. Most of the granites and quartz monzonites have assimilated country rocks; this assimilation indicates that their emplacement temperatures exceeded liquidus temperatures, although some heat for assimilation may have been derived from crystallization. Experimental data also suggest that granitic melts are not saturated in water at the time of their formation (Maaloe and Wyllie, 1975), but may become saturated during the late stages of crystallization. Two factors suggest that the igneous rocks of the high-Si and high-K groups had low water contents at the time of emplacement: 1) the sparsity of pegmatites, aplites, and evidence for hydrothermal alteration and 2) normative compositions clustering around the minimum in the Q-Ab-Or system at low water pressures (5001000b) (fig. 39). Because K-feldspar seems to have crystallized later than biotite in most plutons, there is a large allowable range in water contents (2.5-20 percent) at the time of emplacement—if the experimental results of Maaloe and Wyllie (1975) are applicable. Mirolitic cavities in part of the Los Pinos pluton suggest that this body was saturated with water at the time of its emplacement.

Depths of granite intrusion are not easily estimated. If the granite and quartz monzonite magmas were water-saturated (or close to water-saturated) and emplaced at a temperature of about 700° C, the experimental data of Tuttle and Bowen (1958) indicate a maximum depth of emplacement of about 7 km (2kb). Field and experimental data—as well as the results of Barker and others (1975) on the Pikes Peak granite, which is strikingly similar in mineralogy and composition to members of the high-Si and high-K groups—suggest that plutons of these groups were emplaced at depths of only 3-7 km. Granodiorites and the Priest quartz monzonite were probably emplaced at greater depths of 7-10 km. Andalusite formed in contact metamorphic aureoles of some plutons in this latter group, indicating that intrusion did not occur on the prograde metamorphic curve shown in fig. 30 because this curve lies outside of the andalusite stability field. Rapid uplift, with only a small decrease in temperature ($\leq 50^\circ$ C), prior to granite intrusion probably brought the metamorphic section into the andalusite stability field. Continued uplift and granite emplacement then occurred along a somewhat steeper geothermal gradient that crossed the andalusite field.

Experimental, geochemical, and isotopic data clearly

indicate that mafic magmas are produced in the upper mantle, and such a source is proposed for the Precambrian tholeiites in New Mexico. Granitic magmas may form by fractional crystallization of more mafic magmas or by partial melting of lower crustal rocks. Recent experimental studies strongly favor the latter origin for most granites (Brown and Fyfe, 1970; Whitney, 1975). Such experimental results indicate that initial melts of parent rocks that range from granite to diorite in composition fall close to the minimum in the system Q-Ab-Or at low water pressures. This process provides a plausible mechanism for the production of granitic melts of the high-Si and high-K groups.

Geochemical model studies were undertaken to reach a better understanding of the origin of the magmas that produced the Precambrian igneous rocks of central and south-central New Mexico. Both major- and trace-element data were used to test fractional crystallization and partial melting models; a statistical mixing program (modified after Wright and Doherty, 1970), the Rayleigh fractionation law, and trace-element melting relationships (both equilibrium and fractional) were employed. The approach is similar to that described for Archean volcanic and granitic rocks (Condie, 1976a; Condie and Harrison, 1976; Condie and Hunter, 1976). Models were tested at various depths using liquidus and solidus phases determined from experimental studies and summarized in Condie and Hayslip (1975). In the fractional crystallization calculations, the compositions of the granitic rocks are assumed to represent liquids. Parent rocks tested in melting models were lherzolite, garnet peridotite, gabbro, amphibolite, garnet amphibolite, garnet granulite, eclogite, siliceous granulite, diorite, and granodiorite. Average compositions of the tholeiite and depleted tholeiite and of the high-Ca, high-Si, and high-K (low- and high-REE subgroups) groups were used in the calculations. Trace-element distribution coefficients were estimated from published data (see Condie and Harrison, 1976 and Condie and Hunter, 1976 for references). Although unique models cannot be attained by this approach, many models can be eliminated and attention can be focused on the most acceptable models.

All of the New Mexico Precambrian tholeiites are best explained by partial melting (25-35 percent) of a depleted olivine-pyroxene-spinel lherzolite source similar to that proposed for modern rise tholeiites (Kay and others, 1970) and depleted Archean tholeiite (Condie, 1976b). If not due to alteration, the progressive increase in light REE from groups I to III (fig. 35) may be explained by a decrease in the amount of melting (from about 30 to 20 percent), which does not affect heavy REE. REE data do not allow residual garnet, amphibole, or plagioclase in the source area. The small Eu anomalies in some samples may reflect minor plagioclase removal or accumulation or later alteration.

A detailed account of geochemical model studies of the granitic rocks are published elsewhere (Condie, 1978). The results indicate that models involving 30-50-percent partial melting of siliceous granulites in the lower crust produce the best overall agreement of both

major- and trace-element distributions for the production of granitic melts of the high-Ca group. On the other hand, magmas of the high-K and high-Si groups are best explained by fractional crystallization of parent granodiorite magmas in the crust under conditions of varying oxygen fugacity. None of the granitic magmas

seem to be readily obtainable by direct partial melting of upper-mantle rocks. The relatively high initial Sr^{87}/Sr^{86} ratios of many of the granitic rocks (fig. 32) are also consistent with the results of the geochemical model studies in indicating a crustal origin.

Tectonic setting and geologic evolution

The tectonic setting of Precambrian rocks in the Southwest is poorly known. Our knowledge of this problem may be enhanced by comparing the overall features of the Precambrian rocks in New Mexico and Phanerozoic eugeocline, miogeocline, and continental-rift assemblages. Average rock-type distributions of these three associations are shown in histogram form in fig. 46. These data were compiled from measured stratigraphic sections, published estimates of rock-type distributions (Schwab, 1971), and relative proportions scaled from geologic maps. Because the relative proportions of sediments and mafic and siliceous volcanics vary significantly within and between young continental rift systems, the averages given in the figure for continental rifts may or may not be representative. The most striking signature of continental-rift systems appears to be the association of immature arkosic sediments and shales with bimodal (dominantly mafic) volcanics (basalt-rhyolite or basalt-phonolite). Also shown in fig. 46 are the relative distributions of rock types in the Precambrian of central and south-central New Mexico. The typical New Mexico Precambrian assemblage is clearly not similar to either eugeocline or miogeocline assemblages. The absence of graywacke and intermediate volcanic rocks distinguishes the New Mexico assemblage from eugeoclinal associations, and the absence of carbonate and presence of significant quantities of volcanic and/or hypabyssal rock is strikingly different from Phanerozoic miogeoclinal assemblages. Of the three Phanerozoic assemblages, the Precambrian assemblage is most similar to the continental-rift assemblage.

Although equivocal, existing evidence suggests that the Precambrian rocks of central and south-central New Mexico reflect the development of an incipient-rift or multiple-rift system. The overall lithologic assemblage, structural setting, and geochemical features of the igneous rocks are all consistent with—although they do not demand—a rift model. The very persistent north-northwest to north-northeast trends throughout most of the area (reflected by faults, fold axes, and foliation directions) suggest that these features are controlled by widespread extensional fault systems in the basement; major compressive forces generally result in poly-phase deformation involving nappe structures and complex fold interference patterns, but neither are observed in the New Mexico Precambrian. The minor thrust faults

uniform, long-lived (≥ 500 m.y.), northwest-southeast compressive stresses. On the other hand, the folds may have developed in response to vertical motions along normal faults. Sediments and volcanics may have been draped over uplifted fault blocks with penecontemporary faulting producing the folds trending dominantly north-northwest to north-northeast. A similar model was suggested by Van Schmus (1976) for folds developed during the Penokean orogeny in the Great Lakes area. The minor Precambrian thrust faults in New Mexico (such as the Tijeras fault) could result from rising horsts, which rupture overlying sediments and volcanics or from gravity sliding of large blocks into rift valleys.

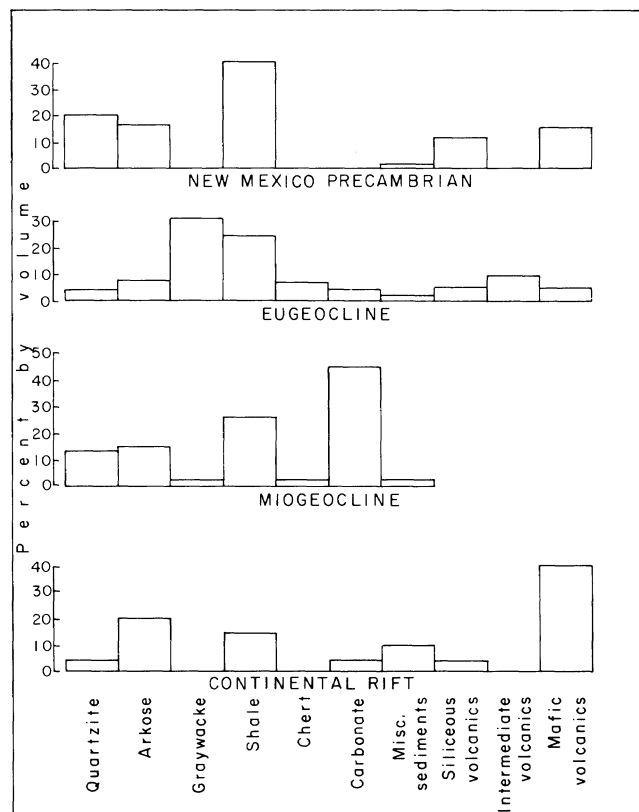


FIGURE 46—ROCK-TYPE DISTRIBUTION IN THE PRECAMBRIAN OF CENTRAL AND SOUTH-CENTRAL NEW MEXICO COMPARED TO ROCK-TYPE DISTRIBUTIONS IN PHANEROZOIC ASSEMBLAGES (COMPILED FROM MANY SOURCES).

Extensive sections of immature arkosic sandstones and conglomerates, such as those that occur in the Ladron and San Andres Mountains, reflect rapidly filled fault-bounded basins where unroofed high-K granitic rocks and quartzite dominated in the source regions. More chemically mature quartzite sections, such as those characterizing much of the SMP block and the Pederal Hills, seem to have been derived from dominantly quartzite source rocks and hence reflect reworking and perhaps recycling. Recycling is not unexpected in an evolving multiple-rift system where clastic sediments may be rapidly buried, metamorphosed, and uplifted to provide detrital input for new basins. Extensive thicknesses of shale occurring in parts of all the exposed sections (figs. 24 and 25) seem to have accumulated during periods of relative tectonic quiescence and reflect more distant source areas of less relief. Precambrian stratigraphic units cannot readily be correlated from area to area in New Mexico—a fact also consistent with an evolving multiple-rift model. Different rift valleys would be in different stages of development. Hence, at a given time, mafic volcanism may dominate in one valley and arkosic sedimentation in another.

The field occurrences of the mafic meta-igneous rocks in New Mexico suggest that most were intruded as dikes and sills and that, in varying quantities, mafic magmas were available at almost all stages of rift evolution. The relatively large quantities of mafic rock in the greenstone complexes of the Manzanita Mountains and in the Salinas Peak complex in the San Andres Mountains reflect localized intense injection and perhaps extrusion of tholeiites into rift sedimentary successions. The siliceous igneous rocks, which represent thick sills with minor amounts of pyroclastics and/or flows, characterize the late stages of development of individual rift valleys. This development is followed by extensive granitic plutonism. Such granitic magmas seem to have originated by partial melting of the lower crust. This melting may have occurred in response to heating of the lower crust by the tholeiitic magmas, which were readily available.

The least mobile trace-element distributions in the New Mexico Precambrian tholeiites are not definitive in terms of assigning tectonic settings. Only the Tijeras Greenstone and upper Pecos River sections bear evidence of plate-margin settings. If the continental-rift model proposed here is correct, the absence of typical continental-rift tholeiites and alkali basalts must be accounted for. Trace-element and Sr-isotope studies of young continental rift basalts indicate an undepleted mantle source, wall-rock reaction, or crustal contamination (or some combination of the three) to explain the origin of these basalts (Gast, 1968; Bell and Powell, 1969; Peterman and others, 1970). If the Precambrian tholeiites from New Mexico reflect a continental-rift tectonic setting, they must have originated in a depleted mantle source (similar to that from which young-rise tholeiites are produced) or somehow avoided wall-rock reaction and/or crustal contamination.

In conjunction with the geochronology summarized in table 7, a brief geologic history, based on an evolving multiple-rift system model, is here described for the Precambrian rocks in central and south-central New Mexico. To place this model in a broader framework,

Precambrian rocks in surrounding states are also included. We propose that a multiple-rift system began to develop about 1.9 b.y. ago in northern New Mexico and southern Colorado (fig. 47). The rift system may have developed in response to an ascending mantle plume that arrived at the base of the lithosphere in this area just prior to 1.9 b.y. The large volumes of tholeiite in the Tijeras Greenstone and Pecos successions, which exhibit REE patterns similar to modern rise tholeiites, may reflect the opening of a major rift (the Pecos Rift, fig. 47) in which oceanic crust developed about 1.7 b.y. ago. Uplift, rapid sedimentation, bimodal volcanism, folding, and regional metamorphism were followed by extensive granitic plutonism at 1.65 to 1.8 b.y. The nature of the continental crust upon which this rift system developed is unknown. However, if the granitic rocks were produced by partial melting of the lower crust—suggested by geochemical model studies previously discussed—the low initial $\text{Sr}^{87}/\text{Sr}^{86}$ ratios (0.701-0.703) for these rocks indicate that the crustal basement upon which the rift system developed was not older by more than about 200 m.y. The excellent preservation of eugeoclinal assemblages 1.7-1.8 b.y. in age in central and western Arizona (Blacet and others, 1971) suggests that these formed in an arc system associated with a northerly trending subduction zone (fig. 47). The relationship between this arc system and the proposed multiple-rift system to the northeast is presently unknown.

The multiple-rift system seems to have increased in area and moved southwesterly so that between 1.4 and 1.7 b.y. ago it was centered over western New Mexico (fig. 48). The outer edges of the area affected by rifting are poorly known due to lack of exposure. The continental rift association has been dated at about 1.7 b.y. in central Arizona, where it gradationally overlies the older arc association (Ludwig and Silver, 1973). This gradation suggests extinction of the subduction zone proposed in fig. 47 at or just prior to 1.7 b.y. ago. The broadening of the multiple-rift system may reflect spreading of the mantle plume, and the change in center may be caused by plume motion and/or movement of the North American plate over the plume. Rifting, rapid arkosic sedimentation, bimodal magmatism, and regional metamorphism of the Barrovian facies series were followed by wide-scale plutonism concentrated at 1.3-1.5 b.y. over a wide area.

Rocks of 1.2 to 1.65 b.y. in age define a belt extending as far east as Illinois (fig. 1). Although—with very few exceptions—these rocks are unexposed, well samples indicate a characteristic rock association very similar to that exposed in New Mexico (with a relatively larger proportion of siliceous volcanic and hypabyssal rocks farther east in the belt, however). If the proposed plume-induced multiple-rift model is correct for the Southwest, it would seem to necessitate several to many plumes delineating a northeasterly trending belt across the central and southwestern United States between 1.2 and 1.9 b.y. ago. The fact that similar rock associations also characterize the Precambrian basement of west Texas, Oklahoma, and Arkansas, and the area of overlap extending into Kansas (fig. 1) between 1.0-1.3 b.y. in age seems to demand a tectonic model similar to that proposed for the Southwest. If so, plume-induced rift

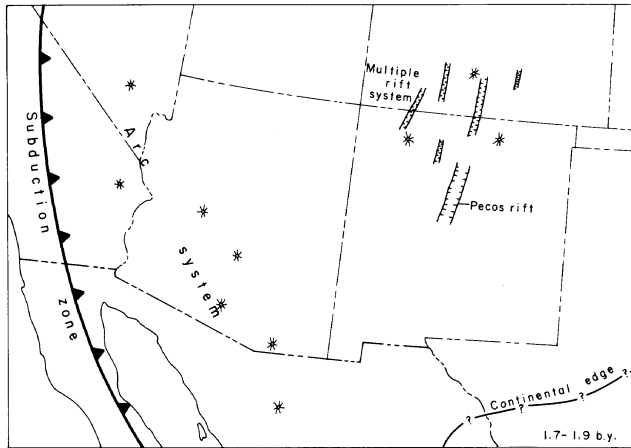


FIGURE 47-POSSIBLE TECTONIC SETTINGS BETWEEN 1.7 AND 1.9 B.Y. IN THE SOUTHWESTERN UNITED STATES. Orientation of rift valleys (parallel lines) is diagrammatic only. Asterisk indicates volcano.

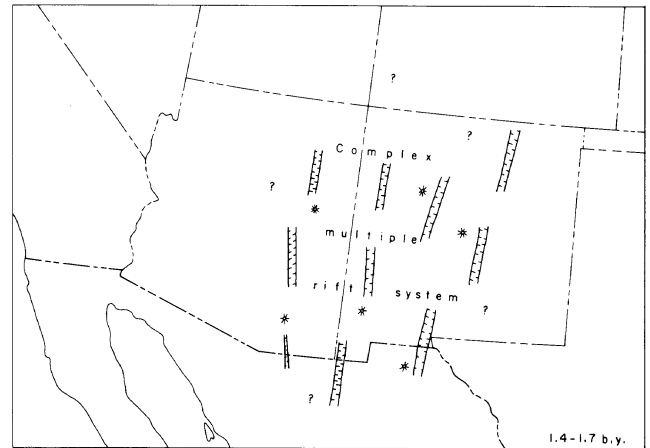


FIGURE 48-DISTRIBUTION OF PROPOSED MULTIPLE-RIFT SYSTEM BETWEEN 1.4 AND 1.7 B.Y. IN THE SOUTHWESTERN UNITED STATES. Orientation of rift valleys (parallel lines) is diagrammatic only. Asterisk indicates volcano.

systems may have characterized most of the southwestern and central United States between 1 and 2 b.y. ago. A similar model involving ductile spreading between transform shear zones has recently been proposed

for rocks between 1.0 and 1.5 b.y. in age that lie in a belt (in part the Grenville Province) extending from Labrador to New Mexico (Wynne-Edwards, 1976).

Mineral deposits

Numerous small veins and fracture fillings of minerals such as barite, fluorite, manganese minerals, magnetite, hematite, and minor sulfides occur in Precambrian rocks of central and south-central New Mexico (Lindgren and others, 1910; Lasky, 1932; Dunham, 1935). None of these have yet proved to be economic. Most or all are Laramide or Tertiary in age. Metallic mineral deposits of known or probable Precambrian age are rare and generally noneconomic. Such deposits fall into three categories: 1) specular hematite deposits, 2) sulfide deposits, and 3) Au-bearing quartz veins. Specular hematite concentrations occur in lenses, veinlets, and fracture fillings and as primary beds in quartzite. Although these deposits are ubiquitous, especially in quartzite, granite, and siliceous metaigneous terranes, they are very small and probably not of economic importance. One specular hematite deposit near the mouth of Sulphur Canyon in the San Andres Mountains (of probable Tertiary age) is associated with malachite and chrysocolla and has been mined for copper (Lasky, 1932). Banded iron formation has also been described from the quartzites in the Pederal Hills (Woodward and Fitzsimmons, 1967). The only Precambrian sulfide deposit of any significance occurs in the Tijeras Greenstone in the vicinity of the York mine (Bruns, 1959; Kelley and Northrop, 1975). This occurrence is characterized by lenses and veinlets in a shear zone that parallels foliation in the surrounding greenstones. Pyrite, sphalerite, and chalcopyrite are the main

sulfides associated with calcite, quartz, or barite. Polished-section studies of Bruns (1959) indicates the mineralization is postmetamorphic or late metamorphic. At the Great Combination mine south of the York mine, gold has been extracted from a mineralized shear zone (Bruns, 1959; Elston, 1967; Kelley and Northrop, 1975). The most extensive Au-bearing quartz lodes occur south of the mouth of Hell Canyon in the greenstone complex (Reiche, 1949). On the Milagros claims, gold occurs in quartz veins. Although quartz veining is locally abundant in many parts of the Precambrian in central and south-central New Mexico, such veins appear to be barren. Amethyst quartz has been mined from a quartz vein at the Juan Torres prospect in the southern Ladron Mountains (Condie, 1976a).

The only major occurrence of pegmatites in the central and south-central Precambrian terranes is in the Rincon Ridge area in the northern Sandia Mountains (Hayes, 1951). These and other minor pegmatites throughout the province appear to be of little economic value. Micas and feldspars are generally small, and rare minerals such as beryl and tourmaline are minor or absent (Hayes, 1951; Herber, 1963a; Kelley and Northrop, 1975). The talc bed in Hembrillo Canyon in the southern San Andres Mountains contains an unknown quantity of potentially commercial talc. Several abandoned mines occur on this unit. Locally, Precambrian rocks have been used as building stones (Kelley and Northrop, 1975) and as railroad ballast (Stark, 1956).

References

- Anderson, E. C., 1948, Briefs from New Mexico Bureau of Mines and Mineral Resources: *Miner and Prospector*, v. 10, no. 9, p. 4
- Arendt, W. W., 1971, The geology of La Joyita Hills, Socorro County, New Mexico: M. S. thesis, University of New Mexico, 75 p.
- Bachman, G. O., 1965, Geologic map of the Capitol Peak NW quadrangle, Socorro County, New Mexico: U. S. Geological Survey, Misc. Geol. Inv. Map I-441
- , 1969, Geology of the Mockingbird Gap quadrangle, Lincoln and Socorro Counties, New Mexico: U. S. Geological Survey, Prof. Paper 594-J, 43 p.
- Bachman, G. O., and Myers, D. A., 1969, Geology of the Bear Peak area, Doña Ana County, New Mexico: U. S. Geological Survey, Bull. 1271-C, 46 p.
- Bachman, G. O., and Harbour, R. L., 1970, Geological map of the northern part of the San Andres Mountains, central New Mexico: U. S. Geological Survey, Map I-600
- Barker, F., 1968, Occurrence and genesis of hematite in Precambrian clastic rocks in southwestern Colorado and northern New Mexico (abs.): Geological Society of America, Spec. Paper 121, p. 481-482
- Barker, F., Peterman, Z. E., Henderson, W. T., and Hildreth, R. E., 1974, Rb-Sr dating of the trondhjemite of Rio Brazos, New Mexico, and of the Kroenke granodiorite, Colorado: U. S. Geological Survey, Journal of Research, v. 2, p. 705-709
- Barker, F., Wones, D. R., Sharp, W. N., and Desborough, C. A., 1975, The Pikes Peak batholith, Colorado Front Range, and a model for the origin of the gabbro-anorthosite-syenite-potassic granite suite: *Precambrian Research*, v. 2, p. 97-160
- Barth, T. F. W., 1959, Principles of classification and norm calculations of metamorphic rocks: *Journal of Geology*, v. 67, p. 135-152
- Basham, W. L., 1951, Structure and metamorphism of the Precambrian rocks of the South Manzano Mountains, New Mexico: M. S. thesis, Northwestern University, 124 p.
- Beers, C. A., 1976, Geology of the Precambrian rocks of the southern Los Pinos Mountains, Socorro County, New Mexico: M. S. thesis, New Mexico Institute of Mining and Technology, 238 p.
- Bell, K., and Powell, J. L., 1969, Strontium isotopic studies of alkalic rocks: the K-rich lavas of the Birunga and Toro-Ankole Regions, east and central equatorial Africa: *Journal of Petrology*, v. 10, p. 536-572
- Blacet, P. M., Silver, L. T., Stern, T. W., and Anderson, C. A., 1971, Precambrian evolution of the Big Bug Group (Yavapai Series) and associated rocks in the northern Bradshaw Mountains, central Arizona (abs.): Geological Society of America, Abstracts with Programs, v. 3, p. 84
- Black, B. A., 1964, Geology of the northern and eastern parts of the Ladron Mountains, Socorro County, New Mexico: M. S. thesis, University of New Mexico, 117 p.
- Blakestad, R. B., Jr., 1976, Geology of the Kelly mining district, Socorro County, New Mexico: New Mexico Bureau of Mines and Mineral Resources, Open-file Rept. 43, 140 p.
- Bolton, W. R., 1976, Precambrian geochronology of the Sevillita metarhyolite and the Los Pinos, Sepultura, and Priest plutons of the southern Sandia uplift, New Mexico: M. S. thesis, New Mexico Institute of Mining and Technology, 45 p.
- Brookins, D. G., 1974, Summary of recent Rb-Sr age determinations from Precambrian rocks of north-central New Mexico: New Mexico Geological Society, Guidebook 25th field conference, p. 119-121
- Brookins, D. G., and Della Valle, R. S., 1977, Rb-Sr geochronologic investigation of the Zuni Mountains, New Mexico (abs.): Geological Society of America, Abstracts with Programs, v. 9, p. 9
- Brown, G. C., and Fyfe, W. S., 1970, The production of granitic melts during ultrametamorphism: *Contributions to Mineralogy and Petrology*, v. 28, p. 310-318
- Bruns, J. J., 1959, Petrology of the Tijeras Greenstone, Bernalillo County, New Mexico: M. S. thesis, University of New Mexico, 119 p.
- Budding, A. J., and Condie, K. C., 1975, Precambrian rocks of the Sierra Oscura and northern San Andres Mountains: New Mexico Geological Society, Guidebook 26th field conference, p. 89-93
- Carmichael, I. S. E., 1963, The crystallization of feldspar in volcanic liquids: *Geological Society of London, Quarterly Journal*, v. 119, p. 95-131
- Chamberlin, R. M., in preparation, Geology of Socorro Peak volcanic center, Socorro County, New Mexico: Ph.D. thesis, Colorado School of Mines
- Condie, K. C., 1967, Petrology of the late Precambrian tillite association in northern Utah: *Geological Society of America, Bull.*, v. 78, p. 1317-1344
- , 1973, Archean magmatism and crustal thickening: *Geological Society of America, Bull.*, v. 84, p. 2981-2992
- , 1976a, Geologic map of Precambrian rocks of the Ladron Mountains, Socorro County, New Mexico: New Mexico Bureau of Mines and Mineral Resources, Geol. Map 38
- , 1976b, Trace-element geochemistry of Archean greenstone belts: *Earth-Science Reviews*, v. 12, p. 393-417
- , 1978, Geochemical models for the origin of Proterozoic granitic rocks in New Mexico: *Chemical Geology*, v. 21, p. 131-149
- Condie, K. C., and Harrison, N. M., 1976, Geochemistry of the Archean Bulawayan Group, Midlands greenstone belt, Rhodesia: *Precambrian Research*, v. 3, p. 253-271
- Condie, K. C., and Hayslip, D. L., 1975, Young bimodal volcanism at the Medicine Lake volcanic center, Northern California: *Geochimica et Cosmochimica Acta*, v. 39, p. 1165-1178
- Condie, K. C., and Hunter, D. R., 1976, Trace element geochemistry of Archean granitic rocks from Swaziland: *Earth and Planetary Science Letters*, v. 29, p. 389-400
- Condie, K. C., and Lo, H. H., 1971, Trace element geochemistry of the Louis Lake batholith of early Precambrian age, Wyoming: *Geochimica et Cosmochimica Acta*, v. 35, p. 1095-1120
- Cookro, T. M., 1978, Petrology of Precambrian granitic rocks of the Ladron Mountains, Socorro County, New Mexico: M.S. thesis, New Mexico Institute of Mining and Technology
- Cserna, E., 1956, Structural geology and stratigraphy of the Fra Cristobal quadrangle, Sierra County, New Mexico: Ph.D. thesis, Columbia University
- Cullers, R. L., Yeh, L., and Chaudhuri, S., 1974, Rare earth elements in Silurian pelitic schists from N.W. Maine: *Geochimica et Cosmochimica Acta*, v. 38, p. 389-400
- Denison, R. E., and Hetherington, E. A., 1969, Basement rocks in far west Texas and south-central New Mexico: New Mexico Bureau of Mines and Mineral Resources, Circ. 104, 13 p.
- Dickinson, W. R., 1970, Interpreting detrital modes of graywacke and arkose: *Journal of Sedimentary Petrology*, v. 40, p. 695-701
- Dorman, J. H., 1951, Structure of the Priest Granite, Manzano Mountains, New Mexico: M. S. thesis, Northwestern University, 46 p.
- Doyle, J. C., 1951, Geology of the Northern Caballo Mountains, Sierra County, New Mexico: M. S. thesis, New Mexico Institute of Mining and Technology, 51 p.
- Dunham, K. C., 1935, The geology of the Organ Mountains: New Mexico Bureau of Mines and Mineral Resources, Bull. 11, 272 p.
- Elston, W. E., 1967, Summary of the mineral resources of Bernalillo, Sandoval, and Santa Fe Counties, New Mexico: New Mexico Bureau of Mines and Mineral Resources, Bull. 81, 81 p.
- Evans, B. W., 1965, Application of a reaction-rate method to the breakdown equilibria of muscovite and muscovite plus quartz: *American Journal of Science*, v. 263, p. 647-667
- Ewart, A., Taylor, S. R., and Capp, A. C., 1968, Trace and minor element geochemistry of the rhyolitic volcanic rocks, central North Island, New Zealand: *Contributions to Mineralogy and Petrology*, v. 18, p. 76-104
- Fallis, J. F., Jr., 1958, Geology of the Pedernal Hills area, Torrance County, New Mexico: M. S. thesis, University of New Mexico, 50 p.
- Feinberg, H. B., 1969, Geology of the central portion of the Sandia granite, Sandia Mountains, Bernalillo County, New Mexico: M. S. thesis, University of New Mexico, 127 p.
- Field, D., and Elliott, R. B., 1974, The chemistry of gabbro/amphibolite transitions in south Norway: *Contributions to Mineralogy and Petrology*, v. 47, p. 63-76
- Flawn, P. T., 1956, Basement rocks of Texas and southeast New Mexico: *University of Texas, Publication No. 5605*, 73 p.
- Foster, R. W., Frenness, R. M., and Riese, W. C., 1972, Subsurface geology of east-central New Mexico: *New Mexico Geological Society, Spec. Pub. No. 4*, 22 p.
- Foster, R. W., and Stipp, T. F., 1961, Preliminary geologic and relief map of the Precambrian rocks of New Mexico: *New Mexico Bureau of Mines and Mineral Resources, Circ. 57*, 37 p.
- Fullagar, P. D., and Shiver, W. S., 1973, Geochronology and

- petrochemistry of the Embudo granite, New Mexico: Geological Society of America, Bull., v. 84, p. 2705-2712
- Gast, P. W., 1968, Trace element fractionation and the origin of tholeiitic and alkaline magma types: *Geochimica et Cosmochimica Acta*, v. 32, p. 1057-1086
- Gonzalez, R. A., 1968, Petrography and structure of the Pedernal Hills, Torrance County, New Mexico: M. S. thesis, University of New Mexico, 78 p.
- Gonzalez, R. A., and Woodward, L. A., 1972, Petrology and structure of Precambrian rocks of the Pedernal Hills, New Mexico: New Mexico Geological Society, Guidebook 23rd field conference, p. 144-147
- Gordon, G. E., and Randle, K., Goles, G. G., Corliss, J. B., Beeson, M. H., and Oxley, S. S., 1968, Instrumental activation analysis of standard rocks with high-resolution γ -ray detectors, *Geochimica et Cosmochimica Acta*, v. 32, p. 369-396
- Green, J. A. and Callender, J. F., 1973, Hornblende-hornfels facies metamorphism in a contact aureole adjacent to the Sandia Mountain pluton, New Mexico (abs.): Geological Society of America, Abstracts with Programs, v. 5, p. 642-643
- Green, T. H., Brunfelt, A. O., and Heier, K. S., 1972, Rare-earth element distribution and K/Rb ratios in granulites, mangerites, and anorthosites, Lofoten-Vesteraalen, Norway: *Geochimica et Cosmochimica Acta*, v. 36, p. 241-257
- Haederle, W. F., 1966, Structure and metamorphism in the southern Sierra Ladrones, Socorro County, New Mexico: M. S. thesis, New Mexico Institute of Mining and Technology, 58 p.
- Hart, S. R., 1969, K, Rb, Cs, contents and K/Rb and K/Cs ratios of fresh and altered submarine basalts: *Earth and Planetary Science Letters*, v. 6, p. 295-303
- Hart, S. R., Erlank, A. J., and Kable, E. J. D., 1974, Sea floor basalt alteration: some chemical and Sr isotope effects: *Contributions to Mineralogy and Petrology*, v. 44, p. 219-230
- Haskin, L. A., Haskin, M. A., Frey, F., and Wildeman, T. R., 1968, Relative and absolute terrestrial abundances of the rare earths: *in* Origin and distribution of the elements, L. H. Ahrens, ed., Oxford, Pergamon Press, p. 880-912
- Hayes, P. T., 1951, Geology of the Precambrian rocks of the northern end of the Sandia Mountains, Bernalillo and Sandoval Counties, New Mexico: M. S. thesis, University of New Mexico, 54 p.
- Herber, L. J., 1963a, Structural petrology and economic features of the Precambrian rocks of La Joyita Hills: M. S. thesis, New Mexico Institute of Mining and Technology, 36 p.
- , 1963b, Precambrian rocks of La Joyita Hills: New Mexico Geological Society, Guidebook 14th field conference, p. 180-184
- Hermann, A. G., Potts, M. J., and Knake, D., 1974, Geochemistry of the REE in spilites from the oceanic and continental crust: *Contributions to Mineralogy and Petrology*, v. 44, p. 1-16
- Holdaway, M. J., 1971, Stability of andalusite and the aluminum silicate phase diagram: *American Journal of Science*, v. 271, p. 97-131
- Hoschek, G., 1969, The stability of staurolite and chloritoid and their significance in metamorphism of pelitic rocks: *Contributions to Mineralogy and Petrology*, v. 22, p. 208-232
- Huzarski, J. R., 1971, Petrology and structure of eastern Monte Largo Hills, New Mexico: M. S. thesis, University of New Mexico, 45 p.
- Jacobs, R. C., 1956, Geology of the central front of the Fra Cristobal Mountains, Sierra County, New Mexico: M. S. thesis, University of New Mexico, 45 p.
- Jahns, R. H., 1955, Geology of the Sierra Cuchillo, New Mexico: New Mexico Geological Society, Guidebook 6th field conference, p. 158-174
- Kalish, P., 1953, Geology of the Water Canyon area, Magdalena Mountains, Socorro County, New Mexico: M. S. thesis, New Mexico Institute of Mining and Technology, 48 p.
- Kay, R., Hubbard, N. J., and Gast, P. W., 1970, Chemical characteristics and origin of oceanic ridge volcanic rocks: *Journal of Geophysical Research*, v. 75, p. 1585-1613
- Kelley, V. C., 1959, Log of preconference trip to Tijeras Canyon, Sandia Mountains, New Mexico: American Association of Petroleum Geologists, Rocky Mtn. Sec., Program 9th ann. mtg., Albuquerque, p. 31-41
- , 1968, Geology of the alkaline Precambrian rocks at Pajarito Mountains, Otero County, New Mexico: Geological Society of America, Bull., v. 79, p. 1565-1572
- , 1972, Geology of the Fort Sumner Sheet, New Mexico: New Mexico Bureau of Mines and Mineral Resources, Bull. 98, 55 p.
- Kelley, V. C., and Northrop, S. A., 1975, Geology of Sandia Mountains and vicinity, New Mexico: New Mexico Bureau of Mines and Mineral Resources, Mem. 29, 136 p.
- Kelley, V. C., and Silver, C., 1952, Geology of the Caballo Mountains: University of New Mexico, Publications in Geology, No. 4, 286 p.
- Kottowski, F. E., 1955, Geology of San Andres Mountains: New Mexico Geological Society, Guidebook 6th field conference, p. 136-145
- , 1959, Sedimentary rocks of the San Andres Mountains: Roswell Geological Society and Society of Economic Paleontologists and Mineralogists, Guidebook 12th field conference, p. 259-277
- , 1960, Summary of Pennsylvanian sections in southwestern New Mexico and southwestern Arizona: New Mexico Bureau of Mines and Mineral Resources, Bull. 66, 187 p.
- Kottowski, F. E., Flower, R. H., Thompson, M. L., and Foster, R. W., 1956, Stratigraphic studies of the San Andres Mountains, New Mexico: New Mexico Bureau of Mines and Mineral Resources, Mem. 1, 132 p.
- Krewedl, D. A., 1974, Geology of the central Magdalena Mountains, Socorro County, New Mexico: Ph.D. thesis, University of Arizona, 128 p.
- Lambert, P. W., 1961, Petrology of the Precambrian rocks of part of the Monte Largo area, New Mexico: M. S. thesis, University of New Mexico, 103 p.
- Lasky, S. G., 1932, The ore deposits of Socorro County, New Mexico: New Mexico Bureau of Mines and Mineral Resources, Bull. 8, 139 p.
- Lindgren, W., Graton, L. C., and Gordon, C. H., 1910, The ore deposits of New Mexico: U. S. Geological Survey, Prof. Paper 68, 361 p.
- Livingston, D. E., 1969, Geochronology of older Precambrian rocks in Gila County, Arizona: Ph.D. thesis, University of Arizona, 224 p.
- Lodewick, R. B., 1960, Geology and petrography of the Tijeras (Cibola) Gneiss, Bernalillo County, New Mexico: M. S. thesis, University of New Mexico, 59 p.
- Loughlin, G. F., and Koschmann, A. H., 1942, Geology and ore deposits of the Magdalena mining district, New Mexico: U. S. Geological Survey, Prof. Paper 200, 168 p.
- Ludwig, K. R., and Silver, L. T., 1973, Precambrian Alder Series and Red Rock Rhyolite, Mazatzal Mountains, Arizona (abs.): Geological Society of America, Abstracts with Programs, v. 5, p. 75-76
- Maaloe, S., and Wyllie, P. J., 1975, Water content of a granitic magma deduced from the sequence of crystallization determined experimentally with water-undersaturated conditions: *Contributions to Mineralogy and Petrology*, v. 52, p. 175-191
- Mallon, K. M., 1966, Precambrian geology of the northern part of the Los Pinos Mountains, New Mexico: M. S. thesis, New Mexico Institute of Mining and Technology, 88 p.
- Mason, J. T., 1976, The geology of the Caballo Peak quadrangle, Sierra County, New Mexico: M. S. thesis, University of New Mexico, 131 p.
- Mathewson, D., in preparation, Precambrian geology and mineral deposits of San Miguel County, New Mexico: Ph.D. thesis, New Mexico Institute of Mining and Technology
- McBride, E. F., 1963, A classification of common sandstones: *Journal of Sedimentary Petrology*, v. 33, p. 664-669
- McCleary, J. T., 1960, Geology of the northern part of the Fra Cristobal Range, Sierra and Socorro Counties, New Mexico: M. S. thesis, University of New Mexico, 59 p.
- Melson, W. G., and Van Andel, T. H., 1966, Metamorphism in the mid-Atlantic ridge, 22° N latitude: *Marine Geology*, v. 4, p. 165-186
- Metz, P. W., and Puhan, D., 1970, Experimentelle Untersuchung der Metamorphose von Kieselig dolomitischen Sedimenten I. Die Gleichgewichtsdaten der Reaktion $3 \text{ Dolomit} + 4 \text{ Quarz} + 1 \text{ H}_2\text{O} = 1 \text{ Talk} + 3 \text{ Calcit} + 3 \text{ CO}_2$ für die Gasamtgasdrucke von 1000, 3000 und 5000 Bar: *Contributions to Mineralogy and Petrology*, v. 26, p. 302-314
- , 1971, Korrektur zur Arbeit "Experimentelle Untersuchung der Metamorphose von kieselig dolomitischen Sedimenten": *Contributions to Mineralogy and Petrology*, v. 31, p. 169-170
- Metz, P. W., and Winkler, H. G. F., 1963, Experimentelle Gesteinsmetamorphose VII Die Bildung von Talk aus kieseligem Dolomit: *Geochimica et Cosmochimica Acta*, v. 27, p. 431-457
- Miller, J. P., Montgomery, A., and Sutherland, P. K., 1963, Geology

- of part of the Sangre de Cristo Mountains, New Mexico: New Mexico Bureau of Mines and Mineral Resources, Mem. 11, 106 p.
- Minyev, D. A., 1963, Geochemical differentiation of rare earths: *Geochemistry*, no. 12, 1963, p. 1029-1149
- Miyashiro, A., 1961, Evolution of metamorphic belts: *Journal of Petrology*, v. 2, p. 277-311
- , 1975, Volcanic rock series and tectonic setting: *Annual Reviews of Earth and Planetary Sciences*, v. 3, p. 251-269
- Muehlberger, W. R., Hedge, C. E., Denison, R. E., and Marvin, R. F., 1966, Geochronology of the midcontinent region, United States, Part 3: *Journal of Geophysical Research*, v. 71, p. 5409-5426
- Muehlberger, W. R., Denison, R. E., and Lidiak, E. G., 1967, Basement rocks in continental interior of United States: *American Association of Petroleum Geologists, Bull.*, v. 51, p. 2351-2380
- Mukhopadhyay, B., Brookins, D. G., and Bolivar, S. L., 1975, Rb-Sr whole-rock study of the Precambrian rocks of the Pedernal Hills, New Mexico: *Earth and Planetary Science Letters*, v. 27, p. 283-286
- Murray, M., and Condie, K. C., 1973, Post-Ordovician to early Mesozoic history of the eastern Klamath subprovince, northern California: *Journal of Sedimentary Petrology*, v. 43, p. 505-515
- Myers, D. A., and McKay, E. J., 1970, Geologic map of the Mount Washington quadrangle, Bernalillo and Valencia Counties, New Mexico: U. S. Geological Survey, Map GQ-886
- , 1971, Geologic map of the Bosque Peak quadrangle, Torrance, Valencia, and Bernalillo Counties, New Mexico: U. S. Geological Survey, Map GQ-948
- , 1972, Geologic map of the Capilla Peak quadrangle, Torrance and Valencia Counties, New Mexico: U. S. Geological Survey, Map GQ-1008
- , 1974, Geologic map of the southwest quarter of the Torreon 15-min quadrangle, Torrance and Valencia Counties, New Mexico: U. S. Geological Survey, Misc. Geol. Inv. Map I-820
- , 1976, Geological map of the north end of the Manzano Mountains, Tijeras and Sedillo quadrangles, Bernalillo County, New Mexico: U. S. Geological Survey, Misc. Geol. Inv. Map I-968
- Noble, E. A., 1950, Geology of the southern Ladron Mountains, Socorro County, New Mexico: M. S. thesis, University of New Mexico, 72 p.
- O'Conner, J. T., 1965, A classification for quartz-rich igneous rocks based on feldspar ratios: U. S. Geological Survey, Prof. Paper 525-B, p. 79-84
- Pearce, J. A., 1976, Statistical analysis of major element patterns in basalts: *Journal of Petrology*, v. 17, p. 15-43
- Pearce, J. A., and Cann, J. R., 1973, Tectonic setting of basic volcanic rocks determined using trace element analysis: *Earth and Planetary Science Letters*, v. 19, p. 290-300
- Perhac, R. M., 1964, Resume of the geology of the Gallinas Mountains; New Mexico Geological Society, Guidebook 15th field conference, p. 87-91
- Peterman, Z. E., Carmichael, I. S. E., and Smith, A. L., 1970, Strontium isotopes in Quaternary basalts of southeastern California: *Earth and Planetary Science Letters*, v. 7, p. 381-384
- Pettijohn, F. J., 1963, Chemical composition of sandstones—excluding carbonate and volcanic sands: U. S. Geological Survey, Prof. Paper 440-5, 21 p.
- Pray, L. C., 1961, Geology of the Sacramento Mountains escarpment, Otero County, New Mexico: New Mexico Bureau of Mines and Mineral Resources, Bull. 35, 144 p.
- Reiche, P., 1949, Geology of the Manzanita and north Manzano Mountains, New Mexico: Geological Society of America, Bull., v. 60, p. 1183-1212
- Reynolds, R. C., Jr., 1963, Matrix corrections in trace elements analysis by X-ray fluorescence: *American Mineralogist*, v. 48, p. 1133-1143
- Rittmann, A., 1952, Nomenclature of volcanic rocks: *Bulletin Volcanologique*, v. 12, p. 75-102
- Robertson, J. M., 1976, Annotated bibliography and mapping index of Precambrian of New Mexico: New Mexico Bureau of Mines and Mineral Resources, Bull. 103, 90 p.
- Schwab, F. L., 1971, Geosynclinal compositions and the new global tectonics: *Journal of Sedimentary Petrology*, v. 41, p. 928-938
- , 1975, Framework mineralogy and chemical composition of continental margin-type sandstone: *Geology*, v. 3, p. 487-490
- Seager, W. R., Hawley, J. W., and Clemons, R. E., 1971, Geology of San Diego Mountain area, Doña Ana County, New Mexico: New Mexico Bureau of Mines and Mineral Resources, Bull. 97, 38 p.
- Shomaker, J., 1965, Geology of the southern portion of the Sandia granite, Sandia Mountains, Bernalillo County, New Mexico: M. S. thesis, University of New Mexico, 80 p.
- Smith, C. T., 1963, Preliminary notes on the geology of part of the Socorro Mountains, Socorro County, New Mexico: New Mexico Geological Society, Guidebook 14th field conference, p. 185-196
- Staatz, M. H., and Norton, J. J., 1942, The Precambrian geology of the Los Pinos Range, New Mexico: M. S. thesis, Northwestern University, 150 p.
- Staatz, M. H., Adams, J. W., and Conklin, N. M., 1965, Thorium-bearing microcline-rich rocks in the southern Caballo Mountains, Sierra County, New Mexico: U. S. Geological Survey, Prof. Paper 525-D, p. D48-D51
- Stark, J. T., 1956, Geology of the South Manzano Mountains, New Mexico: New Mexico Bureau of Mines and Mineral Resources, Bull. 34, 46 p.
- Stark, J. T., and Dapples, E. C., 1946, Geology of the Los Pinos Mountains, New Mexico: Geological Society of America, Bull., v. 57, p. 1121-1172
- Stipp, T. F., 1955, Precambrian rocks of south-central New Mexico: New Mexico Geological Society, Guidebook 6th field conference, p. 62-64
- Taggart, J. E., and Brookins, D. G., 1975, Rb-Sr whole rock age determinations for Sandia granite and Cibola Gneiss, New Mexico: *Isochron West*, no. 12, p. 5-8
- Taylor, S. R., and White, A. J. R., 1966, Trace element abundances in andesites: *Bulletin Volcanologique*, v. 29, p. 177-194
- Thompson, T. B., and Giles, D. L., 1974, Orbicular rocks of the Sandia Mountains, New Mexico: Geological Society of America, Bull., v. 85, p. 911-916
- Turekian, K. K., and Wedepohl, K. H., 1961, Distribution of elements in some major units of the earth's crust: Geological Society of America, Bull., v. 72, p. 175-192
- Turner, F. J., 1968, *Metamorphic Petrology*: New York, McGraw-Hill, 403 p.
- Tuttle, O. F., and Bowen, N. L., 1958, Origin of granite in the light of experimental studies in the system Ab-Or-Q-H₂O: Geological Society of America, Mem. 74, 153 p.
- Van Schmus, W. R., 1976, Early and middle Proterozoic history of the Great Lakes area, North America: Royal Society of London, *Philosophical Transactions*, A, v. 280, p. 605-628
- White, D. L., 1977, A Rb-Sr isotopic study of the Precambrian intrusives of south-central New Mexico: Ph.D. thesis, Miami University, Oxford, Ohio, 88 p.
- Whitney, J. A., 1975, The effects of pressure, temperature, and H₂O on phase assemblage in four synthetic rock compositions: *Journal of Geology*, v. 83, p. 1-31
- Winkler, Helmut, G. F., 1974, *Petrogenesis of metamorphic rocks*: New York, Springer-Verlag, 320 p.
- Woodward, L. A., and Fitzsimmons, J. P., 1967, Precambrian banded iron formation, Pedernal Peak, Torrance County, New Mexico (abs.): New Mexico Geological Society, Guidebook 18th field conference, p. 228
- Woodward, T. M., 1973, Geology of the Lemitar Mountains, Socorro County, New Mexico: M. S. thesis, New Mexico Institute of Mining and Technology, 73 p.
- Wright, T. L., and Doherty, P. C., 1970, A linear programming and least squares computer method for solving petrologic mixing problems: *Geologic Society of America, Bull.*, v. 81, p. 1995-2008
- Wynne-Edwards, H. R., 1976, Proterozoic ensialic orogenesis: The milipede model of ductile plate tectonics: *American Journal of Science*, v. 276, p. 927-953
- Yoder, H. S., Jr., and Tilley, C. E., 1962, Origin of basalt magmas: an experimental study of natural and synthetic rock systems: *Journal of Petrology*, v. 3, p. 342-532

Appendices

APPENDIX 1—COMPOSITE STRATIGRAPHIC SECTIONS OF PRECAMBRIAN ROCKS IN CENTRAL AND SOUTH-CENTRAL NEW MEXICO. (Section numbers also refer to stratigraphic sections, figs. 24 and 25.)

Section 1—Northern Manzanita Mountains from northwestern contact of Cibola Gneiss (2 km south of Tijeras Canyon) to Coyote Canyon (in part after Reiche, 1949, and Bruns, 1959).

Lithology	Thickness (m)
<i>intrusive contact with Manzanita pluton</i>	
arkosite and feldspathic quartzite with two distinct dark quartzite units	430
muscovite-quartz schist	30
quartzites ranging from buff and red to white; massive recrystallized and highly fractured	~ 1,000
amphibolite, metadiabase, chlorite schist and greenstone (Tijeras Greenstone); very minor siliceous meta-igneous rocks	1,600
amphibolite, chlorite schist, mica-quartz schist and minor quartzite	420
<i>Tijeras fault</i>	
quartz-plagioclase gneiss (± sillimanite with minor quartzite beds (Cibola Gneiss))	~ 620
<i>intrusive contact with South Sandia pluton</i>	
total thickness	~ 4,100

Section 2—Manzanita and northern Manzano Mountains between the Comanche Canyon unconformity and Mount Washington (in part after Reiche, 1949).

Lithology	Thickness (m)
<i>angular unconformity</i>	
arkosite (10%), feldspathic quartzite (30%), and mica-quartz-chloritoid phyllite and schist (60%)	≥ 3,500
<i>intrusive contact with Ojita pluton</i>	
greenstone and amphibolite (80%), mica and mica-quartz schist and phyllite (10%), quartzite and feldspathic quartzite (10%)	≥ 2,000
greenstone and amphibolite (35%) and mica and mica-quartz schist and phyllite (65%)	~ 3,000
mica, mica-quartz, and mica-quartz-chlorite schist and phyllite (90%) and feldspathic quartzite (10%)	3,700
granitic sill	30
mica-chlorite-quartz phyllite and schist	70
greenstone and amphibolite	200
<i>intrusive contact with Manzanita pluton</i>	
total thickness	≥ 12,500

Section 3—Central Manzano Mountains between Comanche and Monte Largo Canyons, western limb of syncline (in part after Stark, 1956, and Myers and McKay, 1972).

Description	Thickness (m)
<i>synclinal axis</i>	
<i>Sevilleta Formation:</i>	
siliceous meta-igneous rocks containing about 15% amphibolite layers	1,300
amphibolite (40%), feldspathic quartzite (50%), and mica-quartz schist (10%)	200
<i>White Ridge Formation:</i>	
massive white quartzite and feldspathic quartzite	100
mica-quartz schist	20
massive white quartzite and feldspathic quartzite	220
<i>Blue Springs Muscovite Schist:</i>	
mica-quartz schist and phyllite	800
massive quartzite	20

mica-quartz schist and phyllite	55
quartz schist and banded quartzite	125
mica-quartz schist and phyllite	430

<i>Sais Quartzite:</i>	
massive buff quartzite	75
quartz-mica schist	105
massive white quartzite	150
mica-quartz schist and phyllite with minor interbedded quartzite beds (~ 10%)	2,100
massive white to buff quartzite and feldspathic quartzite	130
<i>angular unconformity</i>	
total thickness	5,830

Section 4—Central Manzano Mountains between New Canyon and Manzano Peak, eastern limb of syncline (in part from Stark, 1956, and Myers and McKay, 1972).

Description	Thickness (m)
<i>synclinal axis</i>	
<i>Sevilleta Formation:</i>	
siliceous meta-igneous rocks containing about 5% thin amphibolite lenses	500
amphibolite (40%), feldspathic quartzite (50%), and mica-quartz schist (10%)	310
amphibolite	160
amphibolite (40%), feldspathic quartzite (50%), and mica-quartz schist (10%)	240
<i>White Ridge Formation:</i>	
quartzite and quartz-mica schist	390
massive feldspathic quartzite	300
massive buff to white quartzite and feldspathic quartzite	500
mica-quartz schist and phyllite (Blue Springs Muscovite Schist)	200
<i>Paloma fault:</i>	
massive white quartzite (Sais Quartzite)	600
<i>Montosa fault</i>	
total thickness	3,200

Section 5—Northern Los Pinos Mountains (in part after Stark and Douglas, 1946).

Description	Thickness (m)
<i>top not exposed</i>	
<i>Sevilleta Formation:</i>	
gray siliceous meta-igneous rock	75
amphibolite	4
gray siliceous meta-igneous rock	300
orange siliceous meta-igneous rock	22
chlorite-hornblende schist	21
gray siliceous meta-igneous rock	27
amphibolite	2
buff to light-green siliceous meta-igneous rock	118
gray siliceous meta-igneous rock	32
quartz-muscovite-feldspar schist	105
white porphyritic siliceous meta-igneous rock	43
amphibolite	1
orange siliceous meta-igneous rock	32
white porphyritic siliceous meta-igneous rock	52
quartz-mica phyllite	10
chlorite-hornblende schist	20
orange siliceous meta-igneous rock	29
quartz-mica phyllite	5

amphibolite	30	brown to gray porphyritic meta-igneous rock	200
quartz-mica phyllite	68	amphibolite	25
amphibolite	1	tan quartz-phenocryst-rich meta-igneous rock	60
quartzite and quartz-muscovite schist	41	amphibolite	7
amphibolite	11	tan quartz-phenocryst-rich meta-igneous rock	25
quartz-mica phyllite	31	sheared and altered meta-igneous rock	80
amphibolite	1	tan quartz-phenocryst-rich meta-igneous rock	50
quartz-mica phyllite	11	sheared and altered meta-igneous rock	25
amphibolite	1	tan quartz-phenocryst-rich meta-igneous rock	7
quartz-mica phyllite	34	amphibolite	6
gray siliceous meta-igneous rock	70	tan quartz-phenocryst-rich meta-igneous rock	12
chlorite-muscovite schist	10	brown porphyritic meta-igneous rock	125
amphibolite	2	gray to black, massive porphyritic meta-igneous rock	35
mica-quartz schist and phyllite	5	amphibolite	3
banded quartz	5	gray to black, massive porphyritic meta-igneous rock	30
amphibolite	70	amphibolite	5
chlorite-muscovite schist	54	gray to black, massive porphyritic meta-igneous rock	550
arkosite	23	amphibolite	4
quartzite and quartz-muscovite schist	29	gray to black, massive porphyritic meta-igneous rock	165
amphibolite	19	amphibolite	10
mica-quartz schist and phyllite	24	gray to black, massive porphyritic meta-igneous rock	10
amphibolite	17	amphibolite	6
mica-quartz schist and phyllite	13	gray to black, massive porphyritic meta-igneous rock	150
amphibolite	8		
mixed quartzite and arkosite	22	<i>fault zone and intrusive contact with Capirote pluton</i>	
amphibolite	3	amphibolite	100
feldspathic quartzite and arkosite	49	buff siliceous meta-igneous rock	20
		amphibolite	30
<i>White Ridge Formation:</i>		mica-quartz schist and phyllite	280
massive buff quartzite and feldspathic quartzite	170	amphibolite	35
muscovite schist and phyllite	16	mica-quartz schist and phyllite	40
massive quartzite schist and phyllite	116	amphibolite, partly layered	105
muscovite schist and phyllite	18	massive white quartzite	35
quartzite	34	amphibolite, partly layered	140
muscovite schist and phyllite	10	massive white quartzite and feldspathic quartzite	
quartzite	18	gradational along strike with conglomeratic quartzite	
massive white quartzite	300	and mica-quartz schist; contains several minor	
		amphibolite units	635
<i>Blue Springs Muscovite Schist:</i>		mica schist	10
muscovite-quartz schist and phyllite; minor quartzite	600	medium-grained, foliated feldspathic quartzite	90
		quartz-mica schist	50
		feldspathic quartzite	50
<i>Paloma fault</i>		quartz-muscovite schist	20
muscovite-quartz schist and phyllite; minor quartzite	400	coarse conglomeratic feldspathic quartzite containing	
massive white quartzite (Sais Quartzite)	340	pebbles 0.5-3 cm long	150
		coarse, foliated feldspathic quartzite	40
<i>Montosa fault</i>		amphibolite dike	20
total thickness	3,572	coarse arkosite with lesser amounts of feldspathic quartzite	
		and several interbedded mica-schist layers	175

Section 6—Northern Pedernal Hills from intrusive granitic contact about 10 km south of Pedernal Peak to northernmost Precambrian exposure (in part after Fallis, 1958, and Gonzalez, 1968).

Description	Thickness (m)		
<i>intrusive contact with Pedernal pluton</i>		<i>fault</i>	
mica-quartz schist and phyllite; minor chlorite schist and amphibolite	2,000	quartz-mica schist	13
mica-quartz schist and phyllite (50%); amphibolite and greenstone (50%)	2,000	white fine-grained quartzite	95
massive white quartzite (85%), quartz-mica schist (10%), and minor amphibolite (5%)	2,500	gray crossbedded quartzite (distinctive unit)	36
<i>base not exposed</i>		coarse white quartzite	76
total thickness	6,500	amphibolite	21
		crossbedded medium-to coarse-grained feldspathic quartzite	35
		massive feldspathic quartzite and siltite exhibiting festoon crossbedding, pull-apart structures, and intraformational conglomerate	50
		amphibolite	8
		medium-grained feldspathic quartzite	12
		brown feldspathic quartzite with 30% of mica-quartz schist	75
		muscovite-quartz phyllite (50%) and quartzite (50%)	46

Section 7—Ladron Mountains from intrusive contact of Capirote pluton along southeasterly trending ridge about 2 km south of Ladron Peak. Also includes meta-igneous sequence on the northwest slope of Ladron Peak (after P. Farquhar, 1976, personal communication).

Description	Thickness (m)		
<i>intrusive contact with Ladron pluton</i>		interlayered buff feldspathic quartzite (80%) and gray feldspathic quartzite (20%); crossbedding well preserved	69
tan porphyritic meta-igneous rock	50	muscovite-quartz phyllite	80
amphibolite	5	coarse quartzite, locally conglomeratic	45
tan porphyritic meta-igneous rock	110	dark feldspathic quartzite	35
granitic sill	3	coarse quartzite, locally conglomeratic	6
amphibolite	5	quartz-mica schist	14
		dark feldspathic quartzite	52
		amphibolite	21
		orange feldspathic quartzite	33
		mica schist	4
		orange feldspathic quartzite	58

<i>intrusive contact with Capirote pluton</i>				
total thickness		4,672		
Section 8—Magdalena Mountains, vicinity of north fork of Water Canyon.				
Description		Thickness (m)		
<i>Water Canyon fault</i>				
buff to gray feldspathic siltite and quartzitic argillite (partly metatuffs)		100	mica-chlorite-quartz schist and phyllite (intruded by the Strawberry Peak pluton)	≥ 250
metadiabase		2	metadiabase	100
buff to gray feldspathic siltite and quartzitic argillite (partly metatuffs)		50	mica-chlorite-quartz and phyllite	400
metadiabase		2	highly sheared mica-chlorite schist and phyllite with quartzite boudins	300
buff to gray feldspathic siltite and quartzitic argillite (partly metatuffs)		60	metadiabase	150
metadiabase		1	mica-chlorite-quartz schist and phyllite	300
buff to gray feldspathic siltite and quartzitic argillite (partly metatuffs)		75	metadiabase	150
metadiabase		8	mica-chlorite-quartz schist and phyllite	200
buff to gray siltite, quartzitic argillite, and phyllite, (partly metatuffs)		370	metadiabase	250
conglomeratic quartzitic argillite (tuff breccia?)		20	mica-chlorite-quartz schist and phyllite	100
buff to gray siltite, quartzitic argillite, and phyllite, (partly metatuffs)		30	massive white quartzite	50
metadiabase		24	mica-chlorite-quartz and phyllite	525
buff to gray siltite, quartzitic argillite, and phyllite, (partly metatuffs)		165	massive white to buff quartzite and feldspathic quartzite (locally crossbedded)	950
metadiabase		8	mica-chlorite-quartz schist and phyllite	350
conglomeratic argillite (tuff breccia?)		8	massive white, purple, and red quartzite and feldspathic quartzite (locally crossbedded)	250
buff to gray siltite, quartzitic argillite, and phyllite, (partly metatuffs)		725	metadiabase	200
<i>base not exposed</i>			massive white to buff, purple, and red quartzite and feldspathic quartzite (locally crossbedded)	400
total thickness		1,648	mica-chlorite schist and phyllite with talc bed near the base	650
Section 9—Central San Andres Mountains from the highest exposed unit east of Strawberry Peak to the Phanerozoic unconformity in Lost Man Canyon.				
Description		Thickness (m)		
<i>top not exposed</i>				
mica-chlorite-quartz schist and phyllite		375	massive feldspathic quartzite (locally crossbedded) with mica-chlorite schist	600
arkosite and feldspathic quartzite		350	metadiabase	50
			massive feldspathic quartzite (locally crossbedded)	250
			metadiabase	18
			massive feldspathic quartzite (locally crossbedded) with mica-chlorite schist	200
			red siliceous metavolcanic rock	5
			massive feldspathic quartzite (locally crossbedded) with mica-chlorite schist	150
			metadiabase	10
			red siliceous meta-igneous rock	3
			feldspathic quartzite and siltite, often crossbedded (50-80%); feldspathic quartz schist and phyllite (10%); mica-chlorite-quartz schist and phyllite (5-10%); minor amphibolite layers thickening in the section south of Dead Man Canyon (5-20%)	≥ 1,900
			<i>unconformity with Bliss Sandstone</i>	
			total thickness	≥ 9,468

Microfiche

APPENDIX 2—Major-element chemical analyses

APPENDIX 3—Trace-element contents

APPENDIX 4—Sample locations

Index

- Ab-An-Or-Q system, 40, 42, 43, 44
ACF values, 34, 35
air-fall tuffs, 20
AKF values, 34, 35
albitization, 45
almandite, 12
alteration, 25, 38, 39, 40, 44, 45, 47
amethyst, 50
amphibolite facies, 18, 34, 36
amygdules, 16
andalusite, 16, 20, 35, 47
andesite, 40
anticline, 32
apophyses, 16
archean rocks, 47
arc system, 49
Arizona, 36, 49
Arkansas, 50
ash-flow tuffs, 18, 19, 20
assimilation, 47
Au-bearing quartz lodes, 50
- banded iron formation, 50
barite, 29, 30, 50
Barrovian facies series, 35, 50
basins, 49
Bent dome, 9
bimodal magmatism, 50
bimodal rocks, 38, 48
Black Range, 38, 39, 40
Bliss Sandstone, 9, 12
Blue Springs Muscovite Schist, 11, 12, 13, 14
boudins, 12, 32
breccia zone, 32
building stones, 50
- Caballo Mountains, 9, 16, 30, 33, 34, 35, 36
 Burbank Canyon, 16, 30
 Longbottom Canyon, 16, 30
Caballo pluton, 30, 33
calc-alkaline basalt fields, 39
California, 7, 36
Capirote pluton, 18, 28, 33, 44, 45
Capitol Peak pluton, 28, 29, 30, 32, 35, 36,
 42, 43
cataclastic deformation, 33
chalcopyrite, 50
channel-fill deposits, 21
chemical analyses, 38
chloritoid, 12, 13, 35
chrysocolla, 50
Cibola Gneiss, 20, 25, 32, 35, 36
Colorado, 36, 40
conglomerate, 14
conglomeratic units, 14, 22
contact aureole, 35
contact metamorphic aureoles, 13, 25, 27, 47
contact metamorphism, 20, 25, 27, 28, 34,
 35, 36
continental-rift systems, 46, 48, 49
cordierite, 35
Coyote Hills, 9, 14, 18, 20, 33, 34, 36
C/Q ratios, 22
crossbedding, 12, 14, 21, 31, 32, 33
cross-micas, 13, 15
cross-muscovite, 19
crust, 47, 48
crustal thickness grid, 40, 43
- De Baca terrane, 7, 21, 24, 38
depths of emplacement, 25, 47
devitrification, 19
dragfolding, 11
- eclogite, 47
epidotization, 45
Eu anomalies, 38, 41, 42, 43, 44, 45, 46, 47
eugeoclinal assemblages, 46, 48, 49
- facies-series evolution, 35
fault breccia, 32
faults, 33, 48
F₁-F₂ discriminant plots, 39
flaser structures, 15, 18, 19, 20
flow breccias, 16
flow cleavage, 13
fluorite, 30, 50
folds, 31, 48
foliation, 12, 13, 14, 15, 17, 19, 25, 26, 28,
 31, 32, 33, 48, 50
forceful emplacement, 32, 33
Fort Bliss Military Reservation, 31
Fra Cristobal Range, 9, 31
fractional crystallization, 43, 47, 48
fracture cleavage, 13
Franklin Mountains, 38
Franklin Mountains igneous terrane, 7
- gabbro, 47
galena, 29
Gallinas Mountains, 9
garnet, 26, 29, 35
garnet amphibolite, 47
garnet granulite, 47
garnet peridotite, 47
geochemical model studies, 47
geothermal gradient, 36, 47
glomeroporphyritic textures, 19, 20
graded bedding, 12
grades of metamorphism, 35
granite emplacement, 47
gravitational gliding, 32
gravity sliding, 48
graywacke, 46
Great Combination mine, 50
greenschist facies, 18, 34, 35
greenstone, 16, 17, 26, 40, 50
Grenville Province, 50
- high-Ca group, 38, 40, 42, 47, 48
high-K group, 38, 40, 42, 43, 47, 48, 49
high-REE subgroup, 40, 43
high-Si group, 38, 40, 42, 43, 44, 46, 47, 48
hornblende-hornfels facies, 35
hornfels textures, 20
- Illinois, 7
initial Sr⁸⁷/Sr⁸⁶ ratios, 36, 38, 48, 49
isoclinal folding, 32, 33
- Juan Torres prospect, 50
- Kansas, 50
Kelly, 17
kyanite, 13, 16, 20, 34, 35
- Labrador, 50
- Ladron Mountains, 9, 11, 12, 13, 14, 15, 16,
 17, 18, 22, 28, 33, 34, 40, 44, 49, 50
 Cerro Colorado, 28, 33
 Ladron Peak, 28, 33
Ladron pluton, 28, 33, 36
Ladron section, 14, 21, 22
La Joyita Hills, 9, 28, 33
La Joyita pluton, 28
Laramide thrusts, 7
Lemitar Mountains, 9, 14, 16, 17, 28, 33
 Corkscrew Canyon, 14, 28
 Polvadera Peak, 28
Iherzolite, 47
lithosphere, 49
Los Pinos Mountains, 7, 11, 12, 13, 14, 15,
 16, 18, 19, 21, 27, 31, 32, 33, 36, 44, 45
 Bootleg Canyon, 27
 Whiteface Mountain, 27
Los Pinos pluton, 27, 36, 47
Los Pinos section, 21
lower crust, 47, 49
low-K basalt fields, 39
low-REE subgroups, 40, 43
- Magdalena Group, 9
Magdalena metagabbro, 36
Magdalena Mountains, 9, 11, 14, 15, 17, 18,
 20, 28, 33, 34
 Garcia Canyon, 17
 Jordan Canyon, 17
 North Fork, 17
 Water Canyon, 11, 14, 33
Magdalena pluton, 17, 28, 33, 36
Magdalena section, 21
magma origin, 38, 47
major elements, 38, 40
malachite, 50
manganese minerals, 50
mantle, 48
mantle plume, 49, 50
mantle source, 49
Manzanita Mountains, 7, 11, 14, 16, 17, 18,
 19, 21, 22, 26, 31, 32, 40, 42, 43, 49
 Coyote Canyon, 14, 18, 32
 Coyote Springs, 26
 Hell Canyon, 16, 18, 40, 50
 North Canyon, 18
 Tijeras Canyon, 16
Manzanita pluton, 7, 21, 26, 31, 40
Manzanita section, 21
Manzano Mountains, 7, 11, 12, 13, 14, 15,
 16, 18, 19, 20, 21, 22, 27, 31, 32, 33, 36, 40,
 41, 45
 Capilla Peak, 14, 18
 Comanche Canyon, 11, 12, 14, 31, 32
 Manzano Peak, 14, 32
Manzano section, 21
Mayberry pluton, 30, 36
 Lost Man Canyon, 30
 San Andres Canyon, 30
mesonorms, 38
metamorphic differentiation, 14
metamorphic grade, 34, 39
metamorphism, 13, 34, 35, 39, 40
metasomatism, 20, 25, 38, 45
metatuffs, 14
miarolitic cavities, 27, 47
migmatites, 20

Milagros claims, 50
 Mimbres River, 39, 40
 Mineral Hill pluton, 30, 36
 miogeoclinal field, 46
 miogeoclinal assemblages, 48
 Mockingbird Gap pluton, 29, 30, 42
 Monte Largo Hills, 7, 14, 16, 18, 20, 30, 31, 32, 34, 36
 Monte Largo Hills pluton, 24, 35
 Monte Largo pluton, 24, 26, 27, 41
 montmorillonite, 35, 36
 Moore fault, 32
 mortar structures, 15, 18, 20
 mud cracks, 12
 multiple-rift system, 48, 49, 50
 mylonite zones, 32
 mylonitization, 33

Nacimiento Mountains, 36
 neutron activation, 38
 New Zealand, 44
 Taupo Rhyolite, 44

Ohio, 7
 Ojita pluton, 21, 24, 26, 27, 31, 36, 38, 41
 Ojita Canyon, 27
 Oklahoma, 50
 ophitic textures, 34
 orbicular granite, 25
 Organ Mountains, 9, 20, 31
 Rattlesnake Ridge, 31
 Organ pluton, 31
 oscillatory zoning, 29
 Oscura Mountains, 9, 28, 29
 Oscura pluton, 28, 29, 36, 42, 43
 oxygen fugacity, 48

Pajarito Mountain, 9, 31, 38
 Pajarito syenite, 7
 Paleozoic formations, 9
 Paloma thrust, 12
 partial melting, 36, 47, 48, 49
 Pecos River, 39, 49
 Pecos succession, 39, 40
 Pederal Hills, 7, 9, 11, 13, 14, 16, 18, 20, 27, 32, 34, 36, 49
 Pederal pluton, 9, 24, 27, 32, 35, 36
 Pederal section, 21
 pegmatites, 20, 24, 26, 27, 28, 29, 30, 31, 32, 47, 50
 pegmatitic phases, 26, 31
 peristerite solvus, 15, 36
 P/F ratios, 22
 Pikes Peak granite, 47
 pillow structures, 16
 Polvadera pluton, 17, 28
 post-tectonic emplacement, 25, 26, 27, 28
 Precambrian crustal provinces, 7
 Precambrian sedimentary environment, 46
 prehnite, 18
 Priest pluton, 24, 27, 35, 36, 42
 Priest quartz monzonite, 47
 provenance, 38, 45
 pseudosillimanite, 35
 pull-apart structures, 14
 pumice fragments, 14, 34

railroad ballast, 50
 Rattlesnake Hills, 9
 Rayleigh fractional law, 47
 Rb-Sr ages, 7, 36, 40
 recumbent folds, 33
 recycling, 49
 Red Hills, 9, 30
 REE, 40, 42, 43, 44, 45, 46, 47
 REE patterns, 39, 40, 43, 44, 45, 49
 REE values, 38
 regional metamorphism, 32, 33, 34, 35, 36, 38, 39, 49, 50
 resorption, 19
 retrograde metamorphism, 18, 34
 rhyodacite, 18, 19
 Rio Grande rift, 7
 roof pendant, 33

Sacramento Mountains, 9, 11
 Sacramento escarpment, 12, 21
 Sais Quartzite, 14, 21, 32
 San Andres Mountains, 9, 11, 12, 13, 14, 15, 16, 17, 18, 20, 21, 28, 29, 30, 32, 33, 34, 36, 38, 40, 49, 50
 Black Mountain, 30
 Black Top Mountain, 14, 20
 Camels Hump Ridge, 20
 Capitol Peak, 17
 Cottonwood Canyon, 20, 29, 35
 Goat Mountain, 14
 Grapevine Canyon, 16, 20
 Gunsight Peak, 14
 Hembrillo Canyon, 9, 11, 12, 18, 19, 20, 32, 35, 36, 50
 Hembrillo-Grandview Canyon, 17
 Hembrillo Wash, 13
 Johnson Park Canyon, 29
 Little San Nicholas Canyon, 20, 30
 Lost Man Canyon, 32
 Mayberry Canyon, 11, 13, 16
 Salinas Peak, 16, 17, 20, 29, 49
 Salt Canyon, 30
 San Andres Peak, 16, 20
 Sheep Mountain, 18, 20
 Strawberry Peak, 12
 Sulphur Canyon, 12, 30, 32
 San Andres pluton, 30
 Little San Nicholas Canyon, 30
 San Andres Canyon, 30
 San Andres section, 14, 21, 22
 Sandia Formation, 7, 9
 Sandia Military Reservation, 26
 Sandia Mountains, 7, 14, 15, 16, 20, 25, 31
 Coyote Canyon, 20
 Embudito Canyon, 41
 Juan Tabo Canyon, 25
 Juan Tabo sequence, 15, 26
 La Luz Trail, 25
 Pino Canyon, 26, 41
 Rincon Ridge, 14, 31, 32, 50
 Tijeras Canyon, 25
 Sandia plutons, 20, 32, 41
 North pluton, 24, 25, 35, 36, 41
 South pluton, 20, 24, 25, 35, 41
 San Diego Mountain, 9, 30
 Sangre de Cristo Mountains, 21
 saussuritization, 18, 19
 septum, 27
 sedimentary basin, 21
 Sepulture pluton, 27, 36

Sevilleta Formation, 14, 18, 27, 31, 36, 44
 Sierra Cuchillo, 9
 sieve textures, 15
 siliceous granulite, 47
 silicification, 27, 33
 sillimanite, 13, 16, 20, 34, 36
 SMP block, 7, 21, 31, 32, 34, 49
 SMP section, 21
 Socorro, 9, 40
 solvus temperatures, 29
 Sonora, 7, 36
 sorting, 14
 sphalerite, 29, 50
 spherulitic K-feldspar, 19
 spherulitic texture, 34
 spilitization, 45
 statistical mixing program, 47
 staurolite, 16, 34, 35, 36
 stilpnomelane, 18
 stratigraphic sections, 21
 Strawberry Peak pluton, 30
 subduction zone, 49
 subophitic textures, 34
 sulfides, 50
 syncline, 31, 32
 synform, 32, 33
 syntectonic emplacement, 25, 26, 28

Tajo pluton, 30
 talc, 12, 35, 36
 tectonic model, 50
 tectonic setting, 39, 46, 48, 49
 temperature, 47
 emplacement temperature, 47
 liquidus temperature, 47
 Texas, 7, 36, 50
 thermal-tectonic regimes, 22
 tholeiites, 38, 39, 40, 47, 49
 tholeiitic magmas, 49
 Tijeras fault, 32, 48, 50
 Tijeras Greenstone, 11, 16, 17, 20, 32, 39, 49
 Ti-Y-Zr discriminant plots, 39
 Tonuco uplift, 30
 trace elements, 38
 transition metals, 45
 Tusas Mountains, 36, 39

unconformity, 31, 32
 Comanche Canyon, 31, 32
 undulatory extinction, 15, 29
 U-Pb zircon dates, 7, 36
 uplift, 47
 upper mantle, 47
 USGS seismic station, 26

vesicles, 16, 18
 volcanic ash, 35

water content, 47
 hydrothermal alteration, 47
 water pressures, 47
 White Ridge Formation, 14, 15, 18, 21, 31
 White Sands Missile Range, 30
 White Sands pluton, 31
 Wisconsin, 7

xenoliths, 25

Yeso Formation, 9
 York min, 50

Type faces: Text in 10-pt. English Times, leaded one point
Subheads in 14-pt.
Display heads in 24-pt.

Presswork: Miehle 38" Single Color Offset
Harris Single Color Offset

Papaer: Cover on 17-pt. Kivar
Text on 70# White matte

Ink: Cover—PMS 320
Text—Black

Press run: 1,000

Pocket Contents

SHEET 1—Precambrian rocks in the SMP block and in Monte Largo Hills, Bernalillo, Torrance, Valencia, and Socorro Counties

SHEET 2—Precambrian rocks from various locations in central and south-central New Mexico (includes figs. 4-13, 17, and 18)

SHEET 3—Precambrian rocks in San Andres and Oscura Mountains, Sierra, Socorro, Doña Ana, and Lincoln Counties

Microfiche

APPENDIX 2—Major-element chemical analyses

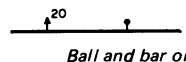
APPENDIX 3—Trace-element contents

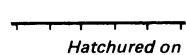
APPENDIX 4—Sample locations

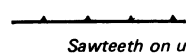
Geologic symbols on color sheets

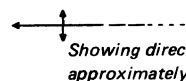
----- Contact
Dashed where approximately located; short dashed where inferred; dotted where concealed

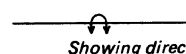
----- Fault
Dashed where approximately located; short dashed where inferred; dotted where concealed

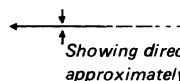
 Fault, showing dip
Ball and bar on downthrown side

 Normal fault
Hatchured on downthrown side

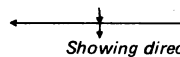
 Thrust fault
Sawteeth on upper plate

 Anticline
Showing direction of plunge; dashed where approximately located

 Overturned anticline
Showing direction of dip of limbs

 Syncline
Showing direction of plunge; dashed where approximately located; dotted where concealed

 Overturned syncline
Showing direction of dip of limbs

 Monocline
Showing direction of plunge of axis

Strike and dip of beds

 70° Inclined

 Horizontal

 Vertical

 Overturned

Strike and dip of foliation

 Inclined

 Vertical

 Horizontal

Note: *Special symbols are shown in explanation*